KINETICS OF NUCLEATION AND GROWTH IN A EUTECTOID PLAIN CARBON STEEL

by

MEHMET BAHA KUBAN

B.Sc., University of Manchester,
Institute of Science and Technology, 1981

A THESIS SUBMITTED IN PARTIAL FULFILMENT OF
THE REQUIREMENTS FOR THE DEGREE OF
MASTER OF APPLIED SCIENCE

in

THE FACULTY OF GRADUATE STUDIES
Department of Metallurgical Engineering

We accept this thesis as conforming
to the required standard

THE UNIVERSITY OF BRITISH COLUMBIA

September 1983

In presenting this thesis in partial fulfilment of the requirements for an advanced degree at the University of British Columbia, I agree that the Library shall make it freely available for reference and study. I further agree that permission for extensive copying of this thesis for scholarly purposes may be granted by the head of my department or by his or her representatives. It is understood that copying or publication of this thesis for financial gain shall not be allowed without my written permission.

Department of METALLURGICAL ENGINEERING

The University of British Columbia
1956 Main Mall
Vancouver, Canada
V6T 1Y3

Date 26/8/83

ABSTRACT

An accurate prediction of the continuous cooling transformation (CCT) history of steels, obtained using isothermal transformation data has been of considerable academic and industrial importance for many years. The Additivity Principle, which is required to permit this calculation, has been defined but in general not completely satisfied. In this thesis the kinetics of nucleation and growth of the austenite-to-pearlite transformation in eutectoid, plain-carbon steels have been measured with the aim of clarifying the limits of applicability of this additivity principle. As a result, a new satisfactory condition, termed "effective site saturation", is proposed.

The pearlite nucleation and growth rates were obtained for a range of austenite grain sizes and transformation temperatures. This data has also been used to develop a grain size parameter which could be included in the empirical transformation equation. The significance of the measured grain size exponent, 'm', in terms of the operational pearlite nucleation sites has been examined.

The relationship between the thermal history of the austenite phase and the resulting austenite grain size has

also been examined. The applicability of an available empirical expression for predicting the austenite grain size as a function of peak temperature and time at temperature has been confirmed.

TABLE OF CONTENTS

LIST OF TABLES

LIST OF FIGURES

Figure | Page

Figure | Page

Figure | Page

Figure | Page

LIST OF SYMBOLS

N_v : Volumetric nucleation rate in the Johnson and Mehl equation (Equation 2.4) in number of nodules per mm^3 per second.

G : Growth rate in mm per second

t : Reaction time

R : Radius of Pearlite Nodule

V_{ex} : Extended volume transformed

V_{true} : True volume after subtracting impinged volume

X : Fraction transformed of pearlite

b : Temperature dependent parameter in the Avrami equation (Equation 2.5).

n : time exponent in the Avrami equation

d : Austenite grain diameter

n_1 : time exponent for high temperature nucleation equation (Equation 2.7).

m : grain size exponent in Equation 2.8.

D_o : Grain diameter at zero time at temperature.(Eqn.2.16)

D : Final grain diameter.

n" : Grain diameter exponent for the grain growth equation.

Q : Heat of activation for the transformation process

A : Grain growth equation constant

D_c : Diffusivity of carbon in austenite

ΔC : Concentration gradient

S_p : Pearlite spacing

a : Grain diameter in the shape factor (Equation 3.1) and the time scale factor (Equation 3.3).

N : Measured nucleation rate in number of nodules per unit volume per unit time

$\overset{*}{D}_0$: Peak temperature independent initial grain size in equation 2.15

ACKNOWLEDGEMENTS

I would like to thank Professor E. B. Hawbolt for the advice and encouragement as my thesis supervisor. Thanks are also extended to Professor J. K. Brimacombe, the other members of the Phase Transformations Study Group and Professor R. G. Butters. Financial assistance was received in the form of a research grant from the American Iron and Steel Institute.

...

Urumelihisarına oturmuşum,
Oturmuşda bir türkü tutturmuşum;
"İstanbulun mermer taşları;
Başıma da konuyor, konuyor aman martı kuşları...."

...

İstanbul Türküsünden

Orhan Veli Kanık

CHAPTER 1

AN EXAMINATION OF THE AUSTENITE DECOMPOSITION REACTION AND THE PREDICTION OF CONTINUOUS COOLING BEHAVIOUR FROM CONSTANT TEMPERATURE DATA

"To make yron or steele hard, take the iuyce of varuen, cold in latine, verbana, and strayne it into a glasse, and ye wil quenche any yron, take thereof, and put to of men's pisse, and the distilde water of wormes so mixe together, and quenche there in so farre as ye will have it hard, but heede it be not too harde, there of take it forth soone after, and let it coole of itself, for when it is well seasoned ye shall see golden spottes on your yron. Also the common hardning of yron or steele is in cold water and snow water, so when the edge shall seeme blue after this hardning, signifieth a good sign, and a right hardning."[1]

This was the standard procedure for heat treating steel in the 16th century and probably long before that.[2] Our knowledge of the hardening mechanisms has been increasing since then, but not without protracted, agonizing research and probing, sometimes in the wrong directions. However, the importance of furthering our fundamental understanding

of the steel decomposition processes is clear for the material progress of human society. An enormous amount of research effort has been expended in this direction and more is required. Early studies employed the metallographic methods to analyze the austenite decomposition at constant temperatures (Fig. 1.1); the classical work of Davenport and Bain is a leading example.[3]

From information on the decomposition reaction at different temperatures, diagrams of a very important and practical nature were obtained. These familiar diagrams, called isothermal transformation or Time-Temperature Transformation (TTT) diagrams, gave valuable information on the start, end and duration of the austenite decomposition reaction, thus making it possible to predict final microstructure and constituents for processes carried out at constant temperatures (Fig. 1.2).

A large number of isothermal transformation diagrams were constructed by Bain and Davenport, and others.[4,5] A variety of steels of different composition and grain size were included.

However, the practical application of TTT diagrams to the heat treatment of steel is limited to those processes

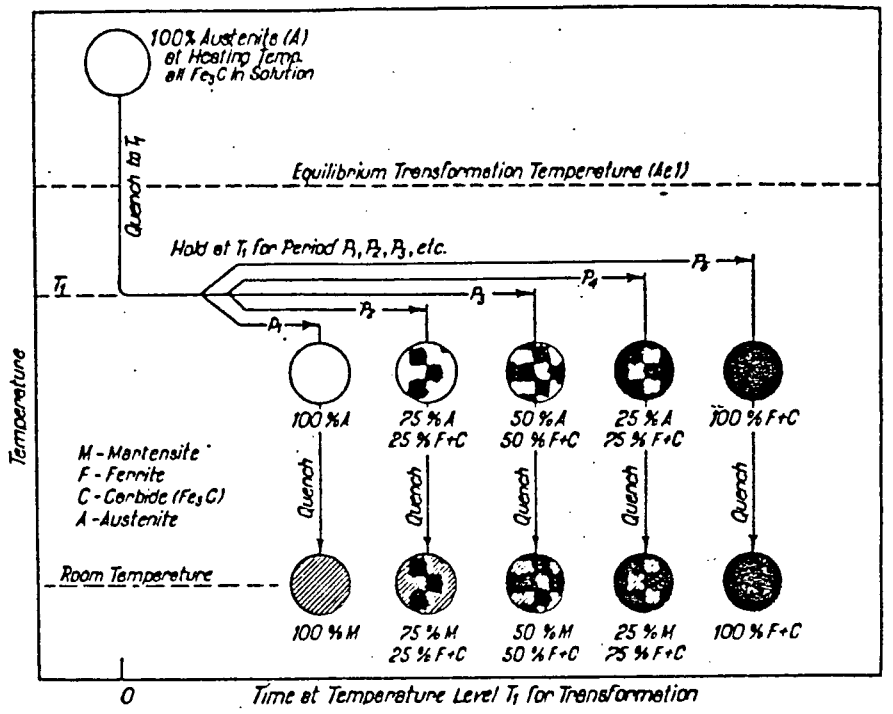

Fig. 1.1 Schematic representation of the heat treating operations involved in following the progress of isothermal pearlite transformation, using the metallographic method (Ref. 6).

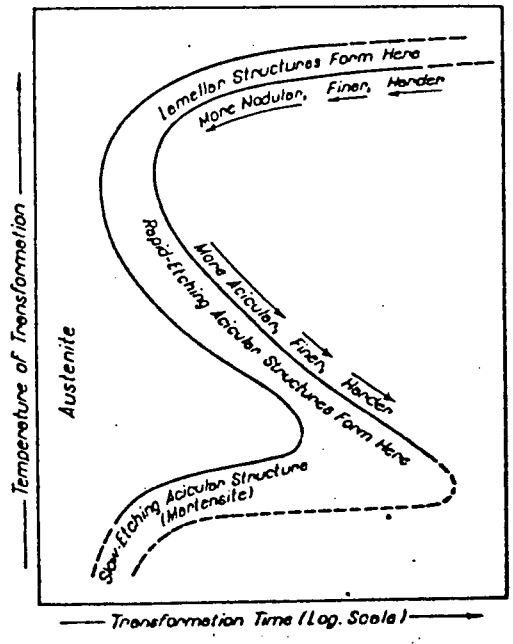

Fig. 1.2 Typical early transformation diagram, with the ranges of temperatures for the formation of lamellar and acicular products indicated (Ref. 7).

which are essentially isothermal in nature. If a steel is cooled rapidly from the austenitising temperature to some intermediate temperature and held there for a certain length of time, the TTT diagram will indicate what the final structure will be. But very few commercial heat treatments occur in this manner. In most heat treatment processes, the metal is heated up to the austenite region and continuously cooled to room temperature. Davenport and Bain, in addition to generating data on isothermal transformations in steels, also pointed out the need for correlating the transformation characteristics obtained during continuous-cooling with those obtained during isothermal treatment. Bain in fact produced a schematic continuous cooling diagram for a 0.85%C steel (Fig. 1.3).[6,7]

A demonstration of the difference between isothermal and continuous-cooling diagrams can best be made by comparing similar treatments for a eutectoid steel. Fig. 1.4 shows, imposed on an isothermal transformation diagram, the altered reaction start and completion times for the designated continuous-cooling curve.[8] After six seconds, the cooling curve crosses the line representing the start of the pearlite transformation for an isothermal reaction at 650°C. A continuously cooled specimen would have been at temperatures above 650°C for the total lapsed time of 6 seconds and would

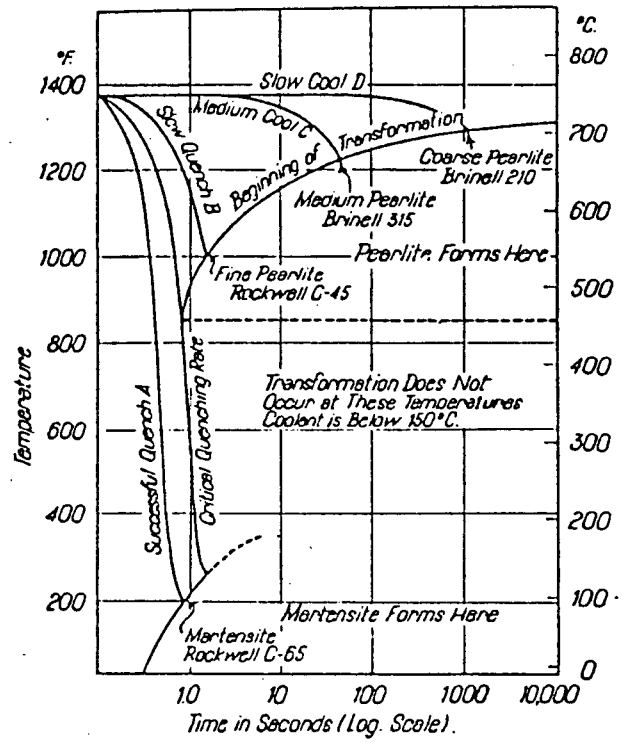

Fig. 1.3 Schematic representation of the relationship between cooling rate and temperature of initial transformation on cooling (Ref.9).

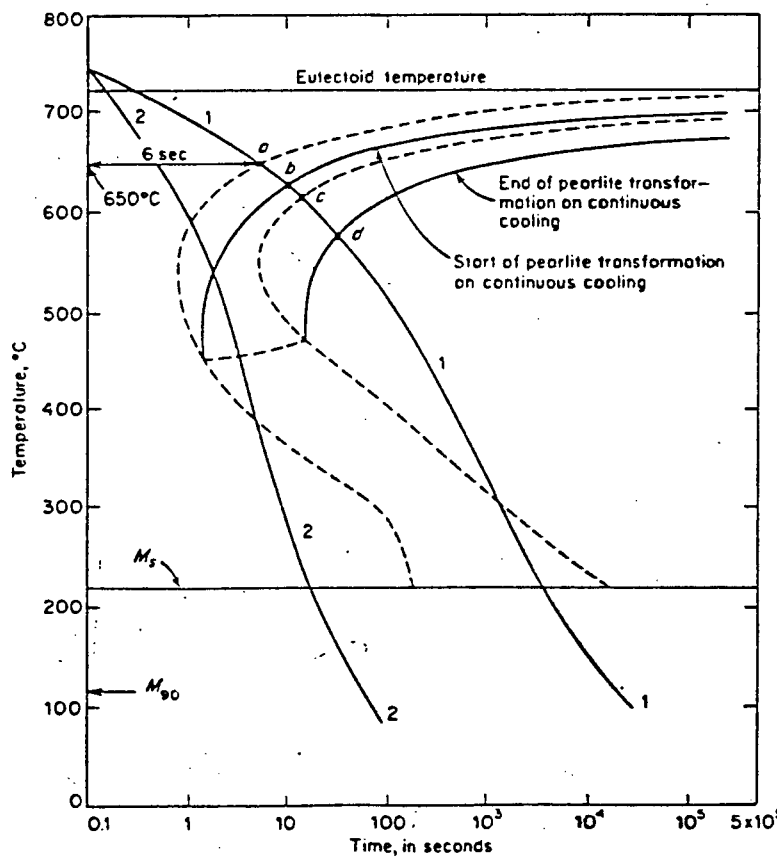

Fig. 1.4 The relationship between the continuous-cooling diagram and the isothermal diagram for an eutectoid steel.(Ref. 8).

only have reached 650°C at the end of 6 seconds. Since the time to start the pearlite reaction, the incubation time, is longer at higher temperatures, a continuously cooled specimen requires a longer incubation time than does an isothermally treated sample. Hence in a continuous cooling process, the reaction start will be depressed to a lower temperature and pushed to a longer time. The most important characteristic of a specimen being allowed to transform over a range of temperatures is the mixed microstructure that results.

In the first attempt to describe experimentally determined Continuous Cooling Transformation (CCT) diagrams, Grange and Kiefer stated, "It is to be noted that in the isothermal case the structure formed at any single temperature level is uniform whereas on continuous cooling, transformation proceeds over a range of temperatures, and the final structure is therefore a mixture or a series of products, each product being substantially indistinguishable from what forms isothermally at the same temperature."[9] They also noted that it would be far more convenient to derive a continuous-cooling diagram from isothermal data, if a satisfactory method of derivation could be developed.

To allow for the experimental determination of a

continuous-cooling transformation diagram, Grange and Kiefer selected a S.A.E. 4340 steel (Table 1.1), whose isothermal diagram indicated sluggish transformation behaviour (Fig. 1.5). A total of 104 specimens, representing seven different constant cooling rates had to be employed to metallographically follow the transformation during cooling. The experimentally constructed CCT diagram can be seen in Fig. 1.6.

Grange and Kiefer also developed an empirical method for deriving a cooling diagram from an isothermal diagram. The essence of their method consisted of respresenting any stage of the cooling by a point on the isothermal diagram which indicates, by its position, the equivalent amount of transformation that has occurred on cooling to that temperature at the specified rate. They carried out a fairly complex construction procedure on semi-log paper, the details of which can be found in their paper,[9] to produce the CCT diagram in Fig. 1.7. In further tests on several grades of low-alloy steels, experimental determinations were found to check satisfactorily with empirical determinations of CCT diagrams. Comparison of experimental and calculated curves for the initiation of the ferrite reaction in 4340 steel can be seen in Fig. 1.8.

One important discrepancy with the empirically

	C	Mn	Si	Ni	Cr	Mo
Composition	0.42	0.78	0.24	1.79	0.80	0.33

Preliminary Treatment—Hot-rolled 1¼ inches round, normalized from 1800 degrees Fahr.
Specimen Size—1¼ inches diameter, half disks ⅛ inch thick
Austenitizing Treatment—1550 degrees Fahr. for 15 minutes
Austenite Grain Size No. 7-8 A.S.T.M.

Equilibrium Transformation Temperatures	Ae_1	Ae_3
	1300 degrees Fahr.	1375 degrees Fahr.

Table 1.1 Composition, thermal history and grain size of S.A.E. 4340 steel used in the study by Grange and Kiefer (Ref.9).

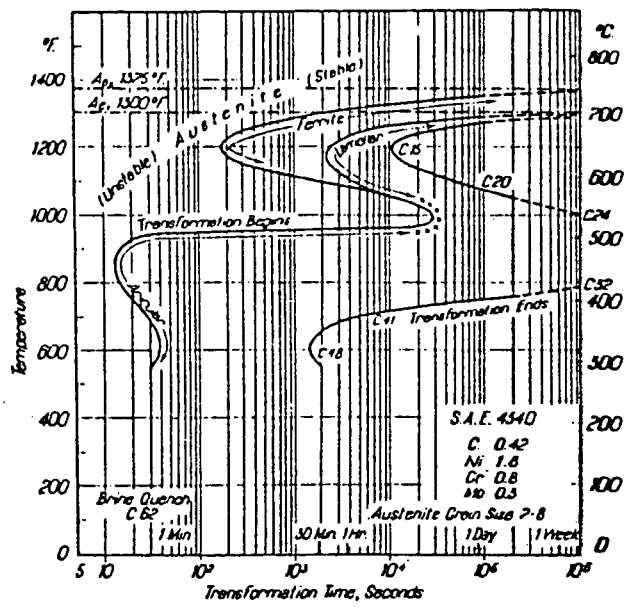

Fig. 1.5 Isothermal Transformation Diagram for S.A.E. 4340 steel (Ref.9).

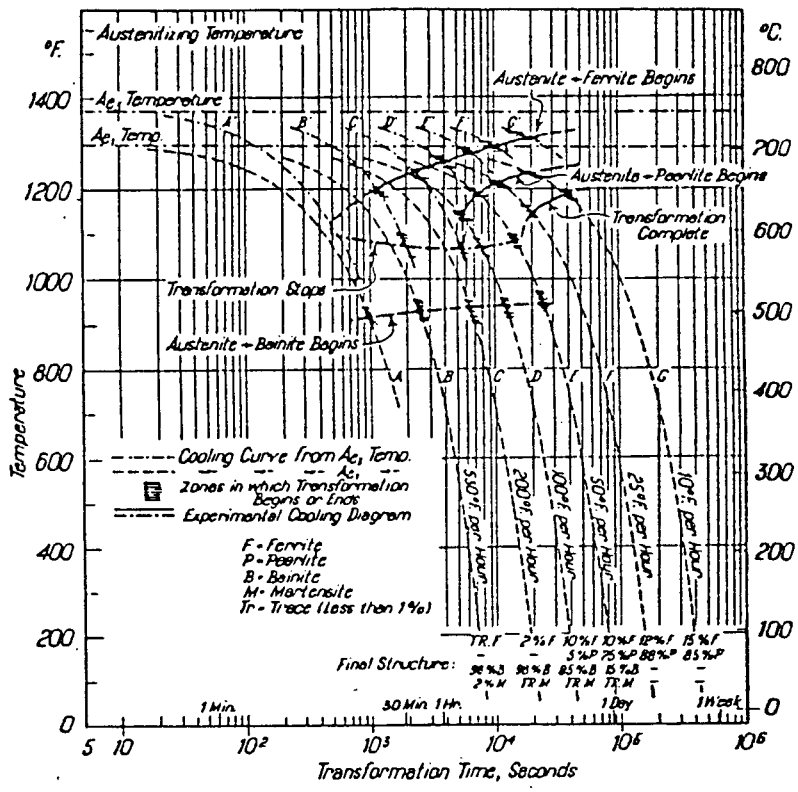

Fig. 1.6 CCT diagram for S.A.E. 4340 steel. Based on experimental data (Ref. 9).

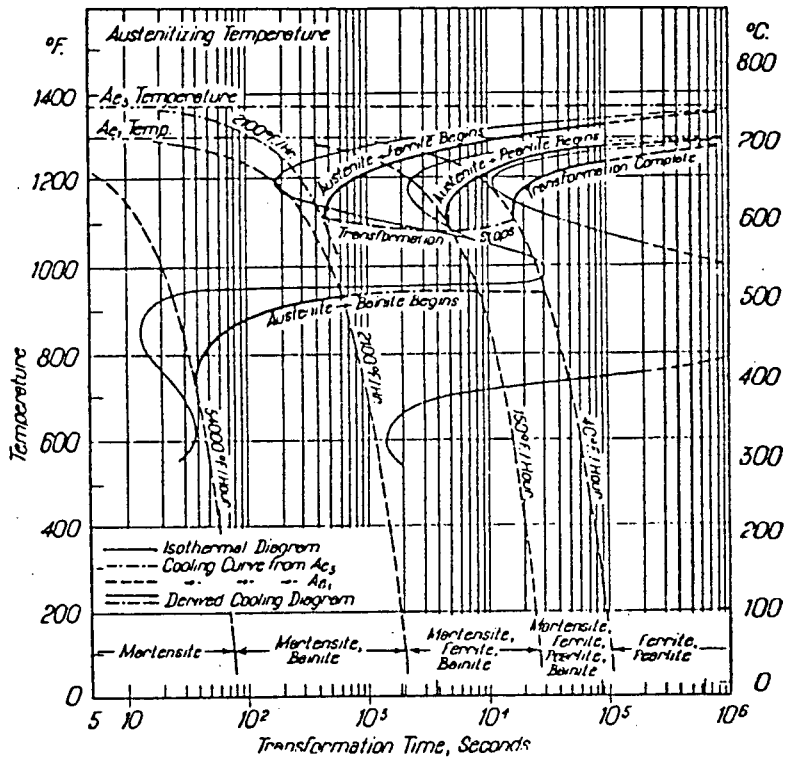

Fig. 1.7 CCT diagram for S.A.E. 4340 steel. Derived from isothermal data (Ref.9).

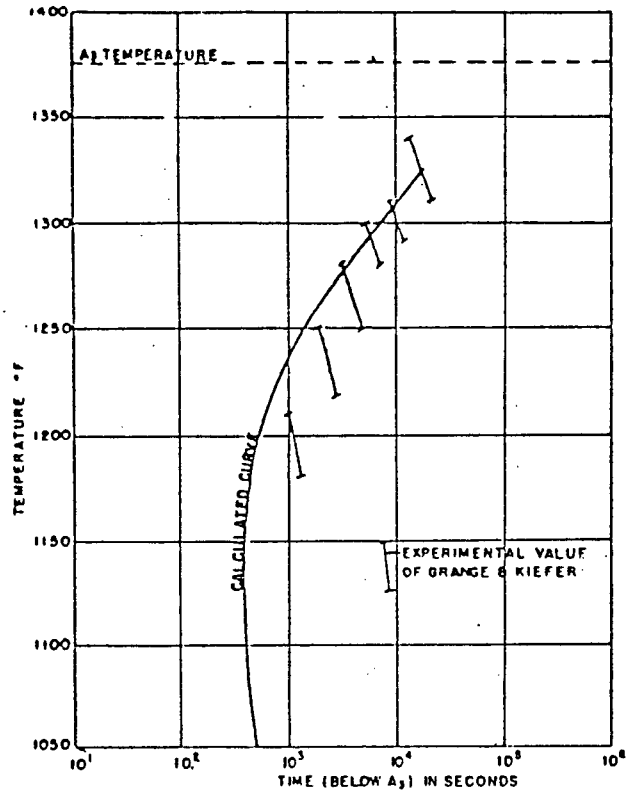

Fig. 1.8 Comparison of experimental and calculated curves for the initiation of the ferrite reaction in a 4340 steel (Ref.13).

determined CCT diagram lay in the location of the curve representing the completion of the pearlite reaction. Grange and Kiefer attributed this to the errors in the determination of the end portion of the transformation (isothermal data for this end of the transformation).

In the case of eutectoid plain-carbon steel Bain had earlier proposed that only pearlite and martensite would be produced because transformation to bainite would be sheltered by the higher temperature transformation to pearlite. Grange and Kiefer, by adopting Bain's argument, could produce somewhat incomplete CCT diagrams.[10]

The suggestion to study the non-isothermal decomposition reactions in the form of combined constant temperature reactions was initially made by Scheil,[11] and later by Steinberg.[12] The TTT to CCT transformation was considered to be possible if the transformation obeyed an additivity rule. If the additivity principle held for a specific non-isothermal austenite decomposition reaction, the continuous cooling reaction events could then be treated as a series of constant temperature reactions. The question then becomes one of determining the effect of partial decomposition at any given temperature upon the subsequent decomposition at a different temperature. In general, the

additivity principle requires that the transformation at any temperature be a function only of the amount already present and the transformation temperature, i.e.

$$F_x = f(f_x, T) \qquad \ldots(1.1)$$

Hence if we consider a phase initially brought to one temperature where it is unstable and partially transforms, and is then brought to a second temperature to tranform further by the same reaction, the additivity principle would require that the reaction at the second temperature be unaffected by that at the initial temperature.[13] This principle can be seen schematically in Fig. 1.9.

Experimental investigations to test the additivity principle for different steel compositions, were carried out by various workers.[14,15,16,17] These included investigating the conditions for and limitations of applying the additivity rule for nucleation and growth reactions.[18]

Avrami[18] defined an isokinetic range of temperatures as one within which the nucleation and growth rates of the transformation reactions are proportional and stated that a reaction that is isokinetic is additive.

Krainer[14] measured the time for initiation of the

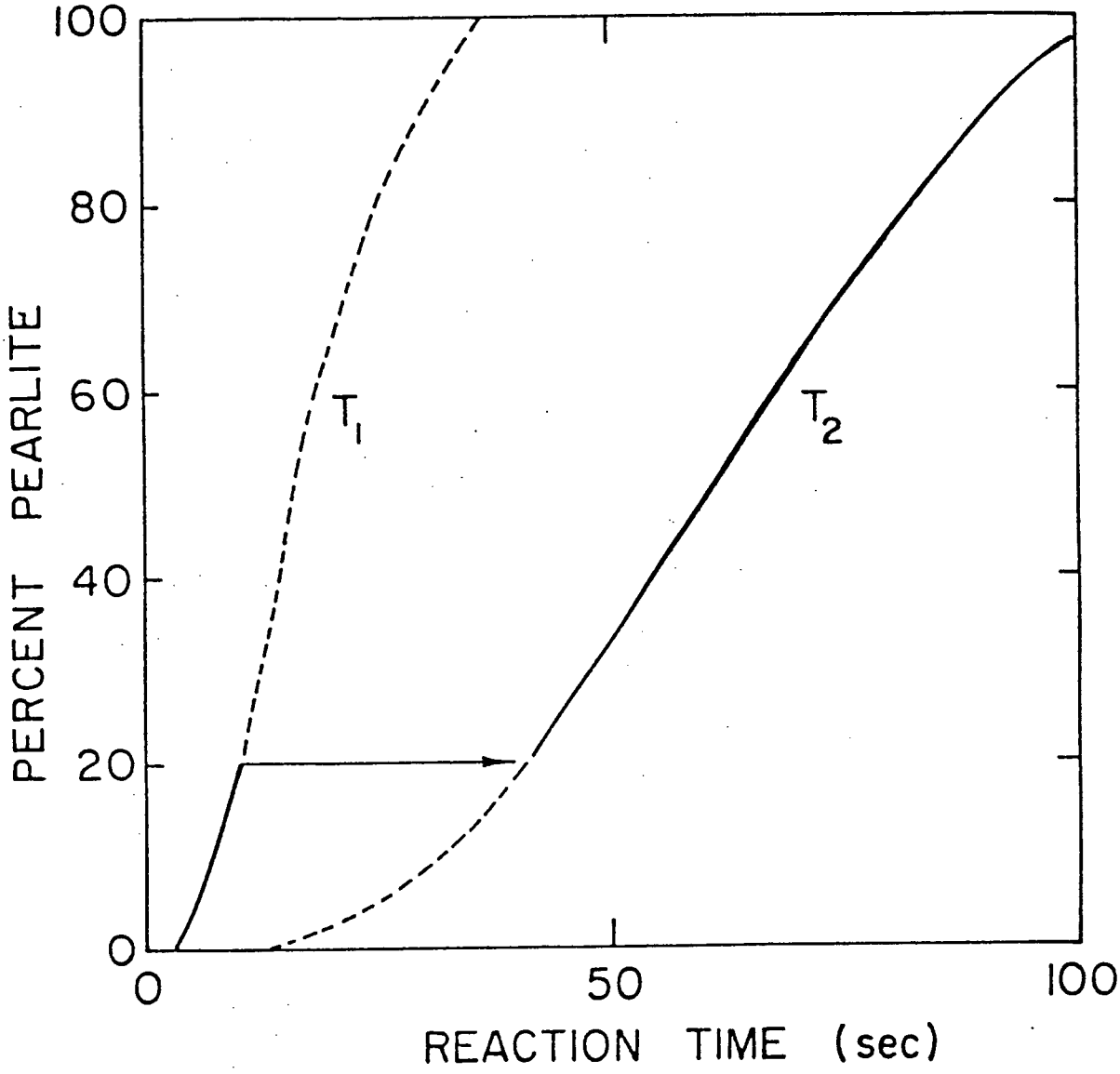

Fig. 1.9 Schematic representation of the additivity principle.

transformation in specimens of SAE 4150 steel (0.5% C, 1.1% Cr, 0.25% Mo) held at single temperatures within the range 590°C to 680°C and at two successive temperatures within this range. His results can be seen in Table 1.2, and show that the initiation of transformation is additive throughout the temperature range investigated.

Lange[15] and Lange and Hansel[16] pointed out that the shape of the curve for percent transformation versus time for the isothermal transformation of pearlite in plain carbon steels varies little with transformation temperature. A change in temperature simply multiplies all times by a factor. This similarity of shape they argued, indicated that the reaction is approximately isokinetic and so, necessarily additive.

Dorn, de Garmo and Flanigan[22] on the other hand, tested the isokinetic condition with a steel of composition 0.92% C, 1.53% Mn, 0.20% Si and 0.26%Mo and found that the pearlite transformation was not isokinetic in the temperature range 620°C to 710°C (Fig. 1.10).

Cahn[20] later added a less restrictive condition for additivity based on site saturation. He observed that for the pearlite reaction at most temperatures, the rate of nucleation becomes irrelevant and the rate of growth

Table 1.2 Steel Containing 0.5 Per Cent C, 1.1 Per Cent Cr, 0.25 Per Cent Mo. Austenitized 30 Minutes at 850°C.

First Temperature			Second Temperature			Sum of Fractional Times
Deg. C.	Minutes Held	Fractional Time	Deg. C.	Minutes to Initiate Transformation	Fractional Time	
	0	0.00	640	8	1.00	1.00
680	9.0	0.25	640	6.15	0.77	1.02
680	18.0	0.50	640	4.10	0.51	1.01
680	27.0	0.75	640	1.95	0.24	0.99
680	36.*	1.00			0.00	1.00
	0	0.00	590	28	1.00	1.00
640	2.0	0.25	590	20.15	0.72	0.97
640	4.0	0.50	590	13.50	0.48	0.98
640	6.0	0.75	590	7.70	0.28	1.03
640	8.*	1.00			0.00	1.00
	0	0.00	590	28	1.00	1.00
680	9.0	0.25	590	21.50	0.77	1.02
680	18.0	0.50	590	14.30	0.51	1.01
680	27.0	0.75	590	6.70	0.24	0.99
680	36.*	1.00			0.00	1.00

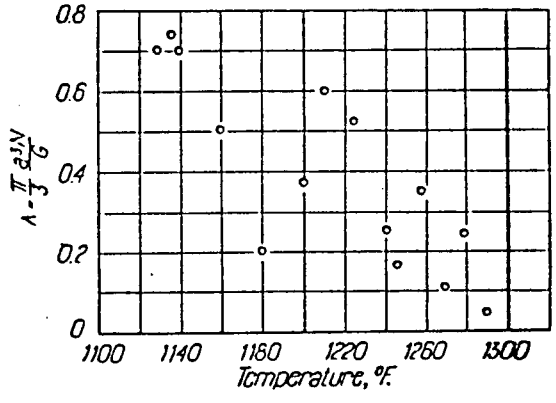

Fig. 1.10 The shape factor as a function of temperature (Ref. 22).

dominates the transformation due to the early exhaustion of available nucleation sites. Tamura et al.,[21] found Cahn's observations to be generally true.

In a recent study conducted in this department by Agarwal and Brimacombe,[23] a mathematical model was formulated to predict the kinetics of the austenite-to-pearlite transformation and the transient temperature distribution in a eutectoid, carbon steel rods during continuous-cooling processes such as Stelmor or Schloemann. This study used isothermal kinetics and assumed that the additivity principle was valid for the austenite-to-pearlite transformation, but showed relatively poor agreement with experimental determinations of continuous-cooling kinetics.

The main factors that were believed to be contributing to this discrepancy were:

1. the inaccuracies in the start and end times in existing isothermal transformation curves; and
2. the validity of using the additivity principle to describe the incubation, nucleation and growth processes.

Hence a more extensive research programme was initiated at the University of British Columbia. This M.A.Sc. thesis

was generated as one part of this research project. The general objectives of the programme were to be:

1. To accurately characterize the kinetics of the austenite decomposition reaction under carefully controlled isothermal as well as continuous cooling conditions.
2. To predict the continuous-cooling behaviour using the additivity rule while clarifying the limitations for use of this principle.

The following variables were to be investigated in the studies; grain size, thermal history, cooling rate, composition and section size. The latter incorporates changes in the cooling rate in a single specimen.

To simplify the transformation behaviour, the initial studies examined the austenite to pearlite reaction in eutectoid plain-carbon steels. This particular component of the study concentrated on characterizing the effect of grain size and thermal history on the isothermal austenite to pearlite decomposition and then investigating the conditions for the application of the additivity rule. Hence the experimental work consisted of:

1. Examining specimens that were given varying thermal

treatment to produce different grain sizes and subsequently reacted at constant subcritical temperatures. A comparison of the transformation rate for the austenite to pearlite reaction was made for different grain sizes.

2. Determining the pearlite nucleation and growth rates employing a series of specimens reacted to a maximum of 20 percent transformation. The data is used to test the present understanding of the additivity rule and to generate another sufficient condition for its use in predicting continuous-cooling kinetics from isothermal kinetic data.

CHAPTER 2

THE INFLUENCE OF GRAIN SIZE ON THE KINETICS OF THE AUSTENITE DECOMPOSITION REACTION IN EUTECTOID PLAIN CARBON STEEL

2.1 GENERAL INTRODUCTION

2.1.1 Grain Size versus Reaction Kinetics

The metallographic features of the constituents present in steel cooled from austenite were observed and fairly well understood as early as the 1890's,[24] despite the confusion in terminologies. Austenite grain size was recognized by Davenport and Bain as having an important influence on the rates of the isothermal austenite decomposition reactions. Bain investigated this subject soon afterwards,[25,26] and contributed to the understanding of the transformation by developing an improved means of revealing and measuring austenite grain size.[27,28]

The role of austenite grain size in affecting the hardening of steel is one of ancient recognition. The French metallurgist Réaumur had in 1722 devised for his blister steel a grain growth test in association with the performance of hardened tool steels and even had a crude

scale for designating the austenite grain size. Bain[29] made the following comment:

> It seems inescapable that the ancients who hardened steel must have made two important observations:
>
> 1. That steel which, after hardening revealed a coarse fracture surface hardened more deeply than that having a fine texture.
>
> 2. That steel which broke easily after hardening had a coarser fracture surface than that which broke only with the application of heavier blows.

In Sweden, as early as 1926, the fineness or coarseness of the fracture surfaces of hardened tool steel was regularly employed as a quantitative measure of certain qualities, the actual rating being made by comparison with five standard fracture surfaces evenly distributed over the full range usually encountered. Shortly afterwards, a ten-step standard scale was adopted and as can be seen in Fig. 2.1, it agreed exceedingly well with the standard ASTM austenite grain size scale.

The influence of austenite grain size on the hardness of a steel section, 1 inch in diameter is demonstrated in Fig. 2.2. Since hardenability is the capacity of a steel to transform to martensite, increasing the austenite grain size can be seen to retard the formation of pearlite, or enhance the formation of martensite. Bain correctly

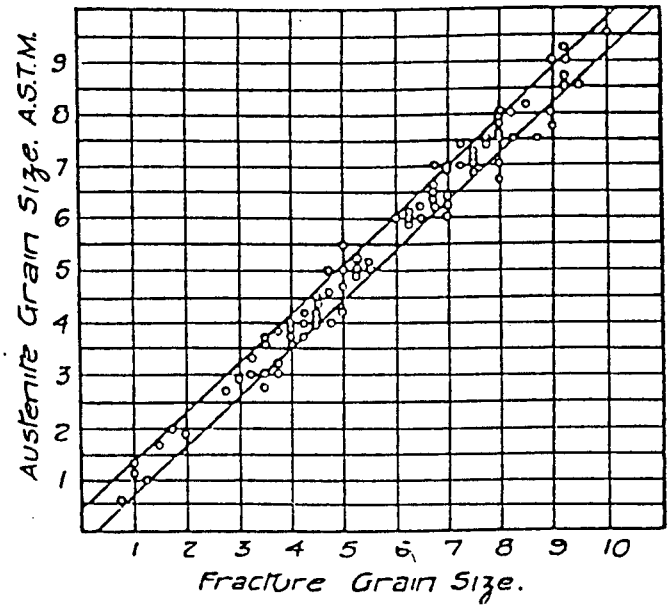

Fig. 2.1 Comparison of A.S.T.M. grain size numbers with the corresponding fracture rating for a range of austenitic grain sizes (Ref. 28).

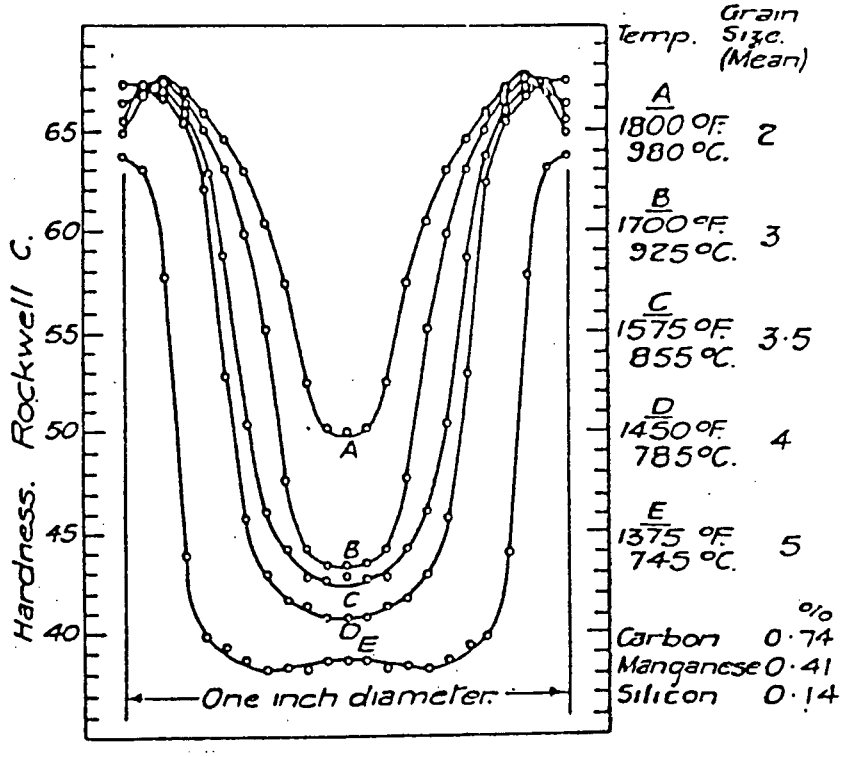

Fig. 2.2 Differences in hardenability caused by changes in austenite grain size in a 0.75% C steel (Ref. 29).

suggests that the real factor at work in controlling hardenability was the pearlite nucleation rate, i.e. the relative number of nuclei appearing per unit time, per unit volume of austenite. In describing the effect of nucleation rate Bain states, "It is comparable to a great number of equally skilled painters scattered over a wall as compared with only a few. The wall is painted sooner by many workmen than by a few."

Metallographic evidence confirmed that both the pearlite nucleation rate and the grain size affected the austenite to pearlite transformation rate, and that in a vast majority of steels, pearlite nuclei were located at the grain boundaries of the austenite. Thus the smaller the grains, the greater was the grain boundary area; the greater the grain boundary area per unit volume, the more numerous the nuclei.

Based on the available isothermal data (TTT diagrams, sometimes called S-curves) and the known major characteristics of the austenite decomposition reaction, Bain and Davenport made the first attempt at explaining the shape of the S-curve and effect of austenite grain size.

The austenite decomposition curve, being a rate curve,

was first compared to rate curves obtained for chemical reactions that occur in gases and liquids. The major difference between two sets of curves was noted at the beginning and end of the transformation plots (Fig. 2.3). Whereas a first order chemical reaction curve started with a maximum velocity, the S-curve did not. In addition, on approaching the end of the transformation curve, the chemical reaction curve approached the 100% transformed line asymptotically, whereas the S-curve appeared to finish in a finite time.

The discrepancies were readily explainable in terms of the nature of the two reactions. The first order chemical reaction rate was determined by assuming the probability of formation of activated molecules had an energy redistribution arising from favourable collision throughout the system; typical of a homogeneous reaction process, whereas the decomposition of austenite is determined by a nucleation and growth process, occurring at interfaces, i.e.; a heterogeneous reaction process.[30]

Since metallographic evidence established that for pearlite formation, the reaction was nucleation and growth controlled, Mehl pointed out the need to derive a

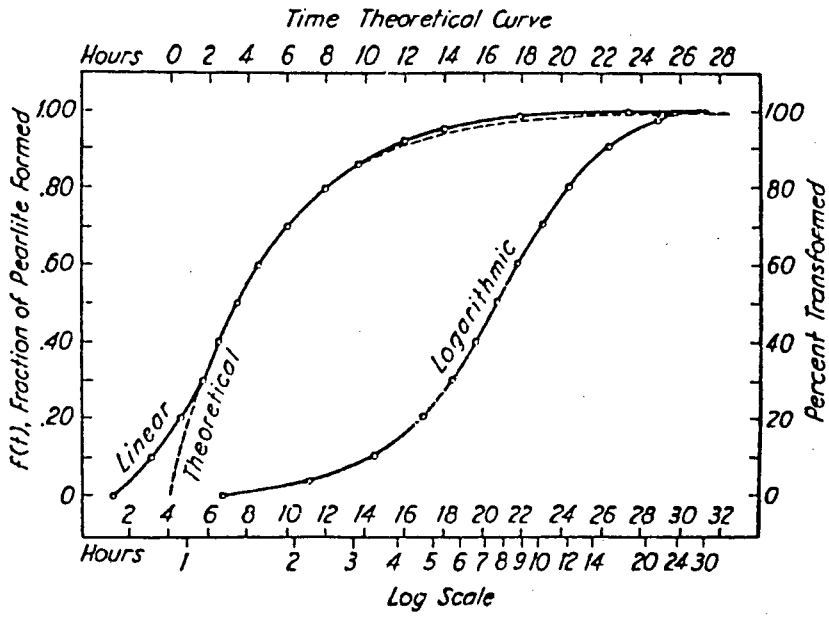

Fig. 2.3 Comparison of the austenite decomposition curve with that of a first order chemical reaction (Ref. 30).

quantitative expression in terms of the real physical parameters, the nucleation rate and the growth rate.[31] Thus the familiar Johnson and Mehl equation which characterizes the reaction rate in terms of nucleation and growth processes emerged. In deriving this kinetic equation for the transformation Johnson and Mehl made the following assumptions:

1. The reaction proceeds by nucleation and growth.
2. The rate of nucleation, N_V, expressed in number of nuclei per unit of time per unit of volume, and the rate of radial growth, G, expressed in units of length per unit of time are both constant throughout the reaction.
3. Nucleation is random, without regard for matrix structure.
4. The reaction products form as spheres except when impingement occurs during growth.

They derived an expression for the extent of reaction versus time in terms of N_V and G using the following approach; the rate of growth of a sphere nucleated at some arbitrary time is calculated; the rate of growth of an actual nodule of pearlite - a sphere that has suffered impingement and thus is no longer spherical - is a fraction of the rate of growth of the sphere; this fraction

is equal to the fraction of untransformed matrix. This determines the rate of growth of one nodule, which when multiplied by the number of nodules nucleated at the same time, gives the rate of growth of all nodules nucleated at this arbitrary time; integrating this expression gives an equation for the volume transformed as a function of time;

$$\int_{t=o}^{t=t} N_v \frac{4}{3}\pi R^3 dt \qquad \ldots(2.1)$$

where for the austenite to pearlite reaction, R is the radius of the pearlite nodule and

$$R = Gt \qquad \ldots(2.2)$$

where G is the growth rate of the pearlite sphere.

This equation will give what was later termed by Avrami,[18] the extended volume, and includes that volume which arises from impingement of nodules. Both Johnson and Mehl and later Avrami calculated the true volume fraction in the following way;

$$V_{true} = 1-\exp(-V_{ex}) \qquad \ldots(2.3)$$

where V_{ex} is the extended volume as determined by the integral given above.

Hence the Johnson and Mehl equation becomes;

$$X = 1-\exp(-\frac{\pi}{3}N_V G^3 t^4) \qquad \ldots(2.4)$$

This equation as stated previously, defines fraction transformed versus time for random nucleation. To characterize the pearlite reaction Johnson and Mehl[19] had to make the following additional assumptions for grain boundary nucleation;

1. Nucleation occurs exclusively at grain boundaries.
2. The matrix is composed of spherical grains of equal size.
3. The nuclei grow only into the grain in which they originate and do not cross grain boundaries.
4. The rate of transformation is retarded by impingement of growing nodules and growth to the adjacent grain boundaries.

Including these additional assumptions enables Johnson and Mehl[19] to quantitatively determine the effect of grain size on the shape and position of the isothermal transformation curve of the pearlite reaction (Fig. 2.4). The increased grain size produces fewer grain boundary nucleation sites per unit volume and requires longer

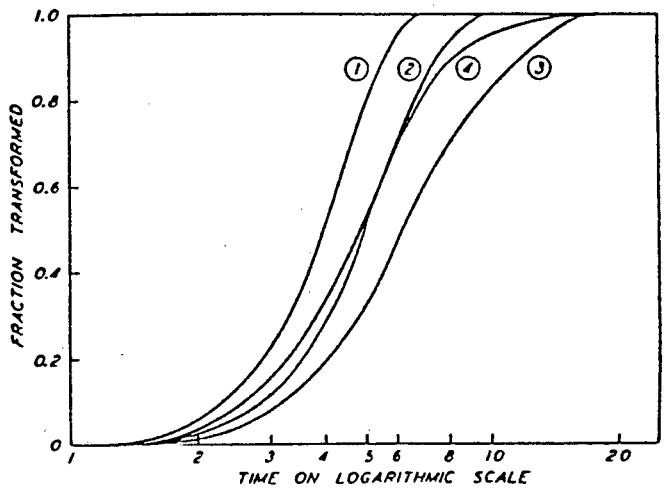

Fig. 2.4 Effect of grain size on the reaction curve (Ref.30).

growth times for the nodules to traverse the austenite grain, i.e. increasing time for completion of the reaction.

This primarily geometrical problem of characterizing a transformation process which includes both nucleation and growth was given a general treatment by Avrami. Avrami also makes the assumption that nucleation occurs only at certain preferred sites which are gradually exhausted. For a three-dimensional nucleation and growth process, he developed the more general relationship between fraction transformed, X, and isothermal reaction time, t:

$$X = 1-\exp(-bt^n) \qquad \ldots(2.5)$$

where $3 \leq n \leq 4$

and b is a constant.

Christian[32] in his analysis of the Avrami equation, suggests that the general expression for the volume transformed remains valid for two-dimensional and one-dimensional growth with $2 \leq n \leq 3$ respectively.

The Avrami equation varies in the same way with different grain size as does the Johnson and Mehl equation; any changes in the volumetric nucleation rate, N_V, will result in a variation of the empirical constant 'b' in the Avrami equation.

One of the important assumptions made by Johnson and Mehl was that nodules of the reaction product would grow only into the grain in which they nucleated. Rothenau and Boas[33] in their exhaustive work with the electron emission microscope, showed that the reverse of this was true for the pearlite reaction in eutectoid plain carbon steels. They observed that pearlite nodules readily cross austenite grain boundaries.

Cahn also attempted to calculate an isothermal reaction rate but excluded the effects of grain boundary growth restraints. Using Clemm and Fisher's analysis of the energetics of particular sites,[34] he included the possibility of nuclei being localized at grain surfaces, grain edges or grain corners.[20,35] Assuming for a grain shape, that of a space-filling tetrakaidecahedron (Fig. 2.5) and determining the numbers of corners, edges and surfaces in terms of the grain diameter, Cahn derived a transformation rate equation assuming that the grain boundaries offer no resistance to a growing nodule. Cahn, analysing the nucleation and growth kinetics measurements of several workers, such as Parcel and Mehl,[65] Lyman and Triano[36] and Hull, Colton and Mehl,[37] came to the conclusion that in most steels, pearlite nucleation was fast enough to cause early site saturation (this concept is to be examined in more

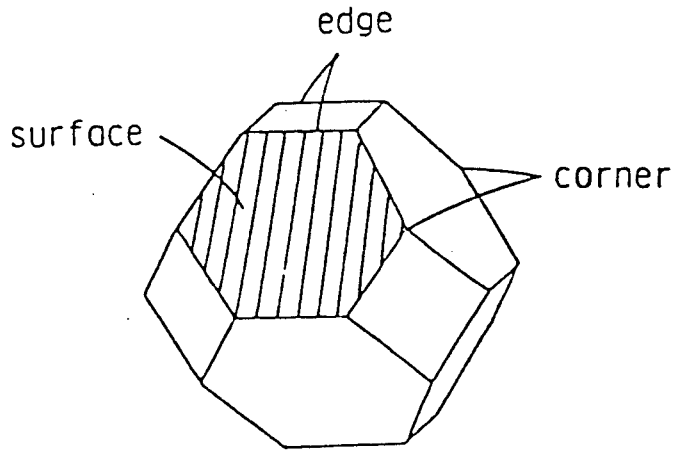

Fig. 2.5 Schematic diagram of the space filling tetrakaidecahedra.

detail in the 3rd chapter) even at fairly high temperatures which resulted in the nucleation event being unimportant to the transformation. The reaction "finish time" was related to the growth rate, G, and the grain diameter, d,

$$t_f \simeq \frac{0.5\ d}{G} \qquad \ldots(2.6)$$

Hence, increasing or decreasing the grain size would have a direct effect on the duration of the reaction.

Cahn however, did derive an expression for transformation at very high termperatures where low nucleation rates predominate and where site saturation may not occur. In such a case a Johnson-Mehl type expression in which the volumetric nucleation rate,

$$N_v = k\ t^{n_1} \qquad \ldots(2.7)$$

k, n_1 : constants

t : reaction time

was derived by Cahn.[20]

Using Cahn's analysis and the dependence of reaction and nucleation rates on the grain size, Tamura et al.,[40] developed a relationship which incorporated into Avrami's empirical rate equation the austenite grain size, d:

$$X = 1-\exp[-b\frac{t^{n'}}{d^m}] \qquad \ldots(2.8)$$

It is important to note that the 'b' contained in equation 2.8 is not the same as that contained in the Avrami equation (Equation 2.5) due to the introduction of the grain size factor.

From their studies of pearlite and bainite transformations, Tamura et al.[39,40] suggested that the exponent 'm' signifies the type of site active in the nucleation process as shown in Table 2.1. It is one objective of this project to test their analysis, to determine the exponents n, and m for a eutectoid plain carbon steel and to investigate by means of metallographic observation the significance attached to 'm'.

2.1.2 Grain Size Versus Thermal History

The austenite grain size of any steel is a result of the prior thermal history and factors such as the composition, peak temperature and duration of heat treatment, etc. It is therefore important to establish a relationship between prior thermal history and grain size, not only for industrial cooling processes but also for predicting heat affected zone microstructures in weld materials. It is therefore necessary to characterize the resulting grain size of a material in terms of the peak temperature and holding time at peak temperature.

TABLE 2.1 The Value of 'm' for Different Nucleation Sites

Nucleation Site	Surface	Edge	Corner
m	1	2	3

The uniform coarsening of the grains in a stress free material held at an elevated temperature is known as grain growth. One can experimentally follow the growth of a single grain on a polished surface, in situ on a heated stage of a microscope. However, the resulting growth is inhibited by the free surface and so the phenomena may not be characteristic of that of bulk grain growth.

Carpenter and Elam,[41] investigated grain growth in a 1.5% antimony, tin alloy with the following results being noted;

1. Growth occurs by grain boundary migration and not by coalescence of neighbouring grains.
2. Boundary migration is discontinuous; the rate of migration of a boundary is not constant in subsequent heating periods and the direction of migration may change.
3. A given grain may grow into a neighbour on one side and be simultaneously consumed by a neighbour on another side.
4. The consumption of a grain by its neighbours is frequently more rapid just as the grain is about to disappear.

Using the same material, Sutoki[42] added;

5. A curved grain boundary usually migrates towards its centre of curvature.

In addition, Harker and Parker[43] observed:

6. Where boundaries in a single phase metal meet at angles different from 120 degrees, the grain included by the more acute angle will be consumed.

Different mechanisms and different sources for the driving force of grain growth have been proposed. Extensive reviews have been published by Burke and Turnbull,[44] and Nielsen.[45] It is generally recognized that in a completely recrystallized material, the driving force for grain growth is the reduction of the surface energy of the grain boundaries. As the number of grains per unit volume decreases and their size increases, the grain boundary area per unit volume becomes less, and the overall surface energy is lowered.

Many authors have pointed out the similarities between growth of cells in a froth of soap and grain growth in metals that are recrystallized. For the simple model of cells in a soap foam, using the surface energy of the boundaries as a driving force, a simple formulation of grain growth kinetics can be established;[8]

$$D^2 - D_o^2 = K't \qquad \ldots(2.9)$$

where

D_o = cell size at t = o

D = final cell size

K' = constant of proportionality

t = time

Although it has been shown that the kinetics of growth of cells in a soap froth agrees well with this expression,[46] experimental studies of metallic grain growth have failed to confirm an extension of this equation based on the activation energy for grain boundary migration,

$$D^2 - D_o^2 = A \exp(-\frac{Q}{R'T})t \qquad \ldots(2.10)$$

where

Q : empirical heat of activation for the process

R' : gas constant

T : degrees Kelvin

A : constant

Instead, most of the isothermal grain growth data in metallic systems corresponds to an empirical equation of the form;

$$D^{n''} - D_0^{n''} = K't \qquad \ldots(2.11)$$

where K' is a material dependent proportionality constant.

Hannerz and Kazinczy [47] studied grain growth in austenite in steels with varying alloy contents, and found that carbides and nitrides of Nb, V, Ti drastically reduced the growth rate of the austenite grains and this corresponded to a value of the exponent $n'' \cong 20$, in grain refined steels. They also determined $n'' \cong 5,6$ for as-cast coarse grained steels.

Hu and Roth,[48] reported a variety of n'' values between 2 and 4. Alberry, Chew and Jones[49] found n'' to be 2.73 for their 0.5 Cr, Mo-V steel and Ikawa et al.[50] determined $n'' \cong 4$ for a commercial purity Ni steel. Most of these studies were undertaken to determine the prior austenite grain size in the heat affected zones of welds.

In this thesis, this same method has been used to determine the grain growth kinetics in an eutectoid plain carbon steel and hence can be used to establish the relationship between peak temperature, heating time and final grain size for eutectoid steel.

2.2 EXPERIMENTAL PROCEDURES

Experiments were performed to investigate the isothermal reaction kinetics for different grain sizes and for different

reaction temperatures.

2.2.1 Dilatometric Isothermal Kinetics Measurements

For an accurate control of temperature and a precise measurement of transformation kinetics, the apparatus shown on Fig. 2.6 was used for all isothermal and continuous cooling tests. The progress of the austenite decomposition was measured continuously with a dilatometer consisting of a water cooled, quartz tipped extensometer. Diametral rather than axial dimensional changes were monitored in the middle of the test specimen to prevent errors associated with axial temperature gradients.[76]

The specimen temperature was monitored and controlled using a chromel-alumel intrinsic thermocouple spot welded to the outside surface of the tubular specimen on the same diameter plane as that measured by the diametral dilatometer. A voltage feedback system was attached to the thermocouple and was used to preselect test temperatures. Signals from the extensometer and thermocouple were continuously recorded with a common time base. The overall dimensions of the tubular steel specimens used in this apparatus were; length = 100 mm, O.D.=8 mm and wall thickness = 0.8 mm. All samples were machined from a 1080, eutectoid carbon steel rod, having the composition shown in Table 2.2.

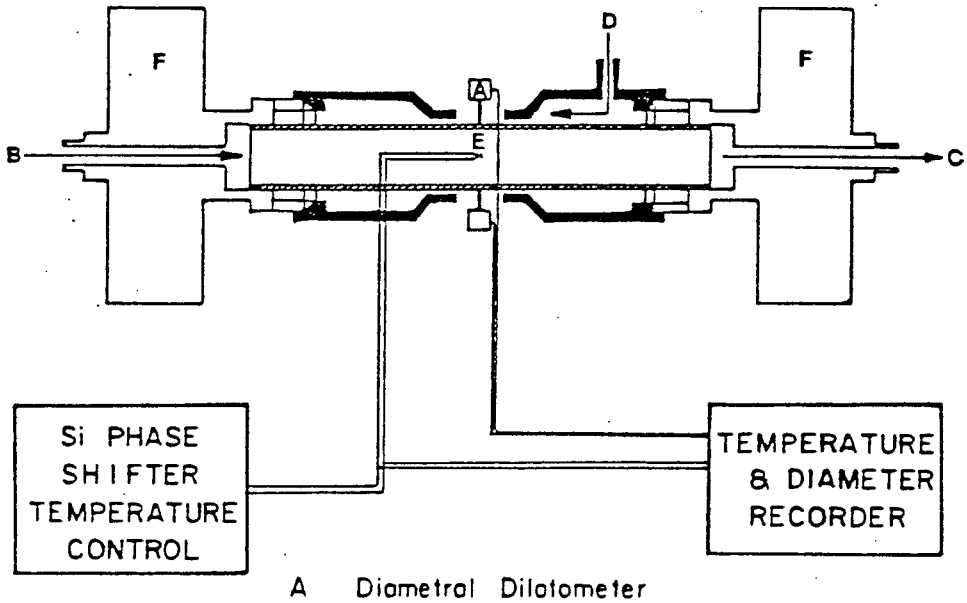

A Diametral Dilatometer
B Inlet for internal gas flow
C Outlet for internal gas flow
D Inlet for external gas flow
E Thermocouple on sample
F Support Structure

Fig. 2.6 Schematic drawing of the apparatus employed for measurement of transformation kinetics.

Table 2.2 COMPOSITION OF EUTECTOID PLAIN-CARBON STEEL (wt%)

C	Mn	Si	S	P	Al
0.79	0.91	0.49	0.029	0.018	0.084

Cu	Cr	Sn	Ni	Mo
0.049	0.062	0.003	0.014	0.002

The austenitising treatment, i.e. time and temperature were preselected and the resultant austenite grain size measured metallographically[51] on water quenched, partially transformed samples. Before selecting a specific austenitising condition, it was decided to investigate the effect of time at austenitising temperature. The austenite to pearlite kinetic results for 1, 5 and 15 minutes austenitising time at 840°C, demonstrated similar transformation kinetics for the 5 and 15 minute treatments and slightly faster kinetics for the 1 minute, as shown in Fig. 2.3. A 5 minutes austenitising treatment was chosen to minimize decarburization while ensuring a homogeneous austenite structure.

Although different austenitising temperatures were used to produce a range of austenite grain sizes, the test sample was always returned to 740°C prior to cooling to the transformation temperature to ensure identical cooling conditions in each test sample. The maximum available cooling rate of 108°C/sec combined with the approximate 1 second TTT nose at 600°C, restricted valid TTT tests to temperatures above 600°C. Two isothermal test temperatures were selected, 690°C to reflect high temperature nucleation and growth conditions and 640°C to depict low temperature pearlite nucleation and growth conditions.

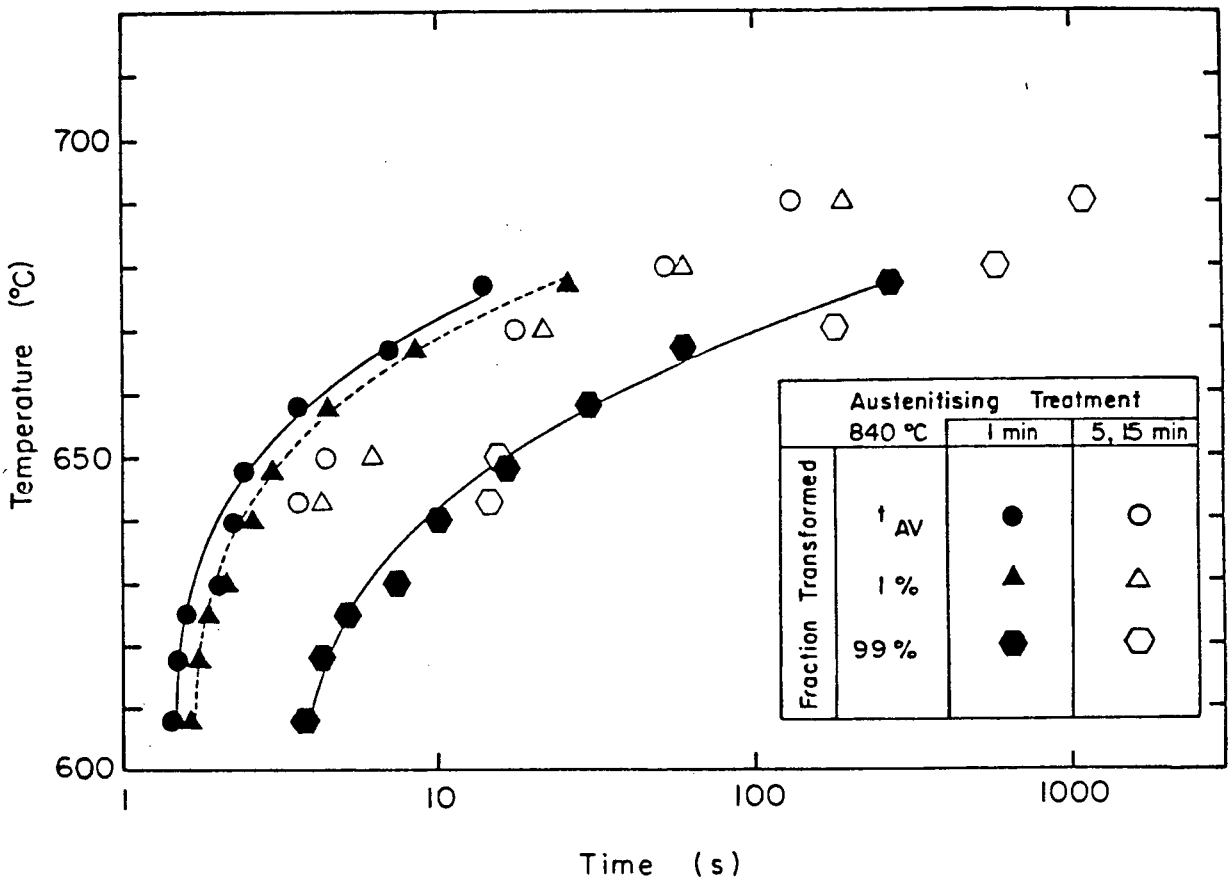

Fig. 2.7 Effect of austenitising time at 840°C on the austenite-to-pearlite transformation kinetics for an eutectoid plain-carbon steel.

2.2.2 Salt Pot Isothermal Kinetics Measurements

Traditional isothermal transformation tests were also performed to compare the measured metallographic transformation results with the dilatometric data. The traditional procedure of transferring relatively thin samples from one salt pot to another and quenching samples after increments of isothermal holding time provides a larger sample area for examination of nucleation and growth rates. This method is also much more suitable for nucleation and growth measurements due to the large number of specimens required.

The test samples, 10 mm diameter x 1-2 mm thickness were austenitised for 5 minutes at temperatures identical to dilatometric tests with the exception of the 1100°C austenitising condition. The grain size was determined metallographically from partially transformed, water quenched specimens.[51]

2.2.3 Salt Preparation

The lowest temperature selected for isothermal tests was to be 640°C. A salt having a melting point of approximately 600°C was required for a working temperature of 640°C. The available high temperature salt was a neutral salt (L.H. 1550) which contained 85% $BaCl_2$, 15% NaCl and had a melting point of approximately 640°C which

was not suitable. To lower the melting point, additions of KCl and NaCl were used. After several trials, the desired melting conditions were obtained using a salt of composition; 100 L.H. 1550, 15 NaCl, 40 KCl. The composition of the component chlorides was, 55% $BaCl_2$, 25% KCl, 20% NaCl. This salt had a melting point of approximately 590°C.

The temperature control for all salt pots was approximately $\mp$ 2°C and the transfer time from pot to pot was less than one second.

After heat treatment which involved austenitising for 5 minutes, transferring the sample to the 740°C salt for 1 minute, then transferring the specimen to the salt maintained at the desired isothermal test temperature, the specimen was quenched in water, cold mounted in bakelite, polished and etched using 2% Nital. The fraction of pearlite was measured directly using a Quantimet 720. The high contrast between the pearlite and martensite ensured that a valid area fraction of pearlite was measured for each field of view.

2.2.4 Specimen Inhomogeneity

Initial isothermal transformation tests conducted in the salt pots yielded the result shown in Fig. 2.8.

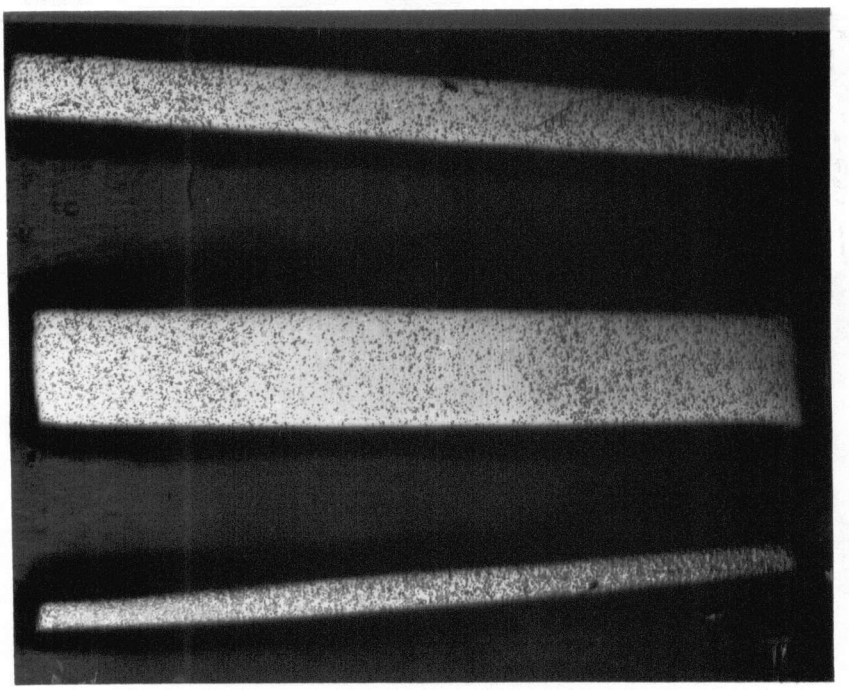

Fig. 2.8 Different levels of transformation on the edges and the middles of salt pot specimens. Mag. X 7.
The figure in the middle is the photograph of a disc specimen ground down to half its diameter. The middle of the specimen therefore, corresponds to the centerline of the wire rod.

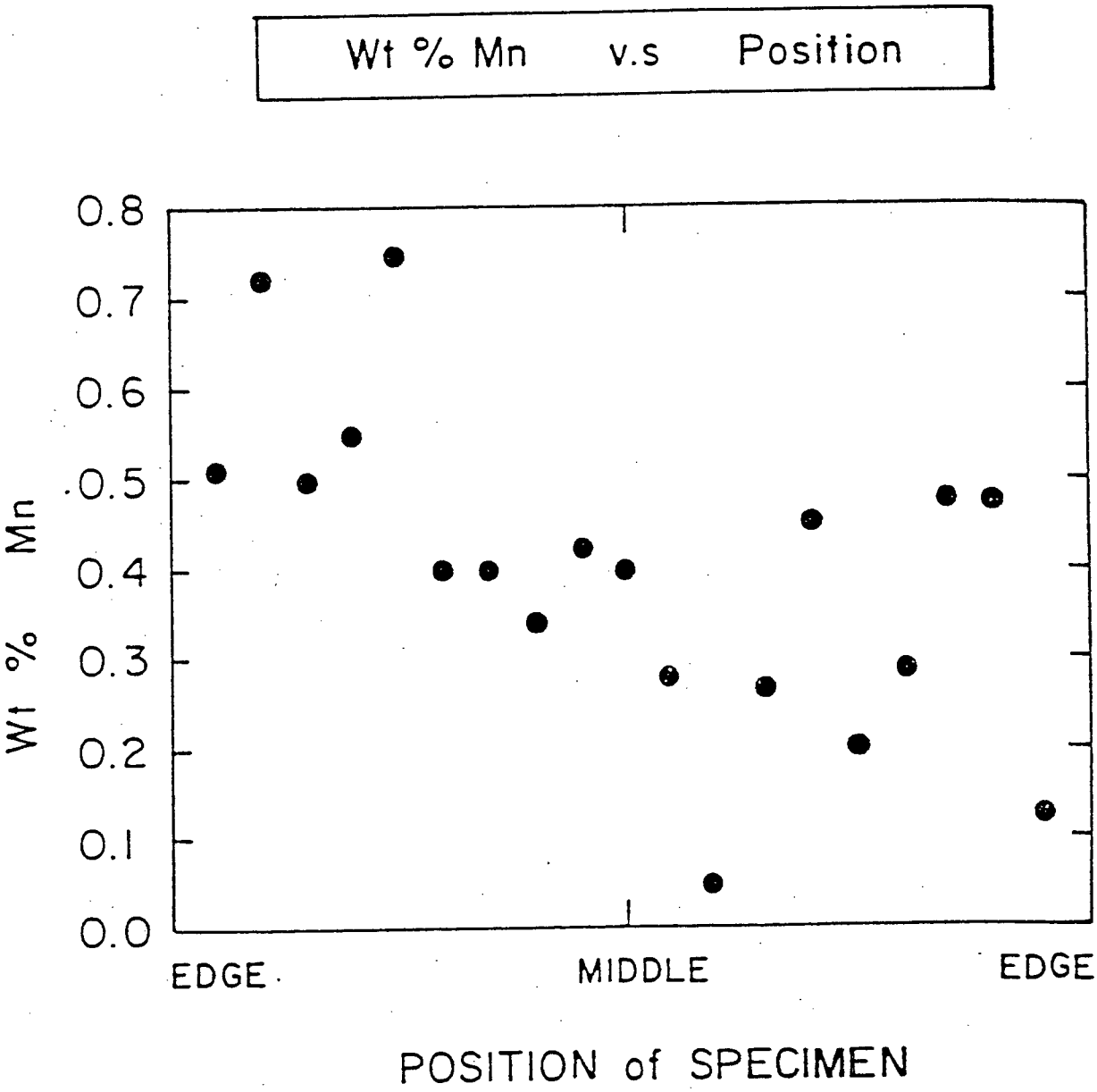

Fig. 2.9 Mn content versus position on the salt pot specimen.

N.B. It must be noted that the average Mn content as can be seen in Fig. 2.9, is lower than the Mn content on Table 2.2 that shows the composition of this steel.

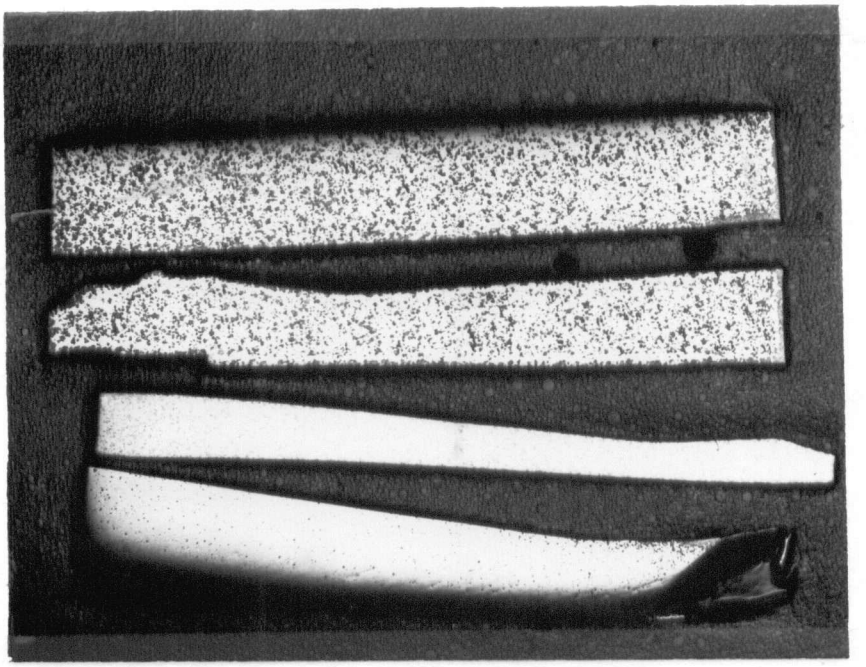

Fig. 2.10 Salt pot specimen demonstrating homogeneity after homogenising treatment. Mag. X 7.

Specimens shown correspond to the diametral cross-section of disc specimens.

The disc specimens demonstrated an enhanced transformation rate at the edges and a slower transformation rate at the center of the specimen. The center corresponds to the centerline of the rod used in the study. The variation in transformation kinetics was attributed to macrosegregation in the original steel rod. Although Mn was thought to be the segregating element, an electron probe examination of the Mn content did not confirm this suspicion (Fig. 2.9). A homogenising treatment of the specimen as recommended in the literature[62,63] was then performed. Specimens were sealed in quartz tubes under vacuum and kept at 1200°C for 15 hours. Tests performed after such a treatment did not show the previously noted inhomogeneity of pearlite transformation (Fig. 2.10). This homogenising treatment was applied to all specimens.

2.2.5 Decarburization

The extent of decarburization on the disc specimens resulting from the austenitising heat treatment in the neutral salts was also determined. Specimens cut from the 1080 rod were heat treated 5 minutes at 850°C, followed by 1 minute at 740°C, a total of 6 minutes to determine the resulting decarburization. The microstructure containing the decarburized layer was then photographed and the depth of decarburization was determined. Using

a maximum allowable decarburized layer of 10% of the specimen thickness, the austenitising at 850°C was found to be acceptable.

2.3 RESULTS AND DISCUSSION

2.3.1 Effect of Grain Size on Transformation Kinetics

The grain sizes obtained with the given austenitising conditions for both the dilatometric and salt pot tests are given in Table 2.3. The effect of grain size on isothermal transformation kinetics can be seen on Fig. 2.11. Also included on this figure is the kinetic data obtained from the salt pot, confirming that the nucleation and growth measurements from bulk specimens treated in the salt pot correspond to that obtained using the dilatometric data. That higher isothermal reaction temperatures decrease the pearlite reaction rate due to slower nucleation and growth kinetics can be seen in Fig. 2.11. The underlying reasons for the temperature dependence of nucleation and growth is well researched,[50,31,38,55] and can be summarized as follows:

The nucleation event is usually concerned with the overcoming of thermodynamical barriers before a new phase can grow with steadily decreasing free energy. The critical particle size beyond which particles become growth nuclei decreases with undercooling from the equilibrium temperature, i.e. the lower the isothermal transformation

TABLE 2.3 Austenite Grain Size

Austenitising Temperature °C	A.S.T.M. Grain Size
740	10.8
800	9.1
840	7.8
900	7.4
950	7.3
1100	3.0

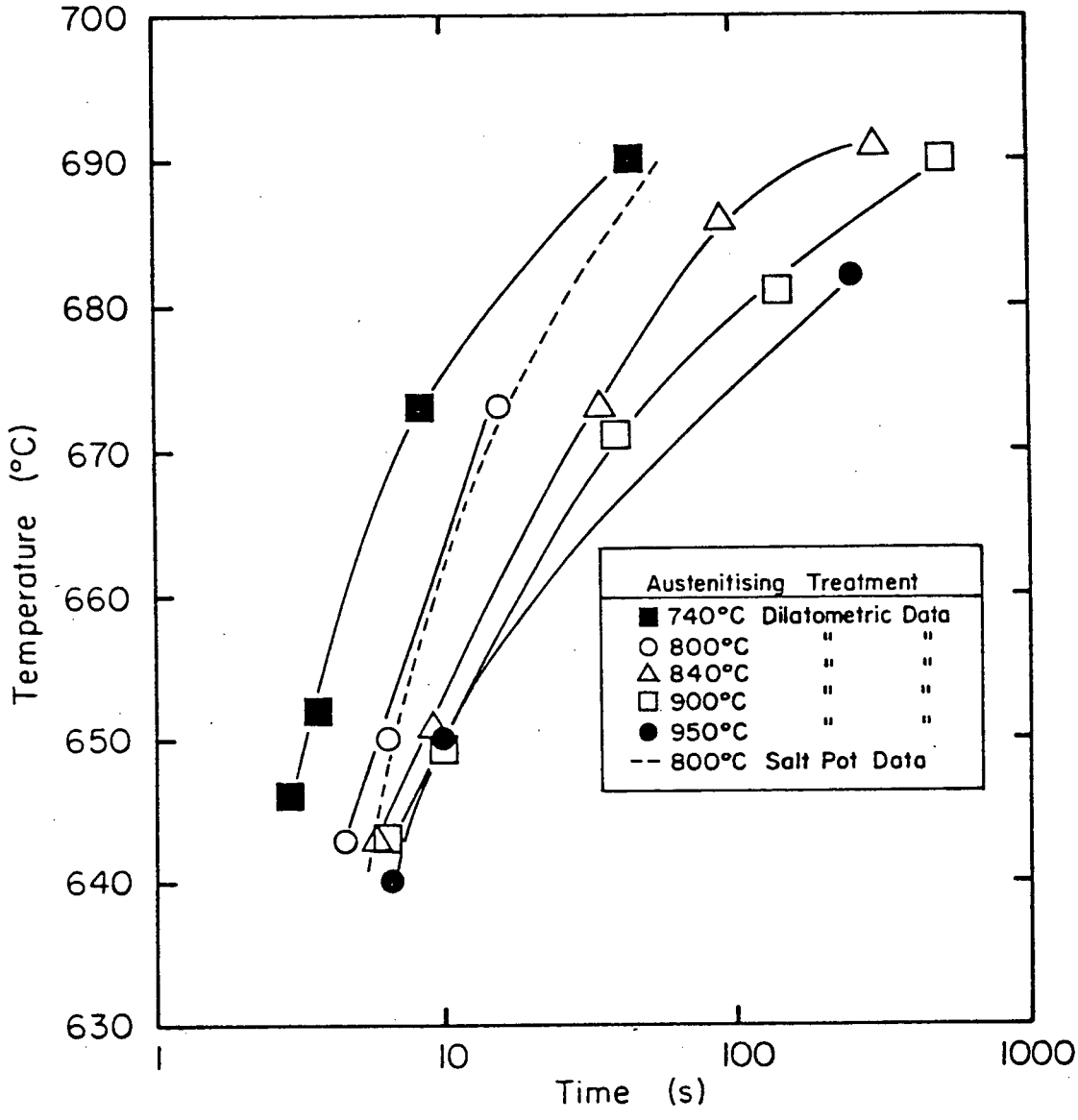

Fig. 2.11 Effect of austenite grain size on the isothermal transformation kinetics; the 10% pearlite transformation line has been shown for each grain size.

temperature, the higher the nucleation rate of pearlite.[61]

The temperature dependence of the growth rate is more complicated and is determined by the interlamellar spacing (the diffusion distance), the diffusion rate and the concentration difference.[8] As the temperature falls, the reduction in the diffusion rate is more than compensated by the decreasing pearlite spacing and increasing concentration gradient. The growth rate therefore increases rapidly to a maximum at a particular temperature, below which the diffusion rate becomes very small, and then decreases.

For the pearlite reaction at a specific isothermal transformation temperature, increasing grain size can be seen to increase the incubation time and to increase the time to complete the transformation. Since the growth rate is essentially structure insensitive and a function only of transformation temperature, the difference in transformation rate with increasing grain size is accountable only by a drop in the nucleation rate, as confirmed by the measurement of this quantity.

Work done earlier on this material has shown that the pearlite reaction can be well characterized by the Avrami equation[73] (Equation 2.5). The kinetic data for each isothermal test was plotted in terms of $\ln \ln \frac{1}{1-x}$ versus $\ln t$ (Fig. 2.12). The exact initiation time for the transformation

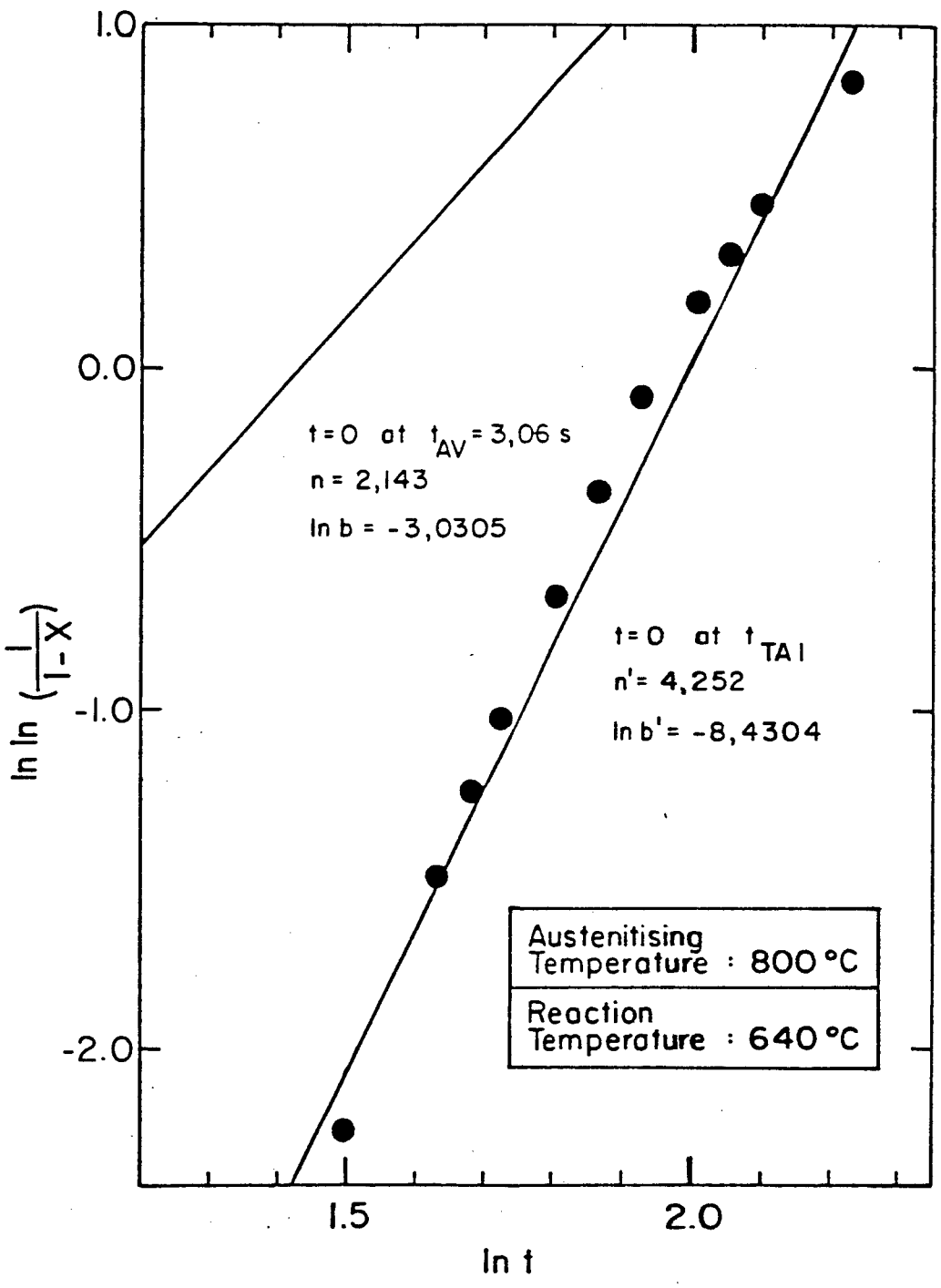

Fig. 2.12 The $\ln\ln \frac{1}{1-x}$ versus ln t graph for isothermal pearlite reaction at 640°C; austenitised at 800°C.

was difficult to determine because the transformation start was estimated by first fitting a least squares line to a minimum of eight points on the ln ln $\frac{1}{1-x}$ versus lnt plot with t = o, based on an approximate start temperature. Then the transformation initiation time was increased by a small increment and again the least squares analysis was performed. This procedure was repeated until a best fit line was obtained for the data points. The resultant initiation time was termed 't_{avrami}'. The resulting 'n' and 'ln b' were determined on the basis of t_{av}. The extremely good fit obtained when t = o at t_{av} is used as the reaction initiation time i.e. excluding the incubation time, can be seen in Fig. 2.13 for a eutectoid plain-carbon steel.

Although the Avrami equation characterizes well the pearlite reaction at constant subcritical temperatures it does not include the grain size as a parameter. This was done by Tamura et al.[40] who incorporated a grain size parameter and studied the pearlite transformation in terms of a more generalized transformation equation (Equation 2.8).

Equation 2.8 can be re-written as;

$$n' \ln t = m \ln d + \ln \ln \frac{1}{1-x} - \ln k \qquad \ldots(2.12)$$

Thus by plotting n' ln t versus ln d the value of the grain size exponent 'm' can be determined.

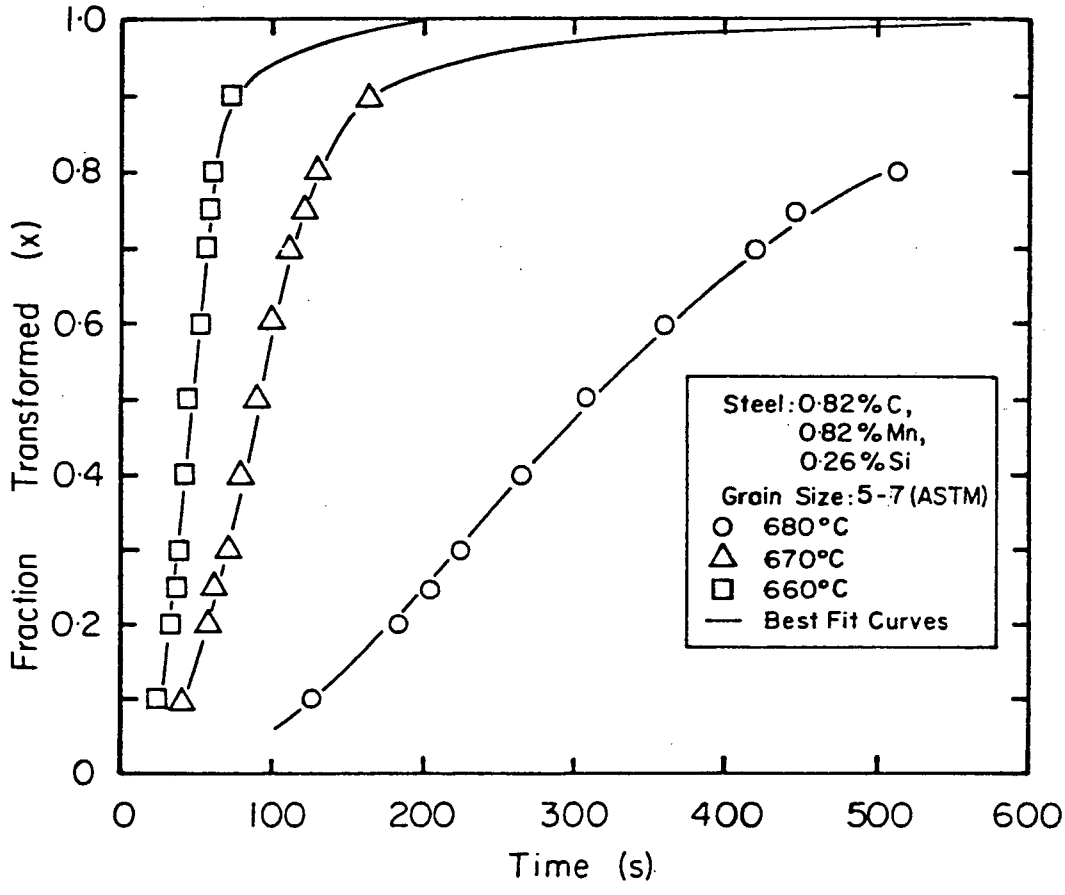

Fig. 2.13 Fit obtained when 't_{av}' is used for reaction initiation time for 0.82 C steel.

To determine whether 'm' is dependent on the fraction transformed, the data was also plotted as $n' \ln t_{0.25}$ versus $\ln d$; $n' \ln t_{0.5}$ versus $\ln d$ and $n' \ln t_{0.75}$ versus $\ln d$; it was found to be independent of fraction transformed (Table 2.4). The plot for 50% transformation is given in Fig. 2.14. A value of approximately 2.2 was determined.

A comparison of 'm' values determined by using two similar composition eutectoid plain-carbon steels with Tamura et al's 'm' values for the pearlite reaction can be seen on Table 2.5.

It must be noted however that Tamura et al. used times calculated from t = 0 at T_{A_1}, and found the value of m = 1.8 for the pearlite reaction. Fig. 2.14 is based on t = 0 at t_{av}, the start of measurable transformation. If the time was calculated based on t = 0 at T_{A1}, the value of 'm' obtained is approximately 3.0 and is higher than that obtained in the study by Tamura et al.

Tamura et al. attached significance to the value of this number as a probable indication of pearlite nucleation sites as summarized in Table 2.1. As will be seen later in the metallographic studies, corner and edge nucleation would seem to be dominant and probably corner is more important, consistent with m = 2.2.

TABLE 2.4 Dependence of the Grain Size Exponent 'm' on the Fraction Transformed of Pearlite.

Pearlite Transormation (%)	'm'
25	2.2
50	2.3
75	2.2

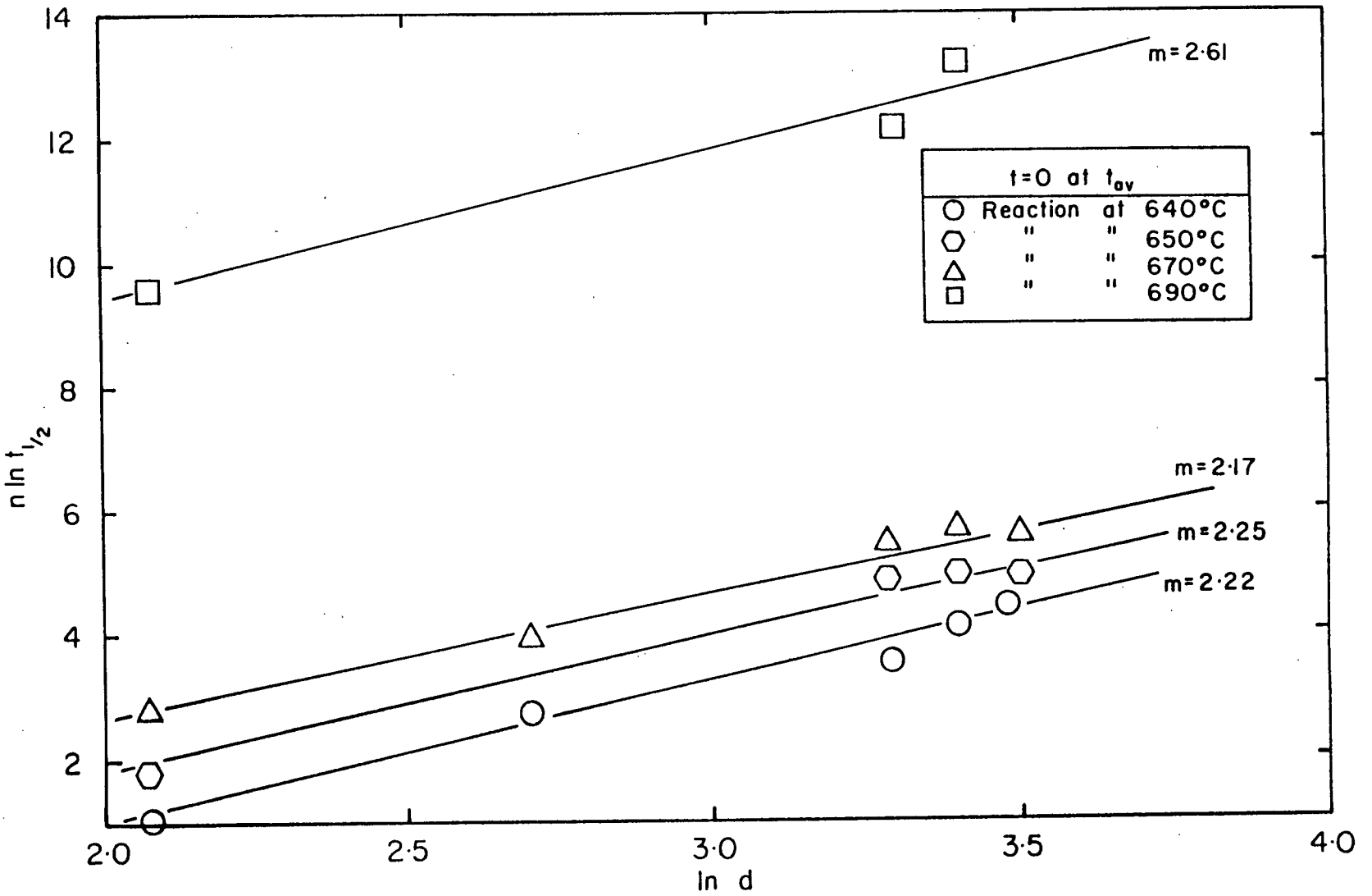

Fig. 2.14 The n ln $t_{1/2}$ versus ln d for t = 0 at t_{av} graph showing a slope 'm' equal to 2.3.

TABLE 2.5 Comparison of 'm' Values

Source		'm'
This work	1080 steel	2.2
	0.77 C steel	2.0
	Tamura et al. (Eutectoid plain carbon steel)	1.8

2.3.2 Grain Size Versus Thermal History

The determination of the grain size versus thermal history relationship developed by Alberry et al.,[49] was based on an examination of the prior austenite grain growth in heat affected zones of welds. After determining grain size for different holding times at constant peak temperature and using the relationship

$$D_1^{n''} - D_2^{n''} = K'(t_1 - t_2) \qquad \ldots(2.12)$$

where D_1 and D_2 are grain sizes obtained after holding at temperature for times t_1 and t_2 respectively, they determined "n" using a series of least squares plots, selected using a maximum correlation coefficient. They found $n'' = 2.73$.

The original relationship[47] i.e. Equation 2.11;

$$D^{n''} - D_o^{n''} = Kt$$

where

$$K = A \exp\left(-\frac{Q}{RT}\right), \qquad \ldots(2.13)$$

and D_o is the grain size at $t = 0$, can be also used, however.

Assuming that the time for the specimen to reach the peak temperature is negligible, i.e. grain size D_o at $t = 0$ is similar for all temperatures then,

$$D_{T_1}^{n''} - D_{T_2}^{n''} = A \exp(-Q/R(T_1-T_2))t \quad ...(2.14a)$$

$$D_{T_3}^{n''} - D_{T_4}^{n''} = A \exp(-Q/R(T_3-T_4))t \quad ...(2.14b)$$

Using the activation energy of austenite grain growth as Q = 460,000 J/mol/K, from Bastien et al.,[53] and grain diameter in mm and the appropriate time, t = 5 minutes, the equations can be solved numerically to determine the value of 'A' and 'n''; the result is:

$$n'' = 3.57$$

$$A = 2.98 \times 10^{12} \text{ min}^{3.57}/\text{s}$$

The specific grain growth equation therefore becomes;

$$D_t^{3.57} - \overset{*}{D}_o^{3.57} = 2.98 \times 10^{12}[\exp(\frac{-460,000 \mp 1000}{RT})]t \quad ..(2.15)$$

For this 1080 steel, compared with

$$D_t^{2.73} - D_o^{2.73} = 1.41 \times 10^{13}[\exp(\frac{-460,000 \mp 33,000}{RT})]t \quad ...(2.16)$$

determined by Alberry et al. for a 0.11 C alloy steel.

N.B. It must be noted that $\overset{*}{D}_0$ in equation 2.15 is different from D_0 in equation 2.16 because $\overset{*}{D}_0$ is not a function of peak temperature.

CHAPTER 3

NUCLEATION, GROWTH KINETICS AND THE ADDITIVITY PRINCIPLE

3.1 INTRODUCTION

The pearly constituent observed in 1864 by Sorby[75] and later named pearlite is probably the metal structure that has been studied in most detail. A great deal of confusion existed in the morphological terminology defining the eutectoid transformation products. Globular, rod-like degenerate, fine, coarse, bearded, massive, banded, reefy, blocky, sorbitic, troostitic pearlites and many other terms were often used. This situation gradually became more logical as the nature of the formation of pearlite was investigated and became better understood

The nucleation and growth character of pearlite was examined as early as 1905 by Arnold and McWilliam[54] and by Benedicks[55,56] and described clearly in the works of Bain and Davenport.[3]

3.1.1 Nucleation of Pearlite

A correct theory for the formation of pearlite was necessary if quantitative relationships for harden-

ability, in steels were to be determined. Theories for the formation of pearlite existed almost as soon as the constituent was observed under the microscope.

An excellent review of the theories for formation of pearlite is given by Hull and Mehl.[56] From experimental evidence accumulated up to the time of their review, they summarized the then current understanding of the genesis of pearlite as follows: "...Pearlite forms directly from austenite by a process of nucleation and growth and colonies of pearlite originate as a result of edgewise growth and sidewise nucleation and growth. Ferrite, cementite or both ferrite and cementite simultaneously may serve to nucleate pearlite."

The question of which constituent served as the active nucleus of pearlite remained a controversial one due to the somewhat contradictory available evidence.[56,57] However it was generally accepted, based on studies of orientation relationships with pro-eutectoid cementite, that cementite was the most probable active nucleus for pearlite.[30]

This generally accepted interpretation had to be modified in the light of new evidence provided by Hillert,[58] Hultgren and Ohlin.[74] Through some critical experiments, they

found that ferrite was an equal partner with cementite in nucleating pearlite and that the growth of colonies took place not by repeated sidewise nucleation and growth but by the branching of existing ferrite and/or cementite plates.

Hence during the random composition fluctuations that occur in the metastable body of austenite, there is a point, structurally and energetically, of no return. The main barrier, i.e. the creation of surface energy acts as a restraining force for nucleation and is inversely proportional to the size of the particle. Therefore there exists a critical size beyond which the thermodynamic driving force favouring the formation of a new phase, dominates. Based on his observations, Hillert envisioned that the ferrite and cementite of pearlite were initially competing with each other and only gradually was cooperation developed. Depending on the level of cooperation, the degree of lamellarity was determined. Hillert argued that all the observed forms of pearlite, lamellar through spheroidal, could be explained by this concept of "level of cooperation".

In such a situation, the nucleation rate can be interpreted as the rate with which these 'embryo' of either ferrite or cementite fluctuate to critical size, beyond which they become stable.

Pearlite nucleation uses essentially pre-existing surfaces such as grain corners, grain edges and grain boundaries, due to the contribution to the driving force of such surfaces, and is therefore heterogeneous.

Johnson and Mehl[19] analyzed the effect of changing nucleation rate using the J.M equation based on the assumptions summarized in the previous chapter. They defined a shape factor 'λ' where:

$$\lambda = \frac{a^3 N}{G} \qquad \ldots(3.1)$$

By selecting different values for this constant by keeping 'a', the grain size and G, the growth rate, constant they determined the effect of different values of the nucleation rate, N, on the isothermal reaction. The result of this can be seen in Fig. 3.1 where the shape factor varies between 1 and ∞, this representing an extreme variation in N. The interesting result of this analysis is that the time of the reaction is changed only by 60%, although N changes from 1 to ∞. The effect of low and high nucleation rates on the rate of the pearlite reaction when the growth rate and grain size are constant can be demonstrated schematically as shown in Fig. 3.2.

To test their equations, real nucleation rates were

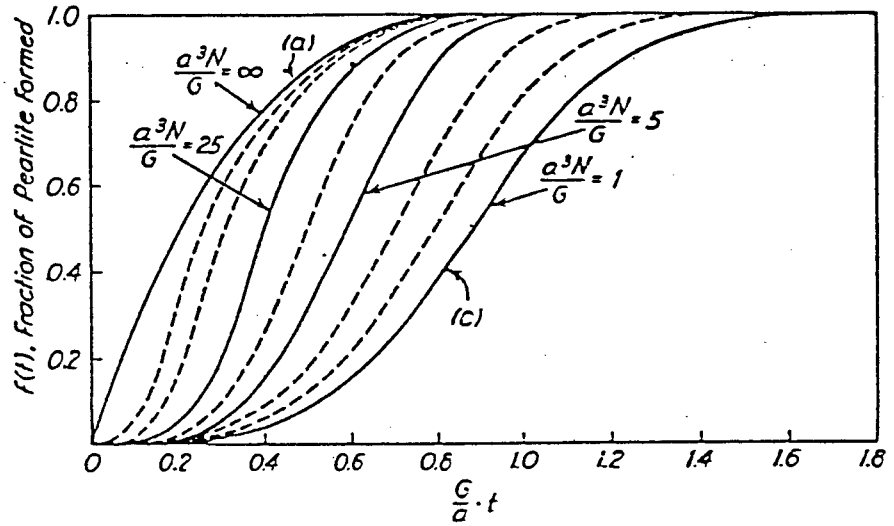

Fig. 3.1 Effect of the nucleation rate on the isothermal reaction curve of pearlite (Ref. 30).

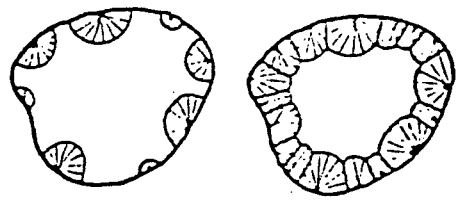

Fig. 3.2 Schematic representation of the effect of varying rates of nucleation on the rate of reaction with grain size and growth rate constant (Ref. 30).

needed; in fact measurements of nucleation rate for the austenite-to-pearlite reaction were made before Johnson and Mehl formulated their equation.

The inherent difficulty in trying to observe the initiation of a transformation is that, invariably the nucleation event occurs on too localized a scale in both space and time to be detected with available techniques. Hence, there is little hope of making direct measurements on the nuclei as they are being created or to ascertain the exact nature of the process. We can at best examine the details of nucleation using models whose predicted behaviour seems to agree well with the observed rate of nucleation and its dependence on known parameters.

The earliest nucleation measurements are reported by Mirkin and Blanter,[59] and Scheil and Lange-Weise,[60] and later a more systematic investigation by Hull, Colton and Mehl.[37] There are two accepted methods for measuring nucleation rate.

1. Determining the nucleation rate by metallographically observing the number of pearlite nodules per unit volume in a series of specimens reacted for different times at one isothermal reaction temperature. The nucleation rate is the time derivative of the number

of nodules. The assumption in this approach is that the nodules are of spherical shape. Scheil and Lange-Weise[60] using this method, measured the rate at which new nodules reached a measurable size in the specimen, i.e. measured the nucleation rate.

2. Determining the nucleation rate by measuring the size distribution of pearlite nodules in a single sample. In addition to assuming spherical nodules, this method also assumes that G is a constant with time and is uniform from nodule to nodule.

In their review of the various methods of measuring the nucleation rate Cahn and Hagel[61] stated that the assumptions necessary for the simple specimen method to work are not valid and that the multi specimen method is the best suited for examining the pearlite nucleation rate.

The nucleation rate is known to be influenced by the austenitising time and temperature, the grain size, and the homogeneity of the austenite. Early nucleation measurements suffer from the lack of specification of information and therefore are difficult to interpret (Table 3.1 and Fig. 3.3).

As can be seen in Table 3.1 and Fig. 3.3, the nucleation rate is usually reported as the number of nodules per

TABLE 3.1 Approximation of Nucleation in Eutectoid Steel, Grain Size 4-5.[60]

Temperature of Formation °C	No. of Nuclei per cm^3 per sec	No. of Nuclei per cm^2 of grain surface area per sec.
717	$5x10^2$	1.6
704	$7x10^4$	$2.2x10^2$
662	$2x10^6$	$6.3x10^3$
620	$6x10^7$	$1.9x10^5$
580	$3x10^8$	$9.4x10^6$

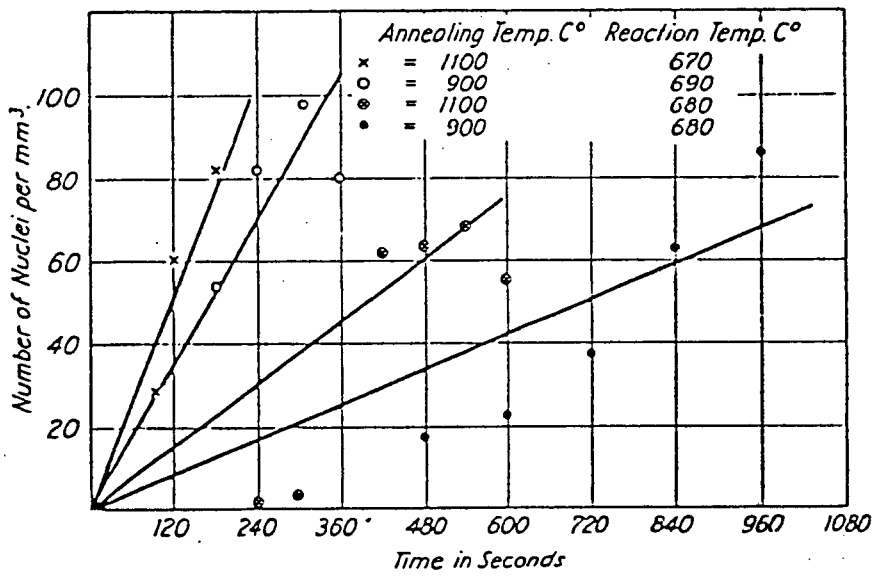

Fig. 3.3 Number of nuclei per unit volume versus Reaction Time for different grain sizes (Ref. 60).

$mm^3.s$ and sometimes as the number of nodules per $mm^2.s$. The main variables affecting the nucleation rate per unit volume can be seen to be grain size and isothermal reaction temperature. The lower the reaction temperature, the larger the driving force for nucleation and the smaller the grains, the more sites available for nucleation at grain corners, edges and surfaces. One shortcoming of the metallographic determination of the nucleation rate is that it can be carried out only until approximately 20% of the sample is transformed, after which impingement of the pearlite nodules makes this method inaccurate.

Recently, measurements of the nucleation rate on a number of steels were carried out by Brown and Ridley.[62,63] They determined the nucleation rates by a number of methods, all employing data from the inverse cumulative distribution curve (Fig. 3.4). Their method (1) uses the d versus t plot (Fig. 3.5) constructed by drawing horizontals to the inverse cumulative distribution curve (Fig. 3.4). By extrapolating graphs of d versus t for different ΣN_V (total number of nodules/unit volume) to zero, the positive intercepts with the time axis gives the time at which there is a corresponding ΣN_V value at d = o. The second method, (2) uses data generated by constructing verticals on the inverse cumulative distribution curve (Fig. 3.6). Finally, the Johnson-Mehl equation (Equation 2.4) is used to determine

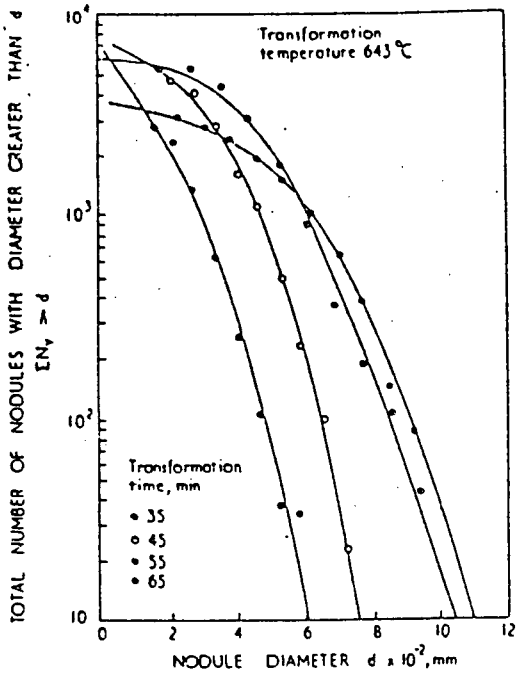

Fig. 3.4 Typical Inverted Cumulative Distribution graph (Ref.62).

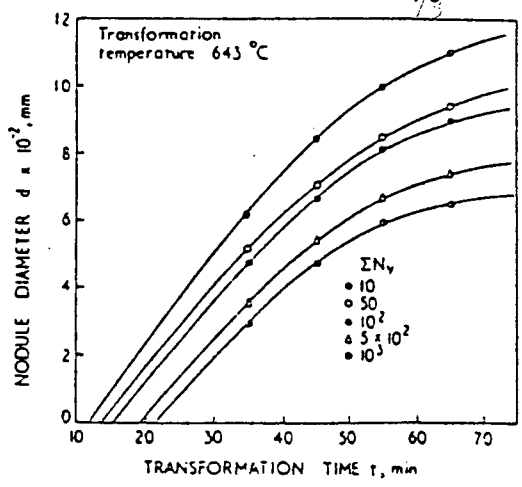

Fig. 3.5 Nodule Diameter (d) versus Transformation Time (t) (Ref.62)

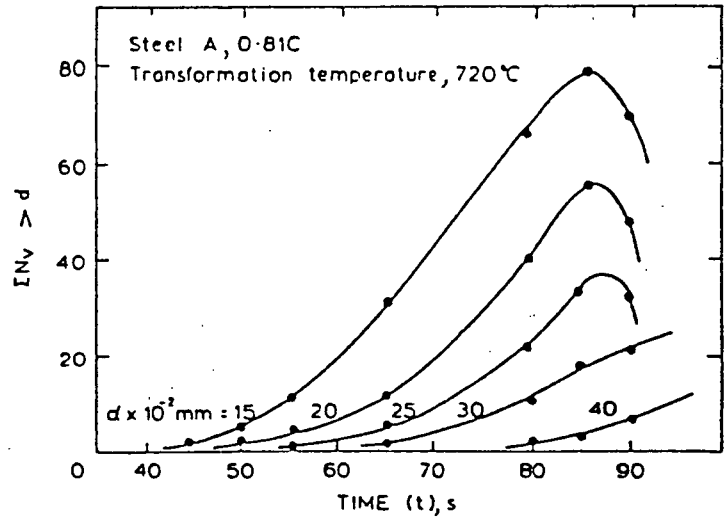

Fig. 3.6 Number of nodules (ΣN) per unit volume versus Reaction Time (Ref. 62).

nucleation rates. The results of all three procedures can be seen on Table 3.2 and demonstrate good agreement. Increasing undercooling can be seen to increase the nucleation rate. Also the nucleation rate seems to exhibit a time dependence at isothermal transformation temperature (Fig. 3.6).

3.1.2 Growth of Pearlite

Any theory to explain the growth of pearlite structures had to take into account: 1) the lamellar structure of the cementite-ferrite aggregate and the dependence of the carbide spacing on the transformation temperature; 2) the magnitude of the growth rate of pearlite colonies and the increase in growth rate at lower temperatures; and 3) the inhibition of growth with alloy additions.

The kinetics of pearlite growth has been examined both theoretically and experimentally by many workers and significant calculations have been carried out by Scheil,[68] Brandt,[69], Zener[70] and Hillert.[71] Apart from its technological importance, the uniformity and reproducability of the lamellar structure has been an area of interest.

The main factors influencing the pearlite growth rate can be demonstrated by using the approximate growth equation that was derived by Mehl and Hagel[5] based on diffusion

TABLE 3.2 Comparison of Nucleation Rates Determined by Using 3 Different Methods.[62,63]

Temperature °C	Nucleation Rates (nuclei, mm^{-3}, s^{-1})		
	Method 1	Method 2	Johnson-Mehl Equation
720	2.7×10^{-1}	9.4×10^{-2}	-2
712	4.2×10^{-1}	5.0×10^{-1}	5.0×10^{-2}
702	5.0	1.0	1.8×10^{-1}
685	33	18	2.8
667	110	20	9

geometry, diffusion of carbon and concentration gradients across the pearlite interface.

At any given temperature,

$$G \alpha \frac{D_c \Delta C}{S_p} \qquad \ldots(3.2)$$

where S_p is the interlamellar spacing of pearlite, ΔC is the concentration gradient and D_c is the diffusivity of carbon in austenite. This equation does not agree very well with experimental data but produces the same shape as experimental data and therefore makes possible certain deductions. The growth rate as can be seen from Equation 3.2 is not dependent on grain size or any other structural factor. Since all of the quantities on the right-hand side of Equation 3.2 are temperature dependent, clearly one would expect the growth rate of pearlite to be temperature dependent as well. With decreasing temperature the gradient term ΔC increases and D_c and S_p decreases. But D_c decreases relatively rapidly and tends to dominate the growth.

The usual way of measuring the growth rate of pearlite has been to metallographically measure the largest nodules on specimens reacted for a series of times at constant temperature. The time rate of change of the nodule size

is taken as the growth rate. This method can only measure growth until impingement occurs, which is usually at approximately 20% transformation. Growth rates measured by Scheil and Lange-Weise[60] (Fig. 3.7), Hull and Mehl[56] (Fig. 3.8) and Hull, Colton and Mehl[37] (Fig. 3.9) all demonstrate a constant growth rate at an isothermal transformation temperature.

Growth rate can also be determined indirectly from inverse cumulative distribution curves (Fig. 3.4). From the same graph of d versus t (Fig. 3.5) drawn by constructing horizontals to the inverse cumulative distribution curve, growth rates can also be obtained by determining the time derivative of these plots. Growth rates determined in this way (1), again compare well with growth rates determined in the traditional maximum nodule size method (2), as can be seen in Table 3.3. However an apparent paradox exists in the graphical determination such that only the growth rate of nodules of constant size can be determined.

The effect of growth rate on the isothermal transformation can be seen by examining the Johnson-Mehl curves. The growth rate will influence both the shape factor (Equation 3.1) and the time scale factor, Z where

$$Z = \frac{G}{a} \cdot t \qquad \ldots(3.3)$$

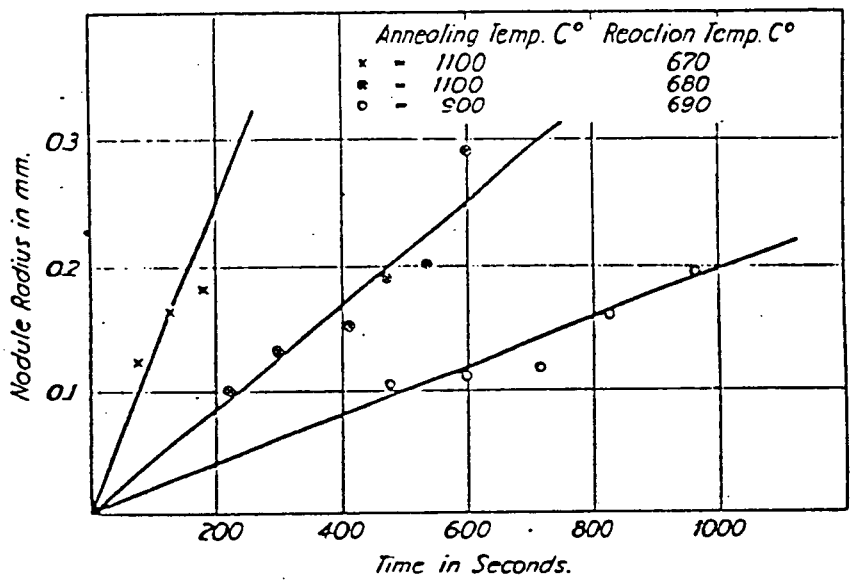

Fig. 3.7 Nodule Diameter versus Reaction Time for different grain sizes (Ref. 60).

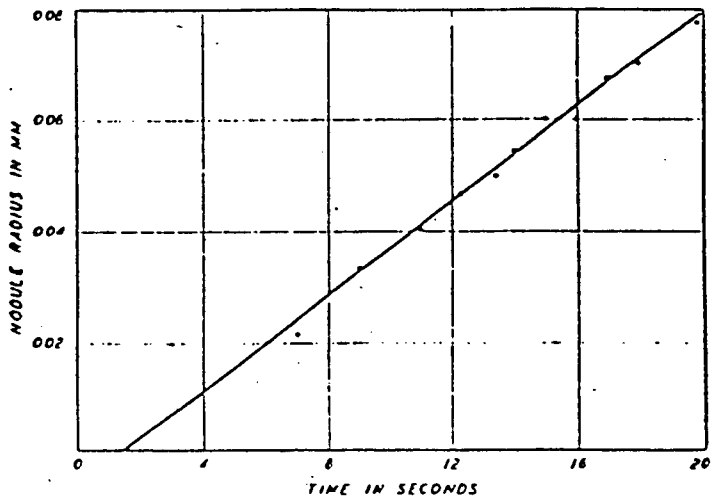

Fig. 3.8 Nodule Radius versus Reaction Time (Ref. 56).

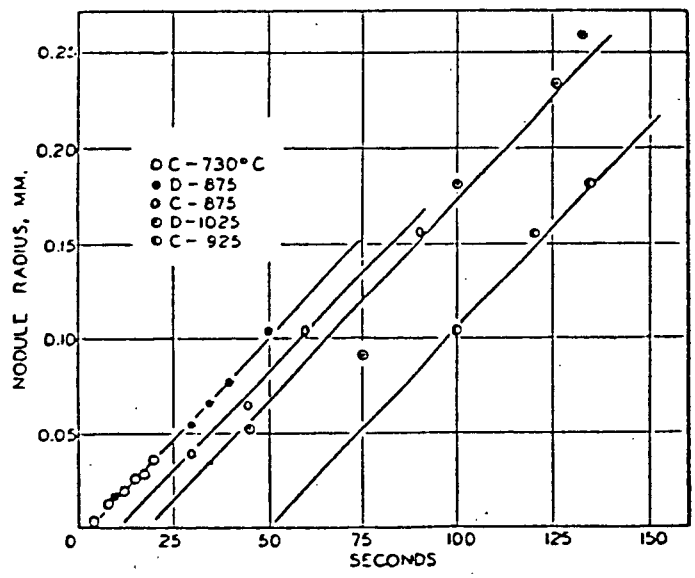

Fig. 3.9 Nodule Radius versus Reaction Time (Ref. 37).

TABLE 3.3 Comparison of Growth Rates Obtained by Using Two Different Methods.[62,63]

Temperature °C	Growth Rates (mm/s)	
	Method 1	Method 2
712	1.1×10^{-4}	1.0×10^{-4}
702	4.3×10^{-4}	5.0×10^{-4}
685	1.6×10^{-3}	2.2×10^{-3}
675	2.2×10^{-3}	3.8×10^{-3}
667	2.5×10^{-3}	5.4×10^{-3}
655	2.7×10^{-3}	8.5×10^{-3}
648	3.3×10^{-3}	1.1×10^{-2}

A change in G that will result in a variation of the shape factor from 0.3 to ∞ can be seen to change the shape of the reaction curve from 'c' to 'a' (Fig. 3.10). It can be seen from Equation 3.3 that increasing the growth rate has a similar effect on the overall transformation kinetics as decreasing the grain size. In reality though, the growth rate is a far more important variable, for it can be varied over a much greater range than grain size, by alloy additions.

3.1.3 Additivity

Due to the independent variation of nucleation and growth rates, to mathematically describe non-isothermal reactions it is necessary to show that the instantaneous reaction rate is only a function of the amount of transformation product present and the reaction temperature. This is the additivity requirement.

To define the concept of additivity Christian[32] considers the simplest type of non-isothermal reaction that is obtained by combining two isothermal treatments, as shown in Fig. 3.11. The assembly is transformed at temperature T_1 where the kinetic law is $f = f_1(t)$ for a time t_1, where f is the fraction transformed. It is then very quickly transferred to a second temperature T_2. If the reaction is additive, the course of the transformation at T_2 will be

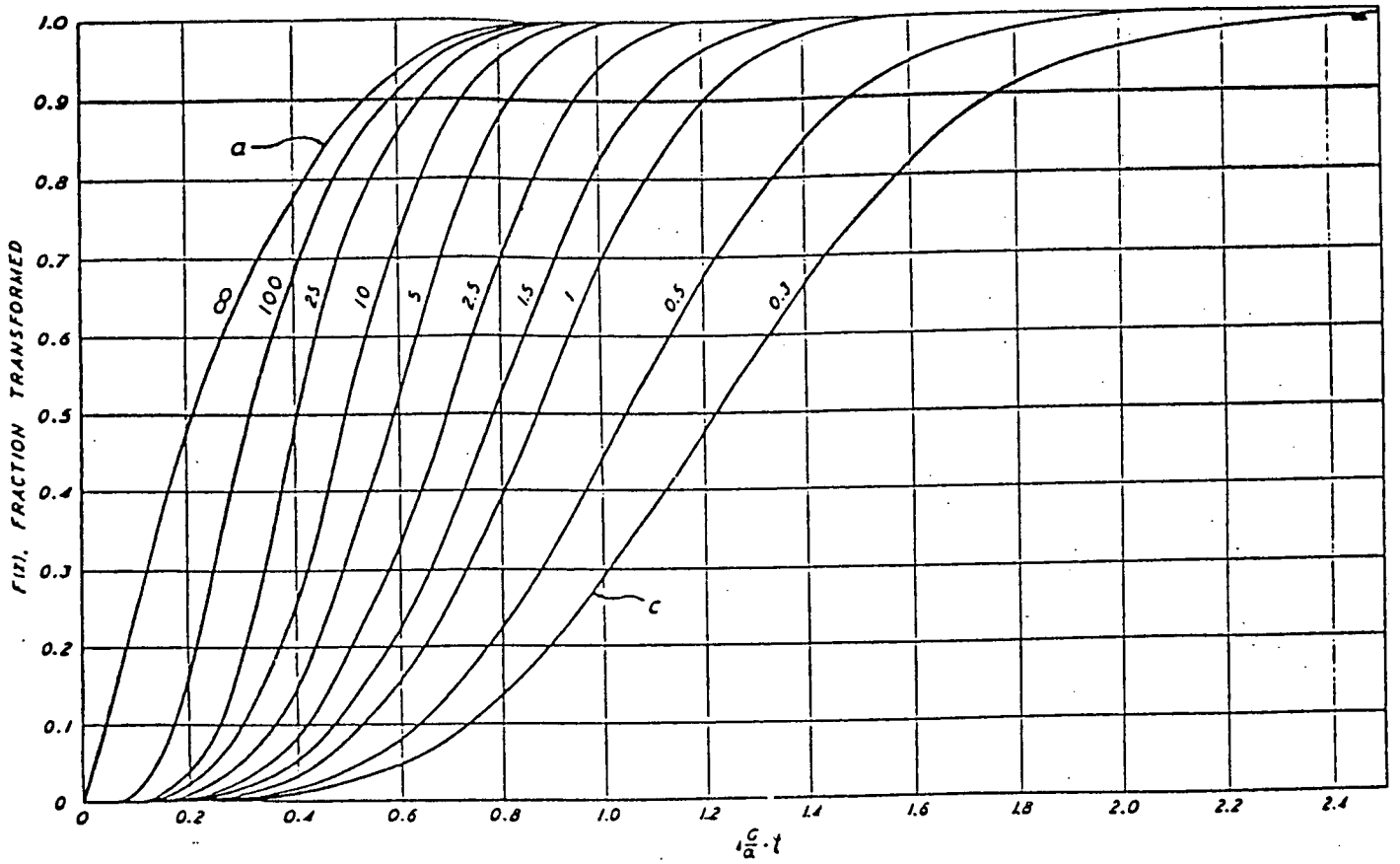

Fig. 3.10 Effect of growth rate on the shape of the reaction curve (Ref. 19).

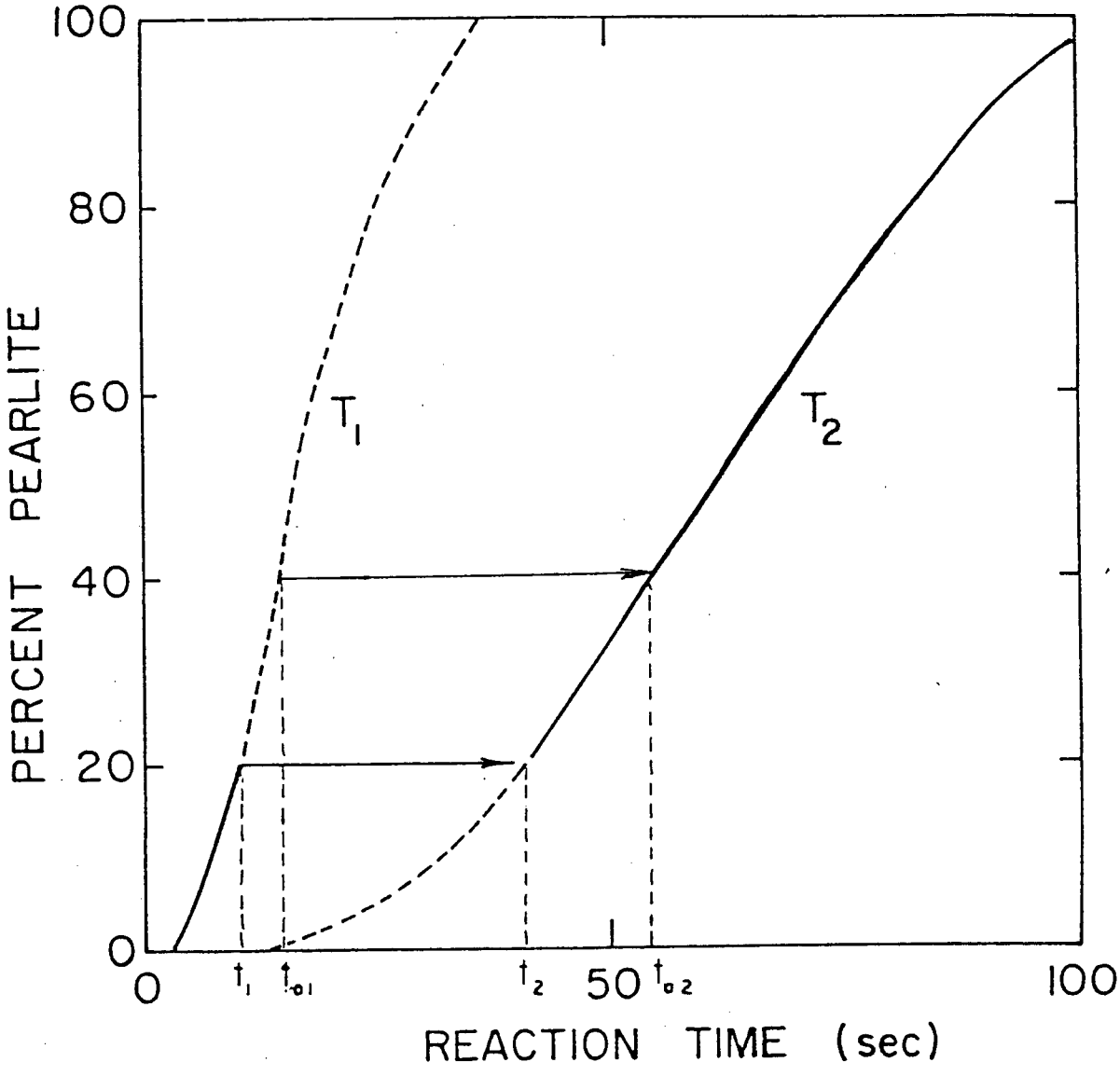

Fig. 3.11 Schematic representation of the principle of additivity.

exactly the same as if the fraction transformed at T_1, $f_1(t_1)$, had all been transformed at T_2. Therefore if t_2 is the time taken at T_2 to produce the same amount of transformation as produced in time t_1 at T_1,

$$f_1(t_1) = f_2(t_2) \qquad \ldots(3.4)$$

and the course of the whole reaction

$$f = f_1(t) \quad t < t_1$$

$$= f_2(t+t_2-t_1) \quad t > t_1 \qquad \ldots(3.5)$$

For example, if t_{a1} is the time taken to produce a fixed amount of transformation 'f_a' at T_1 and t_{a2} is the corresponding time to produce the same amount of transformation at T_2, then in the composite process above, an amount 'f_a' of transformation will be produced in a time,

$t = t_{a2} - t_2 + t_1$ if the reaction is additive.

If
$$t_1/t_2 = \frac{t_{a1}}{t_{a2}} \qquad \ldots(3.6)$$

$$\frac{t_1}{t_{a1}} + \frac{(t-t_1)}{t_{a2}} = 1 \qquad \ldots(3.7)$$

An additive reaction thus implies that the total time to reach a specified amount of transformation is obtained by adding the fractions of the time to reach this stage

isothermally until the sum reaches unity. The generalization of the last equation to any time temperature path is:

$$\int_0^t \frac{dt}{t_a(T)} = 1 \qquad \ldots(3.8)$$

where $t_a(T)$ is the isothermal time to stage 'f_a', and t is the time to 'f_a' for the non-isothermal reaction. This equation can only be derived if Equation 3.6 is true and this relationship will hold only if the reaction rate is dependent only upon:

1. Fraction transformed
2. Temperature

Christian suggests that any transformation for which the instantaneous reaction rate may be written:

$$\frac{df}{dt} = \frac{h(T)}{g(f)} \qquad \ldots(3.9)$$

where h(T) is a function of temperature only and g(f) is a function only of volume fraction transformed, can be expected to be additive.

Both the Avrami equation and the Johnson-Mehl equation can be shown to be of this type.[72]

Consider the Avrami equation.

$$X = 1-\exp(-bt^n) \qquad \ldots\text{Equation 2.5}$$

where n = constant

b = function of temperature only

Rearranging:

$$\log (1-x) = -bt^n$$

$$t = \sqrt[n]{\frac{\log(1-x)}{-b}}$$

Differentiating with respect to 't' (i.e. Equation 2.5)

$$\frac{dx}{dt} = e^{-bt^n} (-nb.t^{n-1})$$

$$= (1-x)(-bn) \left[\frac{\log(1-x)}{-b}\right]^{\frac{n-1}{n}}$$

$$= (1-x)(n).(-b)^{1/n}.[\log(1-x)]^{\frac{n-1}{n}}$$

$$= \frac{n.(-b)^{1/n}}{\left(\frac{1}{1-x}\right)\left[\frac{1}{\log(1-x)}\right]^{\frac{n-1}{n}}} \qquad \ldots(3.10)$$

$$= \frac{h(T)}{g(x)}$$

In the Johnson-Mehl equation:

$$X = 1 - \exp\left(-\frac{\pi}{3} NG^3 t^4\right)$$

where

$$n = 4$$

and

$b = \frac{\pi}{3} NG^3$, hence the J M equation is expected to be additive if N and G are functions of temperature alone.

Avrami[18] suggested that non-isothermal transformation kinetics could be predicted using isothermal kinetic data if the ratio of the nucleation rate to the growth rate, $\frac{N}{G}$, remained a constant over the temperature range of the reaction (i.e. that they have the same temperature variation). This condition was termed the "isokinetic condition".

Early nucleation and growth observations[22,36] showed that the isokinetic condition did not hold. Cahn recognizing that this condition was too restrictive proposed the concept of early site saturation.[35] He observed that the pearlite reaction, exclusively a grain boundary reaction, exhausted the available nucleation sites very early in the reaction (Fig. 3.12). Growth was thus the dominant factor and the transformation consisted essentially of widening of grain boundary slabs of pearlite. Growth being only a function of temperature ensured that the reaction was a function only of temperature and instantaneous fraction transformed and therefore satisfied the additivity criterion.

Cahn went on to propose a series of criteria that would test the site saturation condition. Metallographically he suggested that with a partially transformed specimen, if it is

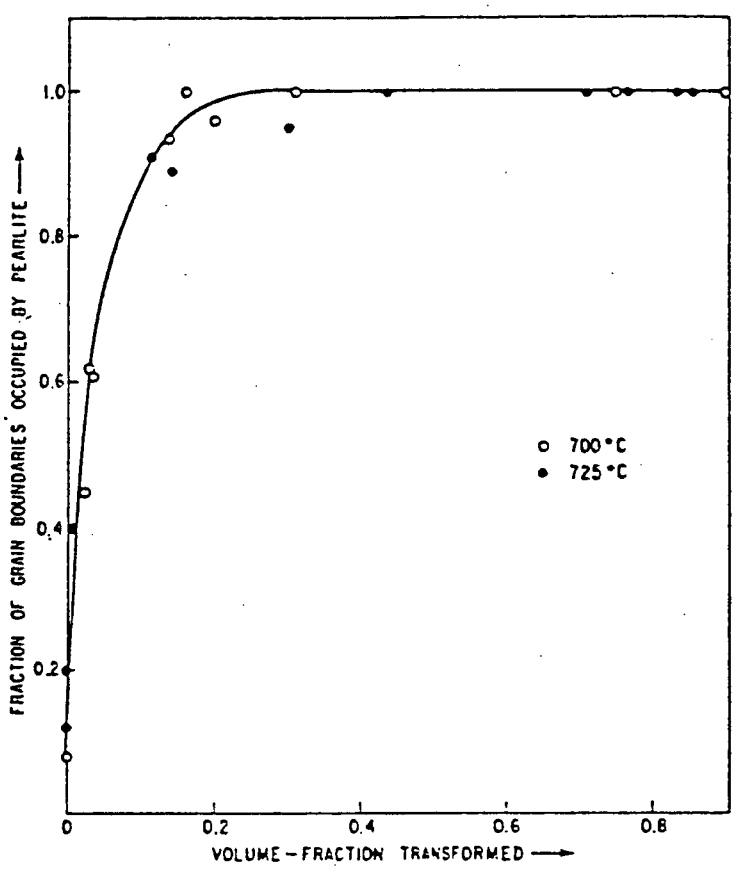

Fig. 3.12 Graph showing fraction of grain boundaries occupied by pearlite as a function of volume-fraction transformed in a Fe-9Cr-1C alloy austenitised for 12 hrs. at 1200°C (Ref. 36).

possible to see one pearlite nodule per grain, site saturation was beginning to occur. Based on at least one nodule per grain, if

$$\frac{G\ t_{0.5}}{d} \leq 0.5 \qquad \ldots(3.11)$$

where d is the grain size, G is the growth rate and $t_{0.5}$ is the time to complete 50% of the transformation. This implies a condition of site saturation.

Cahn's second criteria for site saturation, based on nucleation rates for specific sites was calculated on the basis of a grain shape model and energetics of available nucleation sites as developed by Clemm and Fisher.[34]

The grains of parent austenite were assumed to be equally large tetrakaidecahedra arranged so that they fill space. A tetrakaidecahedra is a body centered-cubic array oriented so that the square faces are on the (100) planes, and hexagonal faces are on the (111) planes. The distance between square faces is designated D, the grain diameter of the austenite (Fig. 3.15). On the basis of a unit volume, Cahn calculated the number of grain corners, length of grain edges and area of grain surfaces as follows:

$$C\left[\frac{\text{number of grain corners}}{mm^3}\right] = \frac{12}{D^3}/mm^3 \qquad ...(3.12)$$

$$L\left[\frac{\text{length of grain edges}}{mm^3}\right] = \frac{8.5}{D^2}\ mm/mm^3 \qquad ...(3.13)$$

$$S\left[\frac{\text{surface area}}{mm^3}\right] = \frac{3.35}{D} mm^2/mm^3 \qquad ...(3.14)$$

The site saturation criteria for specific sites become:

$$N_c > 2.5\ \frac{G}{D^4} \qquad ...(3.15)$$

for corner site saturation

$$N_e > 10^3\ \frac{G}{D^4} \qquad ...(3.16)$$

for edge site saturation

$$N_s > 6x10^3\ \frac{G}{D^4} \qquad ...(3.17)$$

for surface site saturation.

After establishing that the reaction was site saturated, the kinetic laws were easily obtained depending on whether the active growth sites are grain boundary surfaces,

$$X = 1-\exp(-2S\dot{G}t) \qquad ...(3.18)$$

or grain edges,

$$X = 1-\exp(-\pi L G^2 t^2) \qquad \ldots(3.19)$$

or grain corners,

$$X = 1-\exp(-\frac{4}{3}\pi C G^3 t^3) \qquad \ldots(3.20)$$

Cahn did derive a reaction equation for transformations with very low nucleation rates, e.g. at high temperatures, based on Johnson and Mehl's analysis of time dependent nucleation rates,[19] but he stated that even for this condition there was the possibility of local site saturation.

Thus the current state of understanding on the nucleation and growth of pearlite, their relationship to the additivity principle and the ability to predict continuous behaviour from constant temperature data is as follows: 1) The isokinetic condition (N/G = constant) is not a generally observed phenomenon. 2) For the pearlite reaction in the majority of steels, site saturation is a general phenomenon, thereby permitting the application of the additivity principle.

In this thesis metallographic work was undertaken to investigate the nucleation and growth aspects of the pearlite reaction for a eutectoid plain carbon steel and

to test the various criteria for establishing the applicability of the additivity principle for the pearlite reaction.

3.2 EXPERIMENTAL PROCEDURES

Experimental determination of the pearlite nucleation and growth rates was done on samples heat treated in salt pots using the same equipment and heat treatment procedure as previously described in Chapter 2. A series of 10 mm diameter, 1-2 mm thick disc-shaped samples were reacted at constant temperatures for different times to obtain a number of specimens covering the transformation range up to 20% pearlite. These samples could then be examined metallographically and use made of the method employed by Scheil and Lange-Weise,[60] Hull, Colton and Mehl[37] and Ridley and Brown[62,63] for establishing the nucleation rate N, and the growth rate G.

Two reaction temperatures 640°C and 690°C were used, these corresponding to the high temperature, low driving force, flat portion of the TTT diagram (690°C), and high driving force, nose portion of the TTT diagram (640°C).

The austenitising treatment was 5 minutes at peak temperature. The austenitising temperatures, isothermal reaction temperatures and the resulting range of grain

sizes obtained can be seen in Table 2.3.

A 2% nital etching procedure was employed for revealing the microstructural details, the same as that used to determine the reaction kinetics described in Chapter 2. The following pre-etching treatment was required for revealing both prior austenite grain size and the pearlite. After being cold mounted, the specimens were treated in a boiling solution of 2 g picric acid, 25 g NaOH and 100 ml water for 15 minutes. A swab etch with 2% nital was then carried out to reveal the pearlite nodules.

A pearlite nodule counting procedure was performed manually on representative photo-micrographs of each specimen using the Zeiss optical microscope. A particle size distribution was carried out for each specimen per unit area, and these were corrected using the Scheil and Lange-Weise, Schwartz procedure,[67] to obtain the number of nodules/mm^3. An example of the correction procedure can be seen on Table 3.4 for the reaction temperature 640°C and austenitising at 950°C. Corresponding nucleation rates were obtained from graphs of the number of nodules/mm^3 versus reaction time. The slopes of these curves gave

$$N = \frac{\text{nodules}}{mm^3 . s}$$

(Average slope was taken for reactions with increasing nucleation rate.)

TABLE 3.4 Correction Procedure to Determine Number of Nodules Per Unit Volume From Number of Nodules Observed on Polished Surface. Reaction Temperature 640°C, Austenitising Temperature 950°C.

Diameter(mm)	12.5×10^{-2}	25×10^{-2}	37.7×10^{-2}	50×10^{-2}	62.5×10^{-2}
Number of particles per mm^2	135	110	95	55	15
Number of particles with actual $d = 62.5\times10^{-2}$ mm					25
Corrected no.	135	108	91	50	
Number of particles with actual $d = 50\times10^{-2}$ mm				75	
Corrected no.	133	101	76		
Number of particles with actual $d = 37.5\times10^{-2}$ mm			102		
Corrected no.	127	81			
Number of particles with actual $d = 25\times10^{-2}$ mm		93			
Corrected no.	115				
Measured distribution	135	110	95	55	15
Corrected distribution	115	93	102	75	25
Number of particles per unit volume	9200	3720	2720	1500	400
Total number of particles per mm^3	17,540				

The pearlite growth rate was determined from similar salt pot heat treated specimens that had been reacted for times of up to approximately 20-30% of the total transformation. The standard method[37] of measuring the diameter of the largest individual pearlite nodule as a function of isothermal transformation time was used.

The alternative measuring procedures of nucleation and growth rates used by Brown and Ridley[62,63] were also examined, as a check on the magnitudes of the values obtained by the two techniques. This involved construction of inverse cumulative distribution curves for each isothermal transformation reaction. These curves were used for the construction of the plots of nodule diameter versus isothermal reaction time and the $\frac{\text{number of nodules}}{\text{mm}^3}$ versus isothermal reaction time.

3.3 RESULTS AND DISCUSSION

3.3.1 Nucleation Rates

The main method of obtaining the nucleation rate from plots of $\frac{\text{number of nodules}}{\text{mm}^3}$ versus isothermal transformation time can be seen on Fig. 3.13. The slope of the individual isothermal transformation curves gives $\frac{\text{number of nodules}}{\text{mm}^3.\text{s}}$ i.e. the nucleation rate. The influence of the reaction temperature and the grain size on the

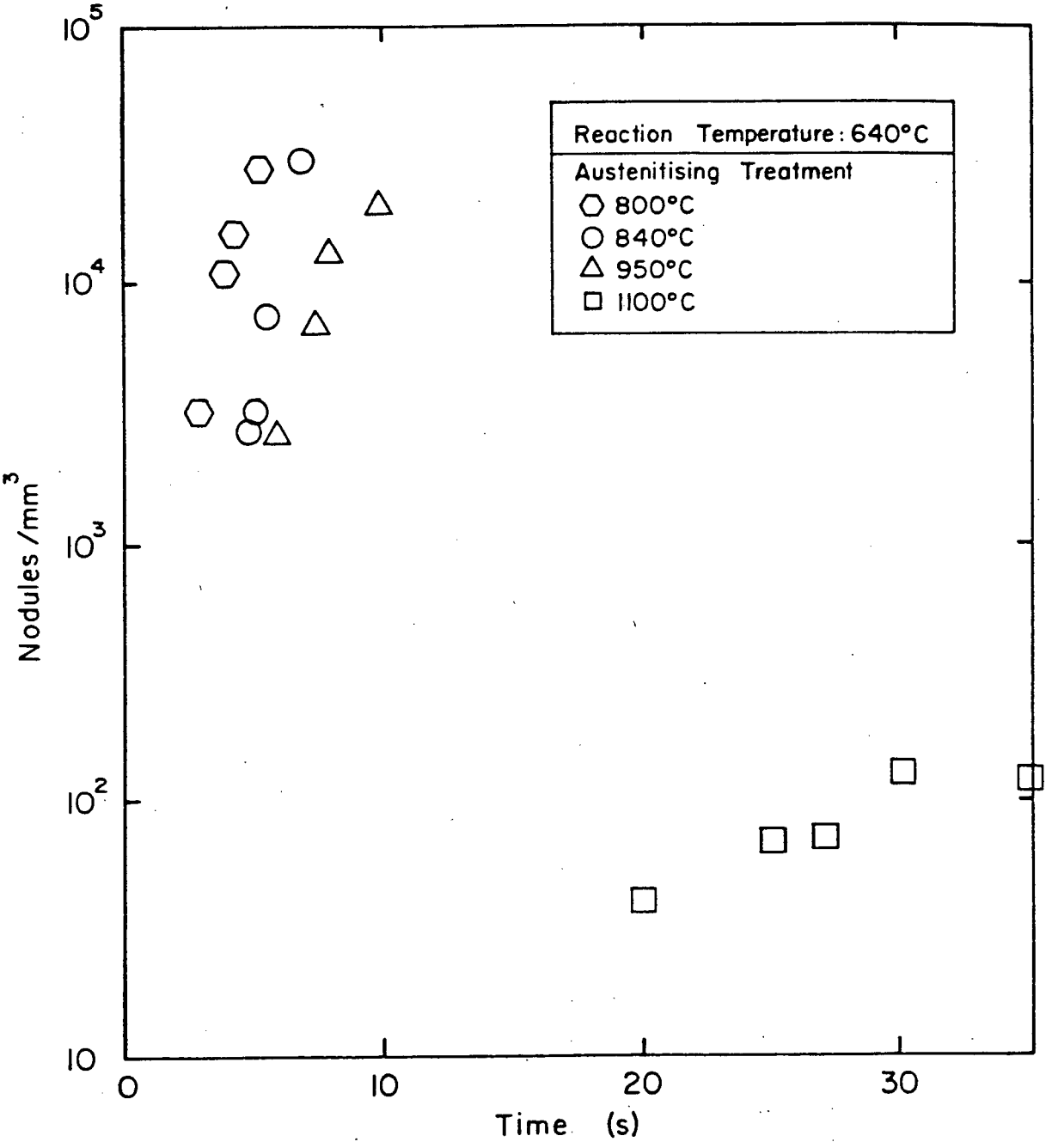

Fig. 3.13a $\frac{\text{Nodules}}{\text{mm}^3}$ versus Reaction Time for isothermal pearlite reation at 640°C.

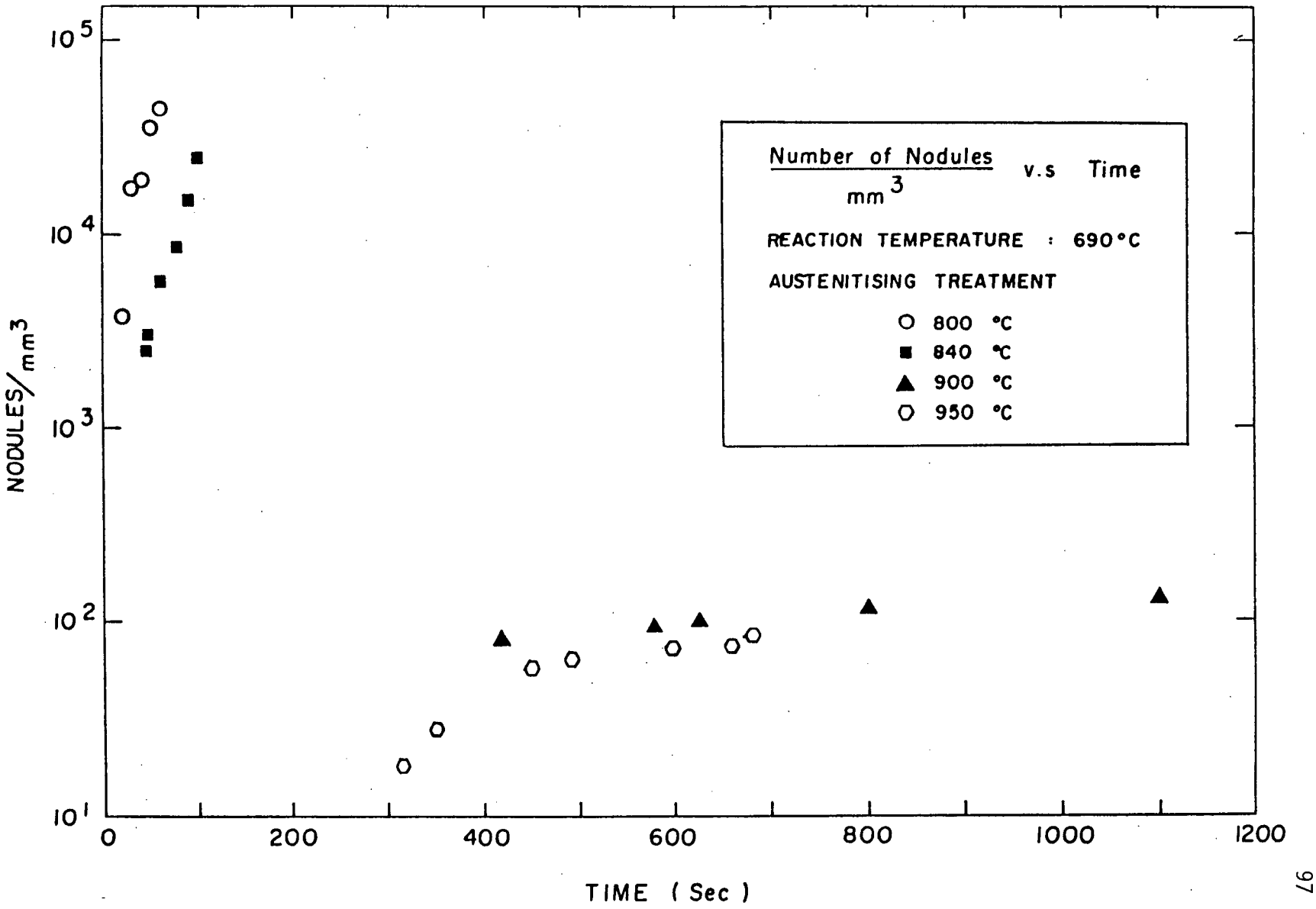

Fig. 3.13b $\frac{\text{Nodules}}{\text{mm}^3}$ versus Reaction Time for isothermal pearlite reaction at 690°C.

resulting nucleation rate can be seen by examining Table 3.5.

Increasing the pearlite grain size reduces the nucleation rate dramatically. This can also be observed metallographically on the photomicrographs shown in Fig. 3.14 where the initial stages of the reaction are compared for small and large grain size specimens.

The alternative method of determining the nucleation rate requires drawing vertical lines on the inverse cumulative distribution curves (Figs. 3.15, 3.16) at values of constant 'd'. This approach yields the reaction time required for obtaining an equivalent size distribution for a given grain size; the resultant graph can be seen on Fig. 3.17. The time derivative of each line on Fig. 3.17 gives the $\frac{\text{number of nodules}}{\text{mm}^3}$, i.e. the nucleation rate. The comparison of nucleation rates obtained by both methods can be seen in Table 3.6 and agree reasonably well.

With increasing grain size from A.S.T.M. 9.1 to A.S.T.M. 3, the number of grain corners, the grain edge length and the grain surface area, on a unit volume basis, are dramatically reduced. This explains the decrease in the nucleation rate. Also it can be seen that with greater undercooling and larger driving force for

TABLE 3.5 Pearlite Nucleation Rate Data

Austenitising Temperature °C	A.S.T.M. Grain Size	Average Grain Diameter (mm)	Nucleation Rate = $\frac{\text{Nodules}}{mm^3/s}$ 640°C	690°C
800	9.1	15	10,400	995
840	7.8	27	18,000	382
900	7.4	30	--	7×10^{-2}
950	7.3	32	3,800	16×10^{-2}
1100	3.0	200	6	-

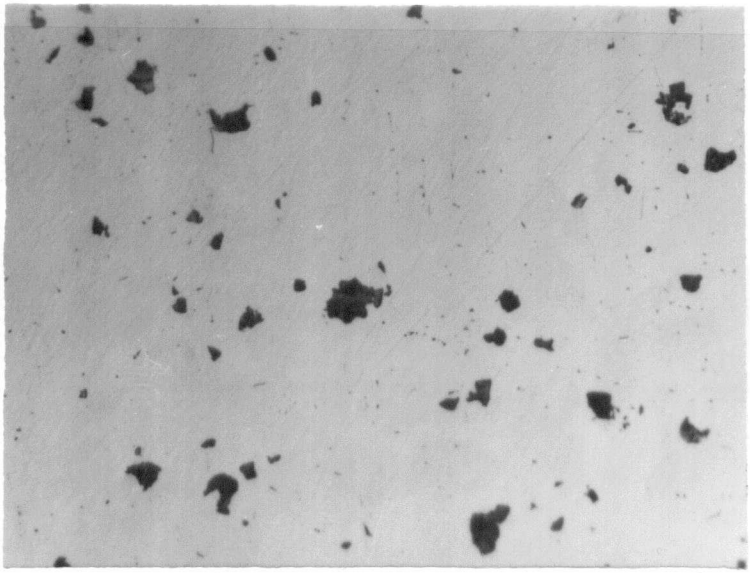

Fig. 3.14a Pearlite nodules in specimen partially transformed to approximately 10% transformation at the isothermal reaction temperature of 640°C. Grain size, A.S.T.M. 7.3 Magnification X160.

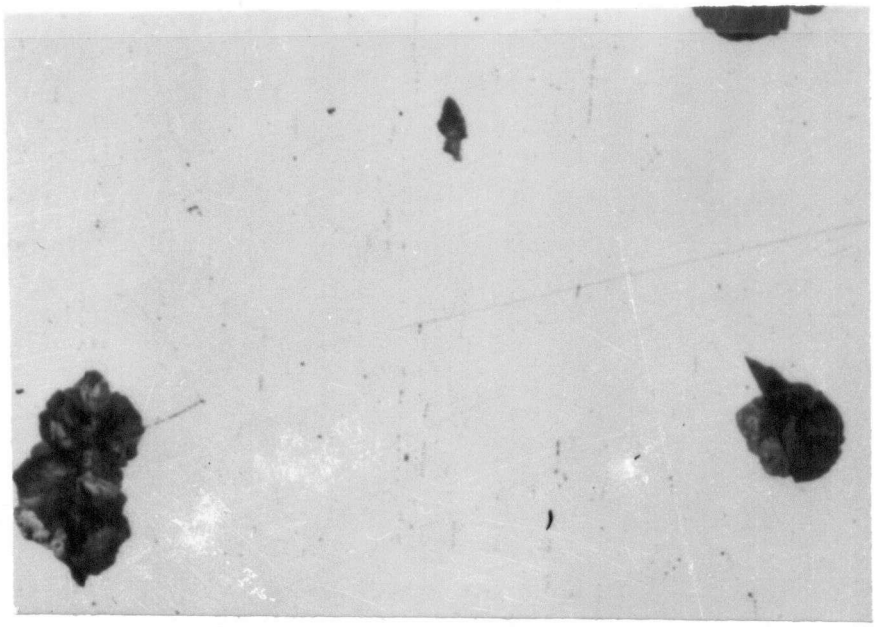

Fig. 3.14b Pearlite nodules in specimen partially transformed to approximately 10% transformation at the isothermal reaction temperature of 640°C. Grain size A.S.T.M. 3 Magnification X160.

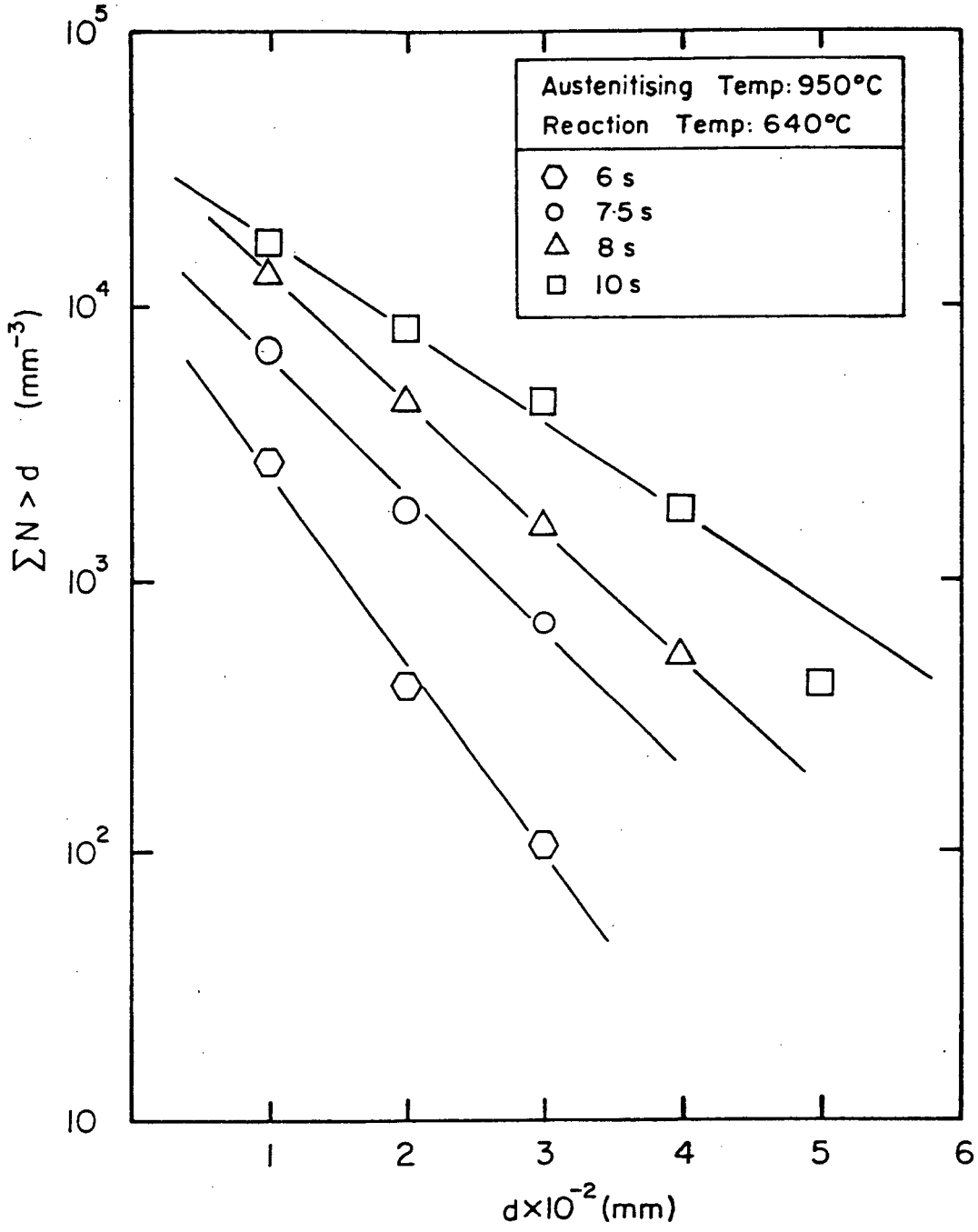

Fig. 3.15 Inverse Cumulative Distribution graph for isothermal transformation at 640°C.

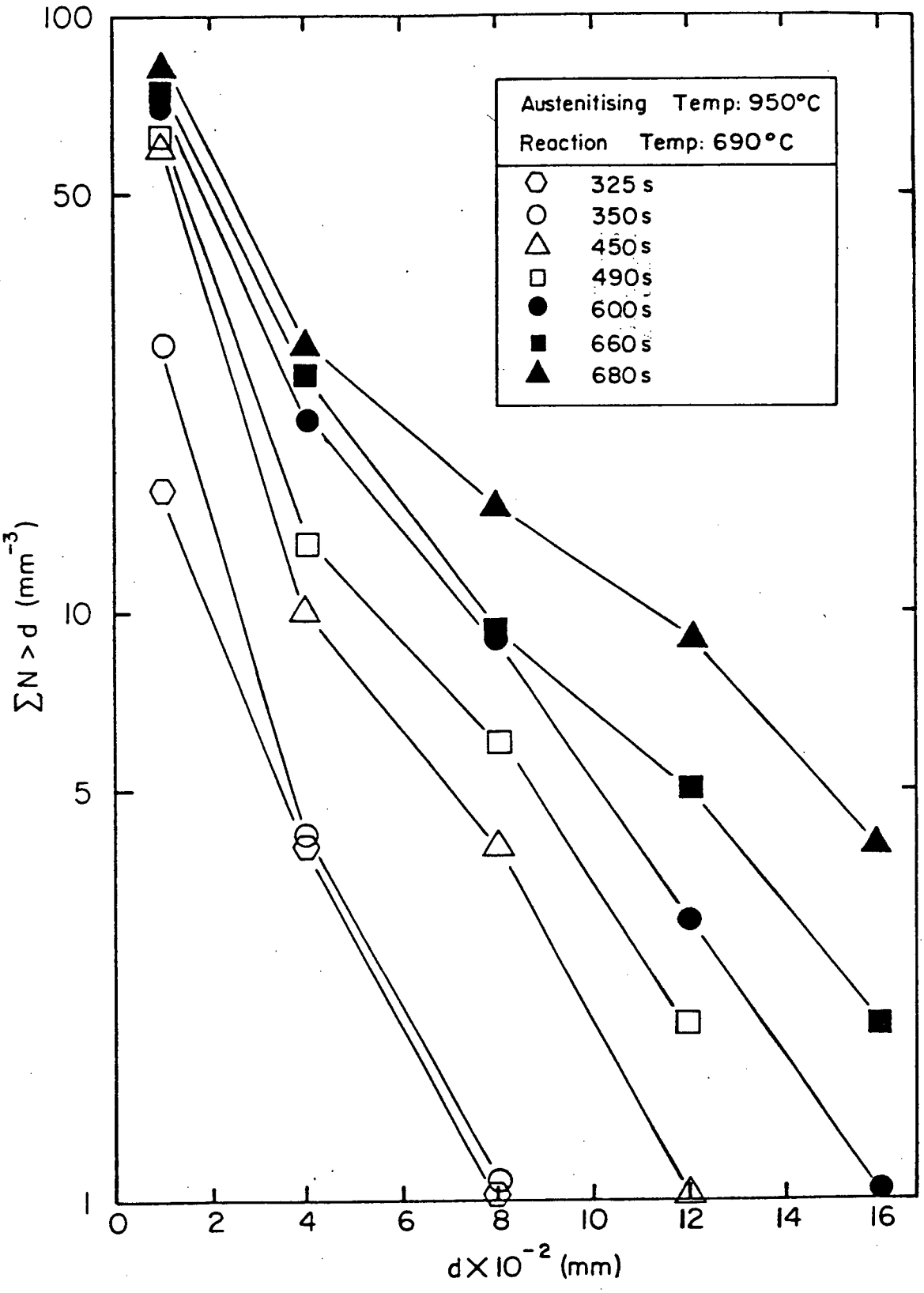

Fig. 3.16 Inverse Cumulative Distribution graph for isothermal transformation at 690°C.

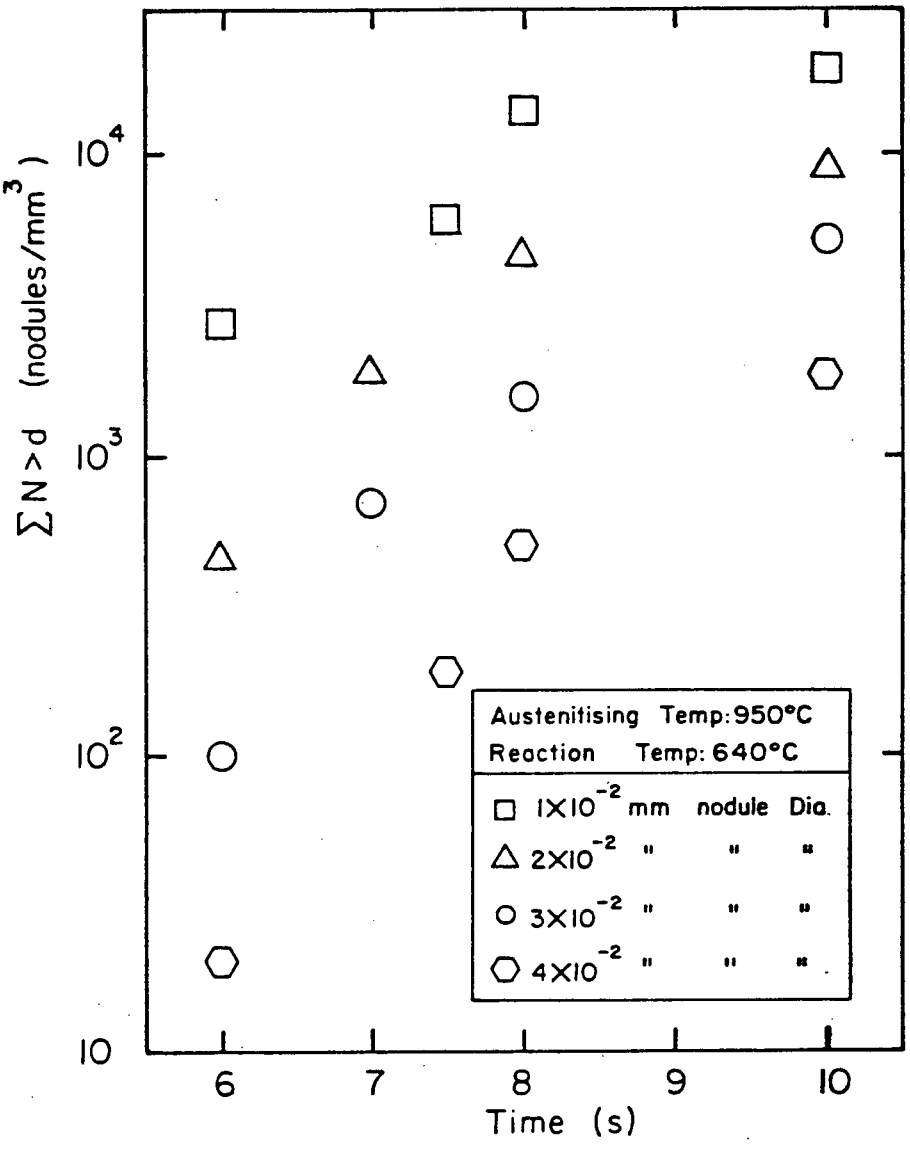

Fig. 3.17a Number of nodules per unit volume versus Reaction Time, obtained by constructing verticals to the Inverse Cumulative Distribution graph. Reaction temperature 640°C, Grain Size ASTM 7.3.

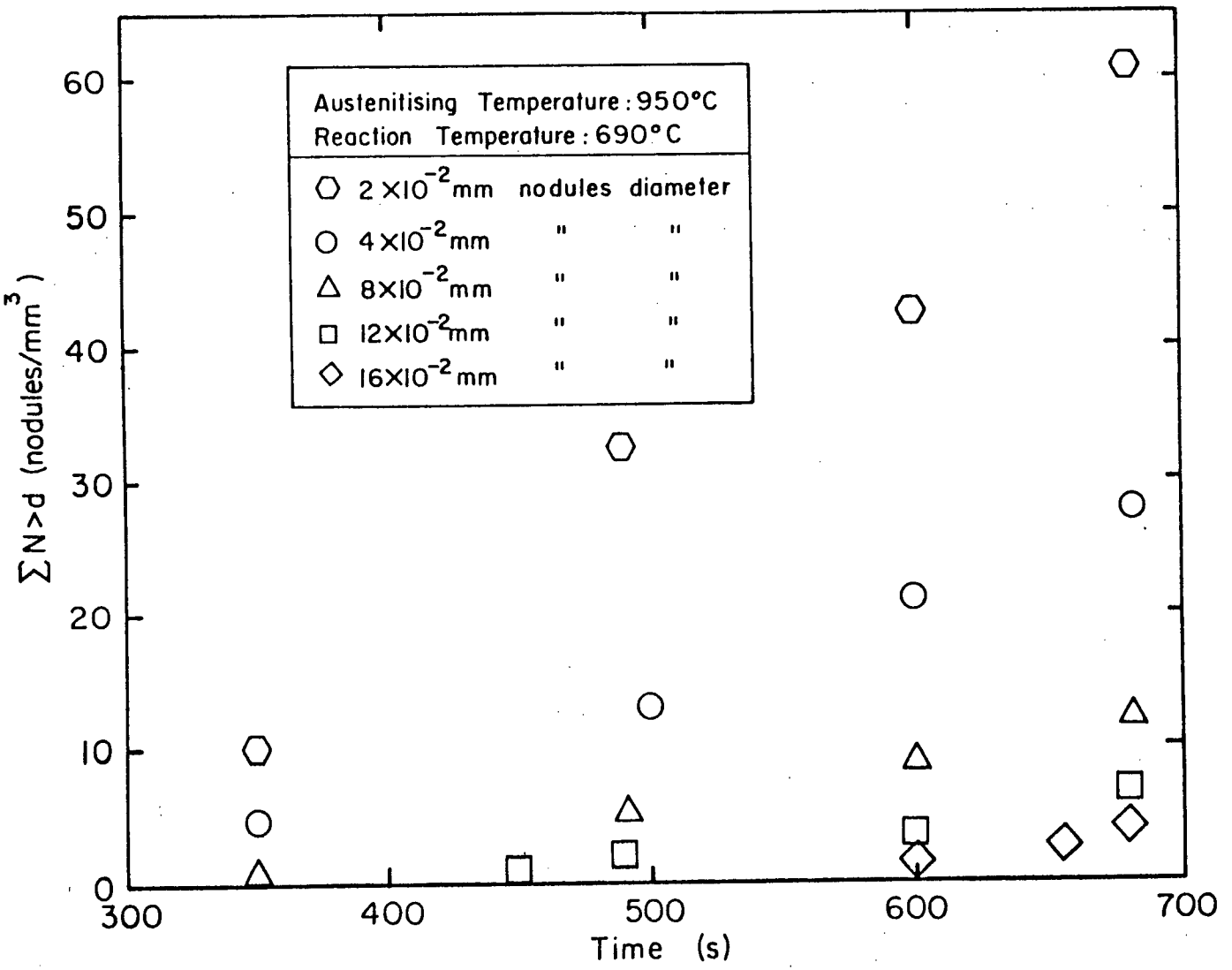

Fig. 3.17b Number of nodules per unit volume versus Reaction time. Reaction temperature 690°C, Grain Size ASTM 7.3.

TABLE 3.6 Comparison of Nucleation Rates Obtained Using Graphical and Metallographic Methods

A.S.T.M. Grain Size	Isothermal Reaction Temperature °C	Nucleation Rate $(\frac{\text{nodules}}{\text{mm}^3.\text{s}})$	Method	Source
7.3	640	3800	Metallographic	1080 steel used in this work
7.3	690	16×10^{-2}	Metallographic	
7.3	640	3000	Graphical (For the smallest size distribution)	
7.3	690	8×10^{-2}	Graphical	
	Literature Values			
5¼	640	47	Metallographic	0.78 C Plain Carbon Steel[37]
5¼	690	5.9×10^{-2}	Metallographic	
4¼	650	36	Metallographic	0.80 C Plain Carbon Steel[37]
4¼	689	6.2×10^{-2}	Metallographic	
0-1	685	18	Graphical	0.81C Plain Carbon Steel[37]

nucleation, the nucleation rate at 640°C is at least an order of magnitude larger than that obtained at the 690°C isothermal reaction temperature. Also on Table 3.6 are results of nucleation rate measurements made by different workers using the different methods.

3.3.2 Growth Rates

Growth rates were determined from plots of the largest single pearlite nodule diameter versus isothermal transformation time (Fig. 3.18). The influence of grain size and reaction temperature on the pearlite growth rate can be seen in Table 3.7.

The alternate way of determining the pearlite growth rate is to construct horizontals to the inverse cumulative distribution curve, (Figs. 3.15, 3.16), at constant values of $\frac{\text{number of nodules}}{\text{mm}^3}$. This yields a relationship between reaction time and nodule diameter for specific nodule size distributions (Fig. 3.19). The time derivative of these curves give the pearlite growth rate. The resulting growth rates are more scattered than those obtained by direct measurement of the largest pearlite diameter as can be seen in Table 3.8; this table also contains the pearlite growth rates measured by various other workers using both methods of measurement.

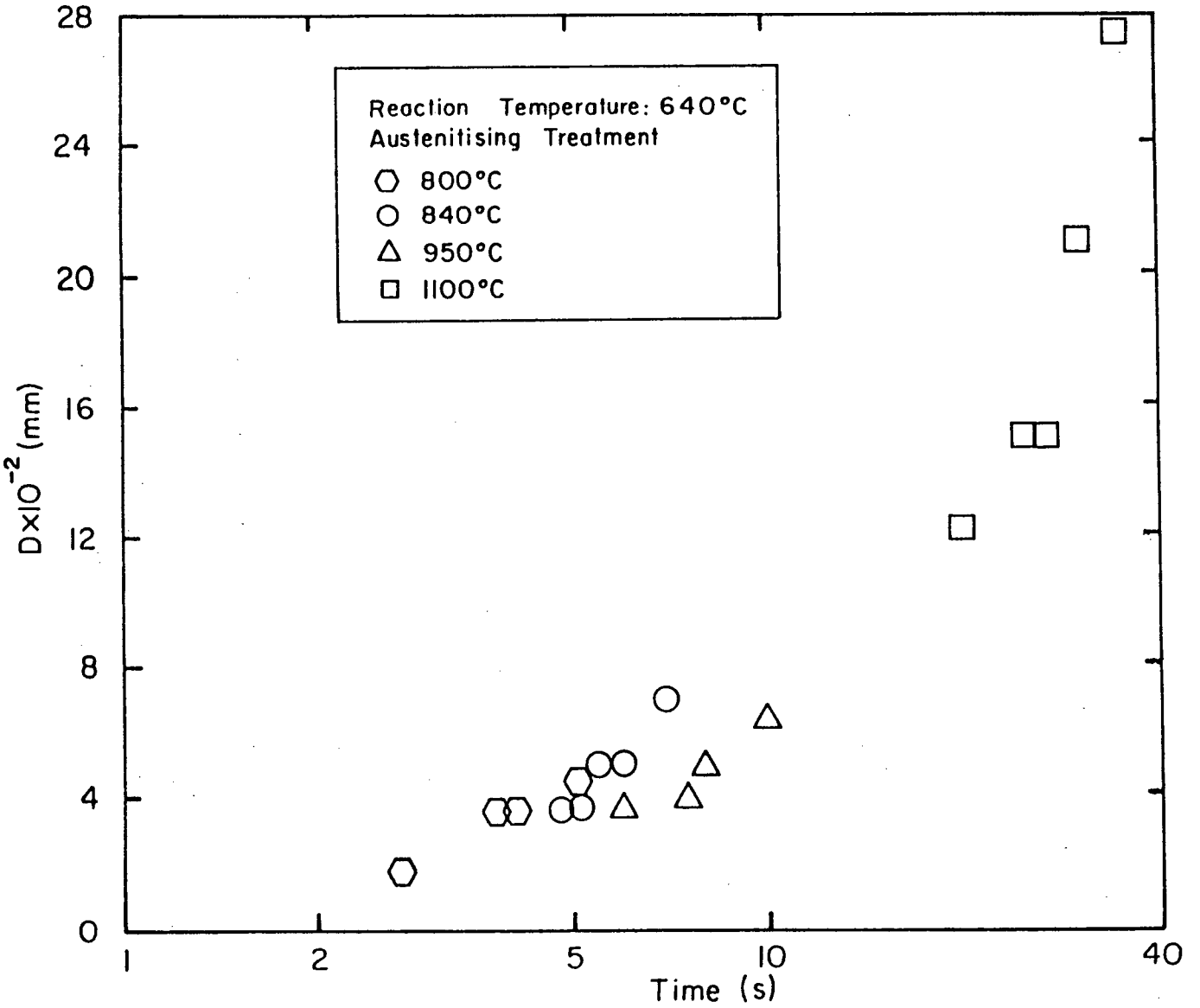

Fig. 318a Largest Diameter versus Reaction Time. The slope of each curve gives the growth rate (mm/s) for different grain sizes. Reaction temperature, 640°C.

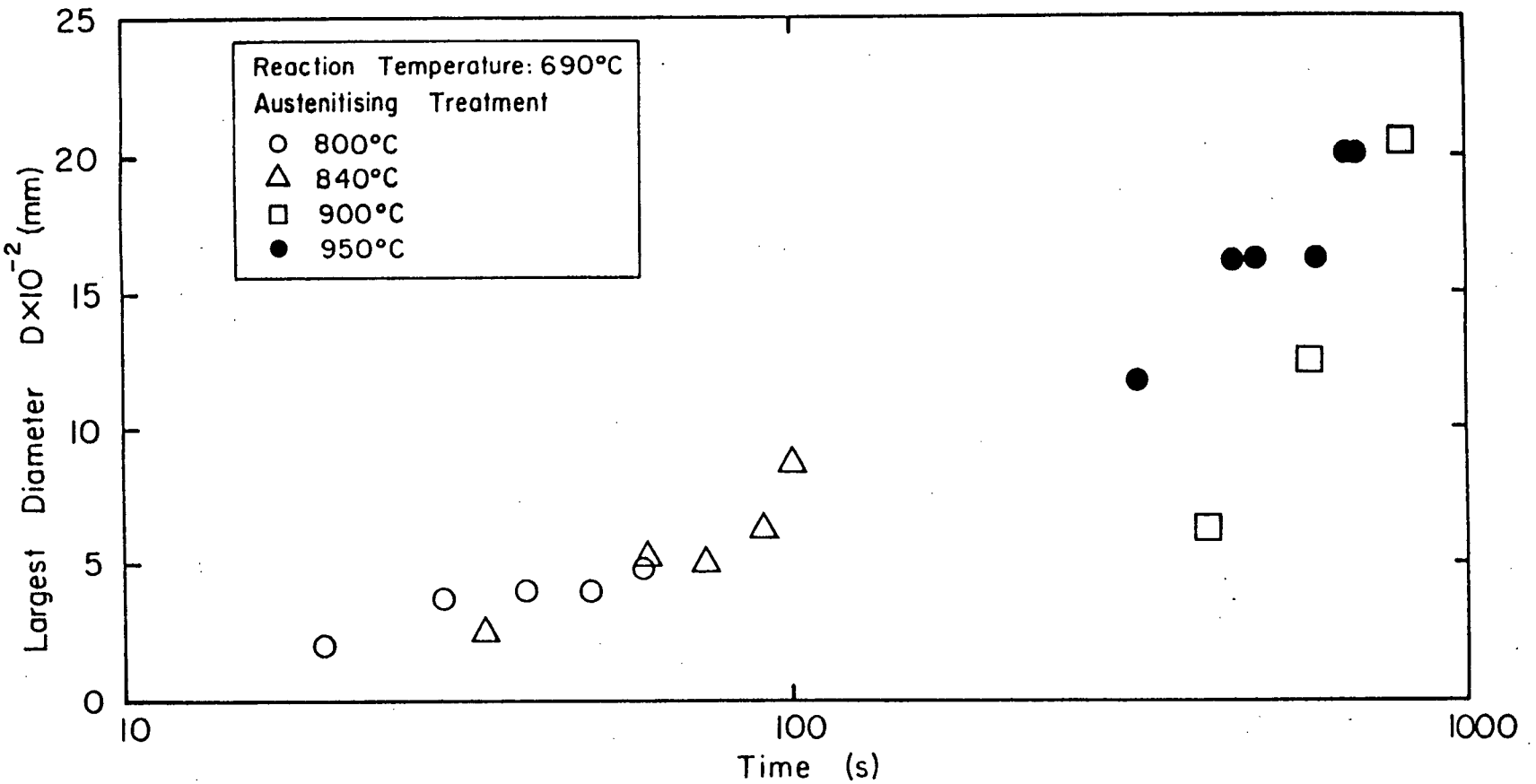

Fig. 3.18b Largest Diameter versus Reaction Time. Reaction temperature, 690°C.

TABLE 3.7 Pearlite Growth Rate Data

Austenitising Temperature °C	A.S.T.M. Grain Size	Pearlite Growth Rate(mm/s) 640°C	690°C
800	9.1	10.6×10^{-3}	5.4×10^{-4}
840	7.8	8×10^{-3}	9.8×10^{-4}
900	7.4	-	2.9×10^{-4}
950	7.3	6.7×10^{-3}	3.3×10^{-4}
1100	3.0	10.7×10^{-3}	-

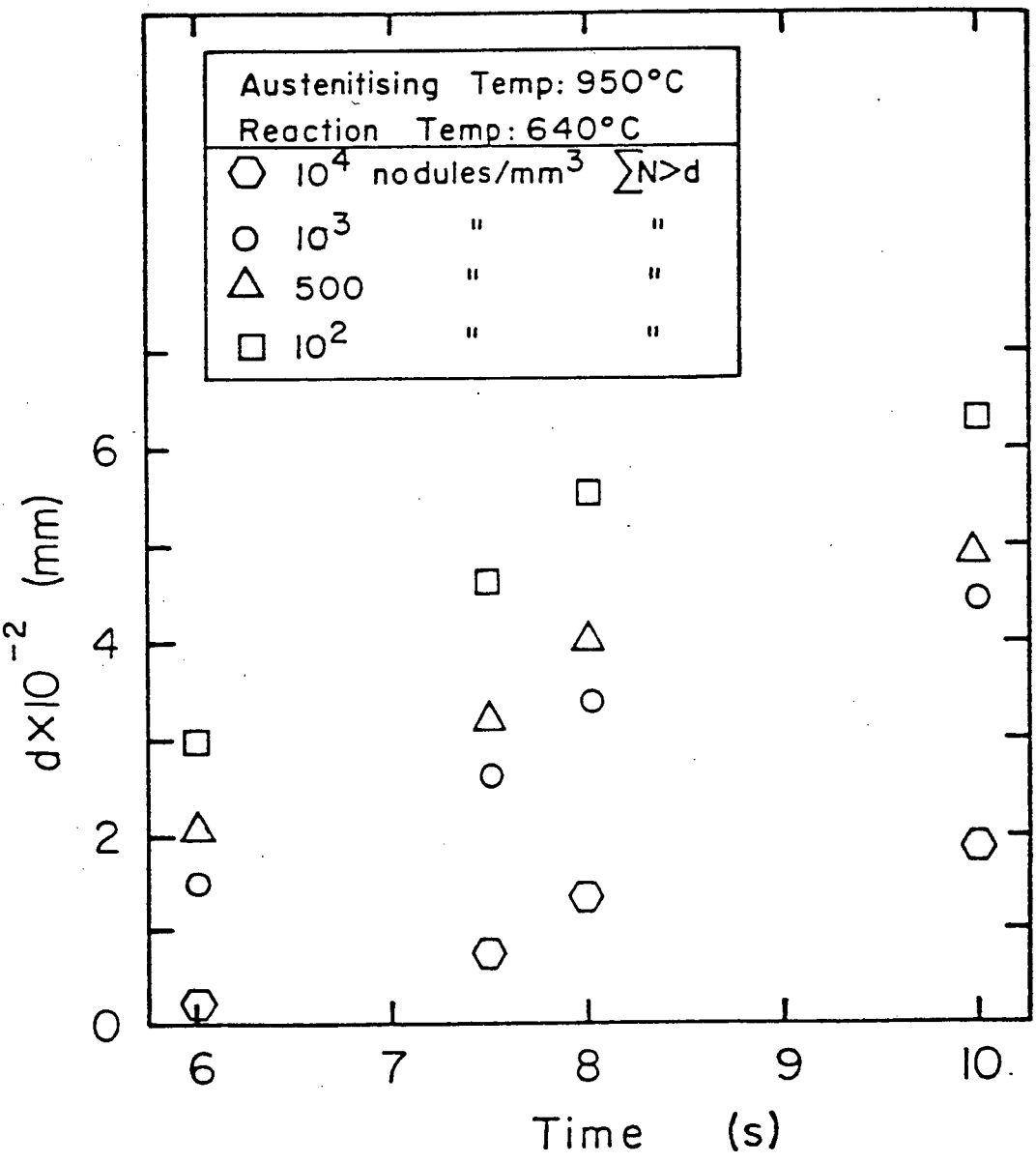

Fig. 3.19a Nodule diameter(d) versus Reaction time (t),obtained by constructing horizontals to the Inverse Cumulative Distribution graph. Slopes of each curve gives growth rate (mm/s). Reaction temperature, 640°C. Grain Size, A.S.T.M. 7.3.

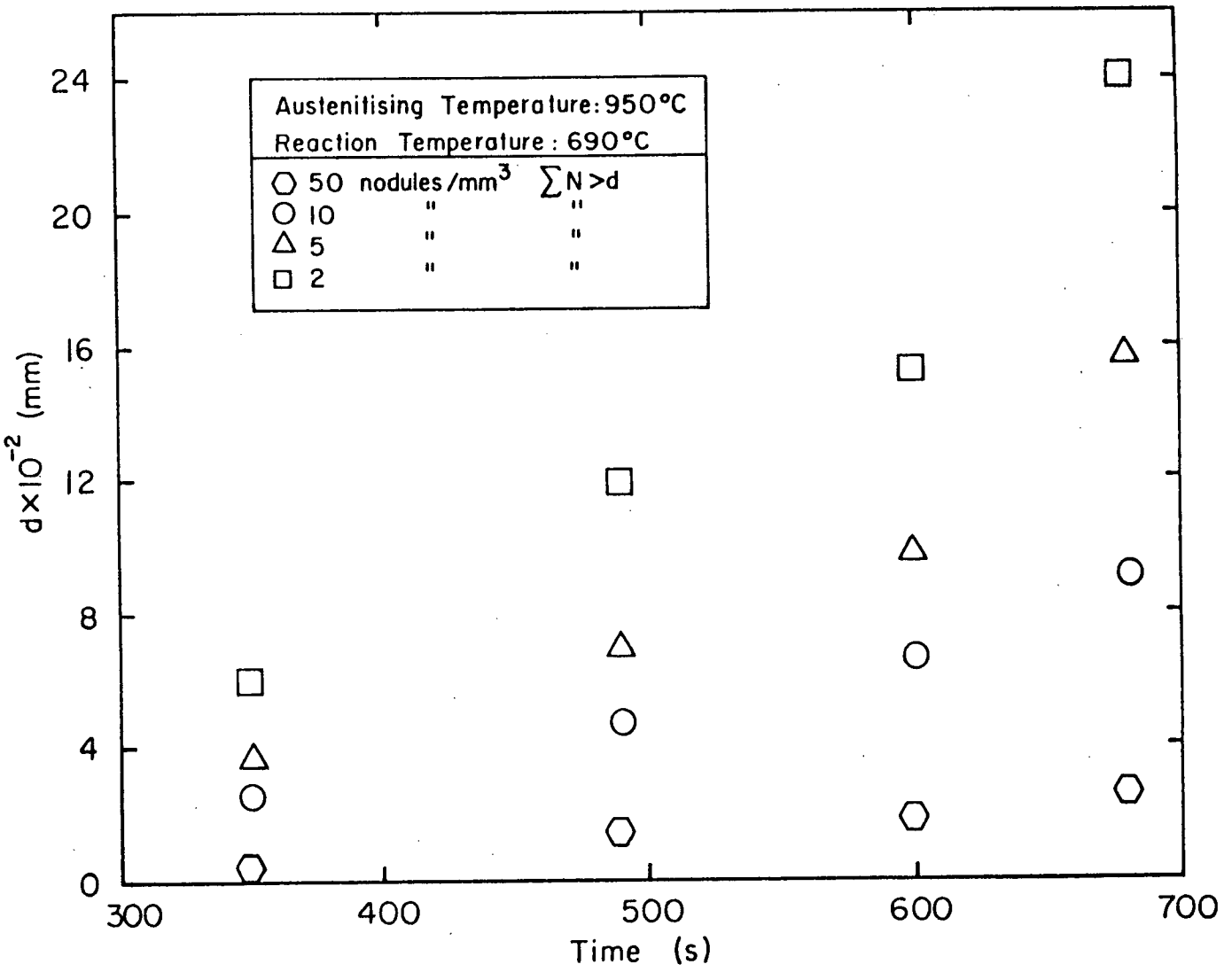

Fig. 3.19b Nodule diameter(d) versus Reaction time (t). Reaction temperature, 690°C. Grain Size, A.S.T.M. 7.3.

TABLE 3.8 Comparison of Growth Rates Obtained by Using Metallographic and Graphical Methods.

A.S.T.M. Grain Size	Reaction Temperature °C	Growth Rate (mm/s)	Method	Source
7.3	640	6.7×10^{-3}	Largest Diameter	1080 steel used in this work
7.3	690	3.3×10^{-4}	Largest Diameter	
7.8	640	8.0×10^{-3}	Largest Diameter	
7.8	690	9.8×10^{-4}	Largest Diameter	
7.3 & 7.8	640	$5\text{-}45 \times 10^{-3}$	Graphical	
7.3 & 7.8	690	$1\text{-}20 \times 10^{-4}$	Graphical	
Literature Values				
5	640	6.2×10^{-3}	Largest Diameter	0.78 C Plain Carbon Steel[37]
5	690	8.5×10^{-4}	Largest Diameter	
4	650	3.6×10^{-3}	Largest Diameter	0.80 C Plain Carbon Steel[37]
4	689	4×10^{-4}	Largest Diameter	
0-1	685	1.6×10^{-3}	Largest Diameter	0.81 C Plain Carbon Steel[62]
0-1	685	2.2×10^{-3}	Graphical	

An important conclusion from the growth rate measurements is the relative independence of growth rate from austenite grain size. For the large range of austenite grain sizes examined, little if any effect is seen on the growth rate of the pearlite. The growth rate is largely determined by the isothermal reaction temperature. This result is consistent with the previous work of Dorn, et al.,[22] Hull, et al.[37] and Scheil et al.[60]

The following observations can be made after an examination of the photomicrographs of the small and large grain size samples shown in Fig. 3.20:

1. Pearlite nodules in the small grain size sample tend to be located at 3 or 4 grain intersections and have an approximately equi-directional growth (spherical), growing into all surrounding grains (Fig. 3.20a).
2. Pearlite nodules in the large grain size sample have a greater tendency to nucleate at 2 grain intersections, grow only into 1 of the adjacent grains and therefore to have non-spherical shapes (Fig. 3.20b).

The possible reasons for these different growth morphologies can be summarized as follows:

1. Pearlite nodules will nucleate at the high energy, multi-grain intersections available in the small grain-sized material. Fewer of these high energy sites per unit volume are available in the

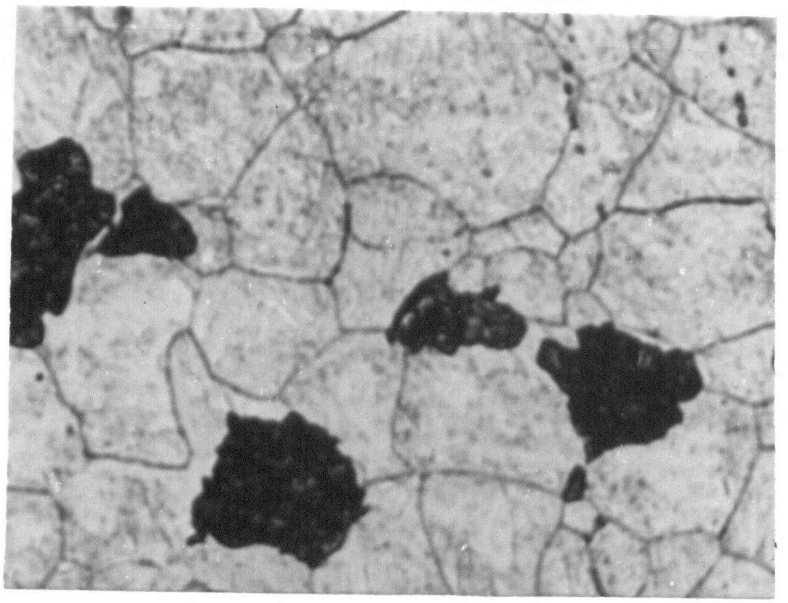

Fig. 3.20a Pearlite nucleation in small grain size specimen (A.S.T.M. 9.1). Mag. X 1200.

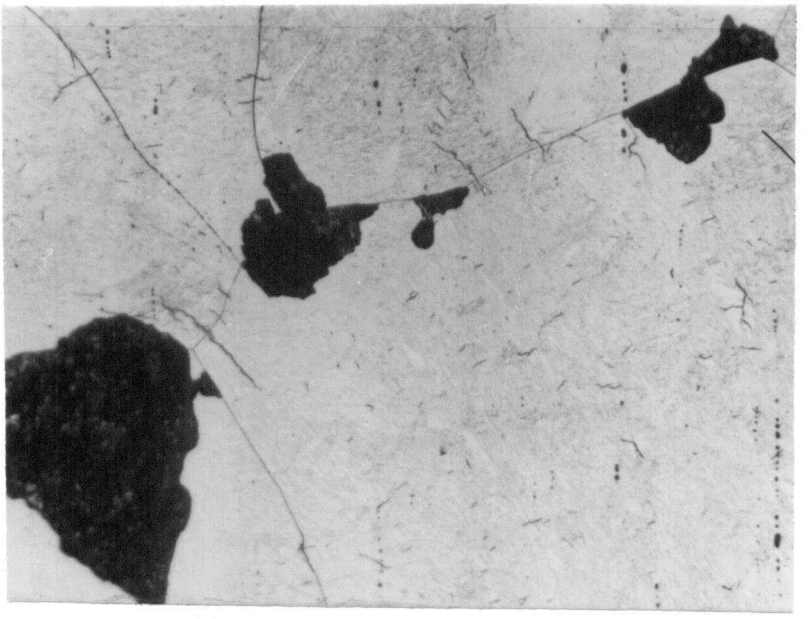

Fig. 3.20b Pearlite nucleation in large grain size specimen (A.S.T.M. 3). Mag. X 230.

coarse grained sample, requiring the nodules to nucleate at two grain intersections in the large grained material.

2. The one-sided (hemi-spherical) growth of pearlite nodules nucleating on the grain boundaries that could be due to lower interface mobility in one direction, suggests the existence of a special orientation relationship, as observed for nodules on the flat grain boundaries of the larger grain size (Fig. 3.20b).

On the other hand for nodules nucleating at multi-grain intersections (i.e. either corner or edge) in the smaller grain-sized sample, a special orientation relationship would be highly unlikely, resulting in predominantly spherical growth (Fig. 3.20a).[58,64,74]

The effect this difference in nucleation and growth morphologies would have on the kinetics of the isothermal pearlite reaction for small and large grain sizes cannot be separated from the effect of differing nucleation rates for the two reactions. Both the lower nucleation rate and the non-spherical nature of growth in the large grained samples will result in a slower isothermal reaction rate.

3.3.3 Additivity and Site Saturation

It has been demonstrated consistently that the

Avrami's equation is able to express the kinetics of non-isothermal pearlite transformations assuming the additivity principle to be valid.[38,39,49,72,73] For this same data the isokinetic condition as defined by Avrami, i.e. the proportionality of $\frac{N}{G}$ over a given reaction temperature range, has been found not to be valid as shown in Table 3.9, consistent with earlier observations (Fig. 1.11). This is a consequence of the more rapid increase in the nucleation rate with increasing temperature as compared with the smaller change in the growth rate.

The site saturation concept as described by J. W. Cahn[20,35] was also examined to explain the applicability of the additivity principle. The number of available nucleation sites/mm^3 for any austenite grain size can be determined using Cahn's austenite grain shape model of a space filling tetrakaidecahedra.

An assessment of the site saturation criteria derived by Cahn, based on the nucleation rate for specific sites can be seen in Table 3.10 for corner site saturation. Since it is experimentally impossible to measure nucleation rates for each individual nucleation site, the comparison was made using the corner nucleation rate. As can be seen, the experimentally determined total nucleation rate,

TABLE 3.9 Test of Isokinetic Condition

- Constant $\frac{N}{G}$ -

Austenitising Temperature °C	A.S.T.M. Grain Size	$\frac{N}{G}$ = $\frac{Nodules/mm^3}{mm/s}$ 640°C	690°C
800	9.1	98×10^4	184×10^4
840	7.8	225×10^4	39×10^4
950	7.3	57×10^4	0.05×10^4

TABLE 3.10 Cahn : Nucleation Rate Criteria

$N_s > 6 \times 10^3 \ G/D^4$

$N_e > 10^3 \ G/D^4$

$N_c > 2.5 \ G/D^4$

Austenitising Temperature °C	Reaction Temperature °C	$2.5 \ G/D^4$ $(1/mm^3.s)$	Total Nucleation Rate $(\frac{nodules}{mm^3.s})$
800	690	26,675	995
	640	528,000	10,400
840	690	4,610	382
	640	37,500	18,000
900	690	895	0.07
950	690	787	0.2
	640	15,900	3,800
1100	640	16.7	5.6

which is $N_c + N_e + N_s$ [20,35,61] is consistently lower than those required for corner site saturation and therefore much lower than is required for edge or boundary nucleation.

Cahn's other criterion for determination of early site saturation was based on a consideration of attaining one pearlite nodule per grain. In a photomicrograph of specimens partially reacted to approximately 15% transformation (Fig.3.21), it can be seen that one pearlite nodule per grain is metallographically far from true. This was confirmed by a calculation based on determining the number of austenite grains per unit volume from the grain diameter and the experimentally measured number of pearlite nodules per unit volume. The results of this calculation done for specimens reacted partially up to approximately 15% transformation is given on Table 3.11. It can be seen that, without exception, for all of the cases examined, the condition of one nodule per grain is likely never attained. Cahn also derived the mathematical expression for this metallographic consideration based on the time it would take one nodule, to consume half of one grain:

$$\frac{G\, t_{0.5}}{d} \leq 0.5 \qquad \ldots(3.11)$$

This would hold if site saturation was taking place. The results of this calculation can be seen to suggest that

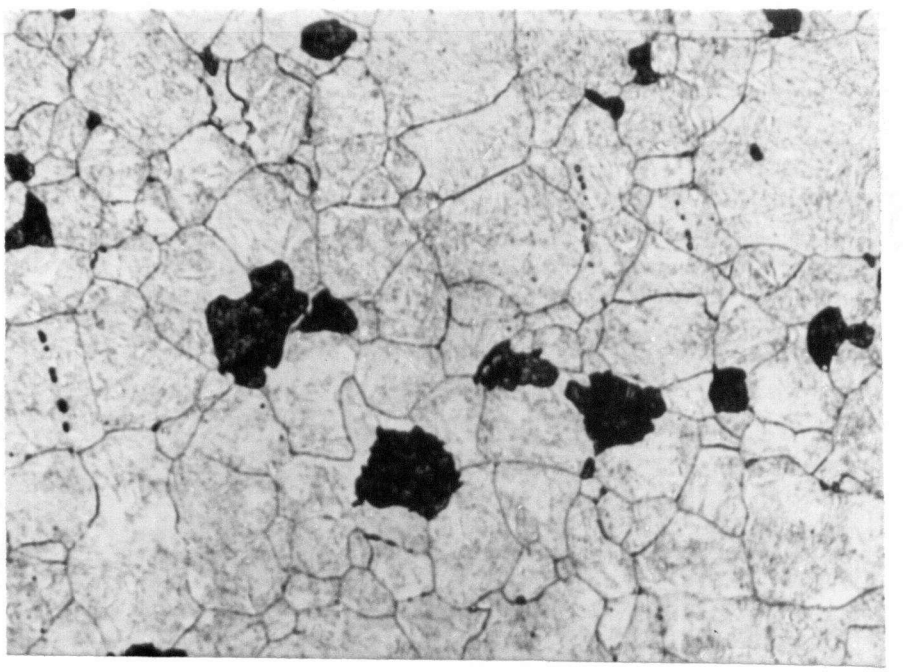

Fig. 3.21 Initial nucleation rate in terms of $\frac{\text{number of nodules}}{\text{grain}}$, metallographically in specimen transformed partially to approximately 15% transformation. Mag. X 600.

TABLE 3.11 Initial Nucleation Rate in Terms of Nodules/Grain

Austenitizing Temperature °C (5 min)	Isothermal Transformation Temperature	A.S.T.M. Grain Size	Initial Nucleation Rate (no/mm^3)	Initial Number Nodules/Grain
800	640	9.1	10,400	1/188
	690	9.1	995	1/141
840	640	7.8	18,000	1/32
	690	7.8	382	1/44
950	640	7.3	3,800	1/19
1100	640	3	6	1/6

TABLE 3.12 Cahn : Early Site Saturation Criterion

$$\frac{Gt_{\frac{1}{2}}}{d} \leq 0.5$$

Austenitizing Temperature °C (5 min)	$\frac{Gt_{0.5}}{d}$ 640°C	690°C
800	4.5	3.0
840	2.5	5.4
900	-	11.0
950	2.1	12.4
1100	2.4	-

this condition for site saturation is not realized (Table 3.12).

In the light of these calculations one would have to conclude that since the isokinetic condition does not hold and site saturation has not taken place, the additivity principle should not be applicable. Yet there is direct evidence that the additivity principle can be applied successfully to predict continuous cooling behaviour.[38,39,40,72,73] It is important to recognize the fact that both Avrami's "isokinetic condition" and Cahn's "site saturation model" were a sufficient condition for the additivity principle to work but were not a necessary condition. An alternative requirement for applying the additivity principle, termed "effective site saturation" was thus investigated.

3.3.4 Effective Site Saturation

An experimentally determined nucleation rate is a measure of the rate at which new centres of transformation product appear. As long as there are available sites, this experimental nucleation rate need not decrease. However, as the transformation approaches completion, one would expect the available sites to be decreasing in number, if not exhausted. The question is; what is the contribution to the total volume fraction transformed of the late-coming centres of growth? If an overwhelming fraction of

the transformed phase is the result of growth of the very early nuclei, although the experimentally measured nucleation rate may be a constant, the late nuclei contribute very little to the total volume fraction transformed and "effective site saturation" will have taken place.

To calculate the volume contribution from nodules nucleating at different times during the course of the transformation, it is necessary to characterize the transformation in terms of the nucleation and growth rates. The Johnson-Mehl (J.M) equation (Equation 2.4) includes these quantities to express the progress of the transformation.

A calculation was carried out using the Johnson and Mehl equation (Equation 2.4), the experimentally determined nucleation and growth rates and the appropriate isothermal reaction times corresponding to approximately 5 and 10% volume fraction transformed. A determination of the resulting time exponent (originally 4 in the J.M equation) was made. The results for the isothermal reaction temperatures of 640°C and 690°C can be seen on Table 3.13. The time exponent values determined confirm that the Johnson-Mehl equation with its n = 4, does not characterize the pearlite reaction for the isothermal reaction temperatures examined.

TABLE 3.13 Calculated Values* of the Time Exponent in the Johnson-Mehl Equation.

Austenitising Temperature °C	Time Exponent for 640°C Isothermal Reaction Temperature	Time Exponent for 690°C Isothermal Reaction Temperature
800	1.4	3.2
840	1.4	2.2
900	-	3.9
950	2.4	3.5
1100	2.8	-

*Calculations based on t = 0 at t_{av}.

The inability of the J.M equation to predict the volume fraction transformed was due to certain non-satisfactory assumptions. The assumptions made in the derivation of the J.M. equation are:

1. The rate of nucleation and the rate of growth are constant.
2. The growth of pearlite nodules is spherical and constant.
3. The nucleation is random (homogeneous nucleation).

Although the first two assumptions are reasonable, the last assumption, in the case of the pearlite nucleation, is definitely incorrect. Pearlite nucleates preferentially at grain corners, grain edges and/or grain boundaries and is therefore a heterogeneous transformation product.

To be able to use the J.M equation that includes nucleation and growth rates and to better simulate the actual transformation, an "inhomogeneity factor" defined as:

$$I = \frac{V_{homogeneous}}{V_{heterogeneous}}$$

has been calculated. The schematic comparison of homogeneous versus heterogeneous reactions is made in Fig. 3.22.

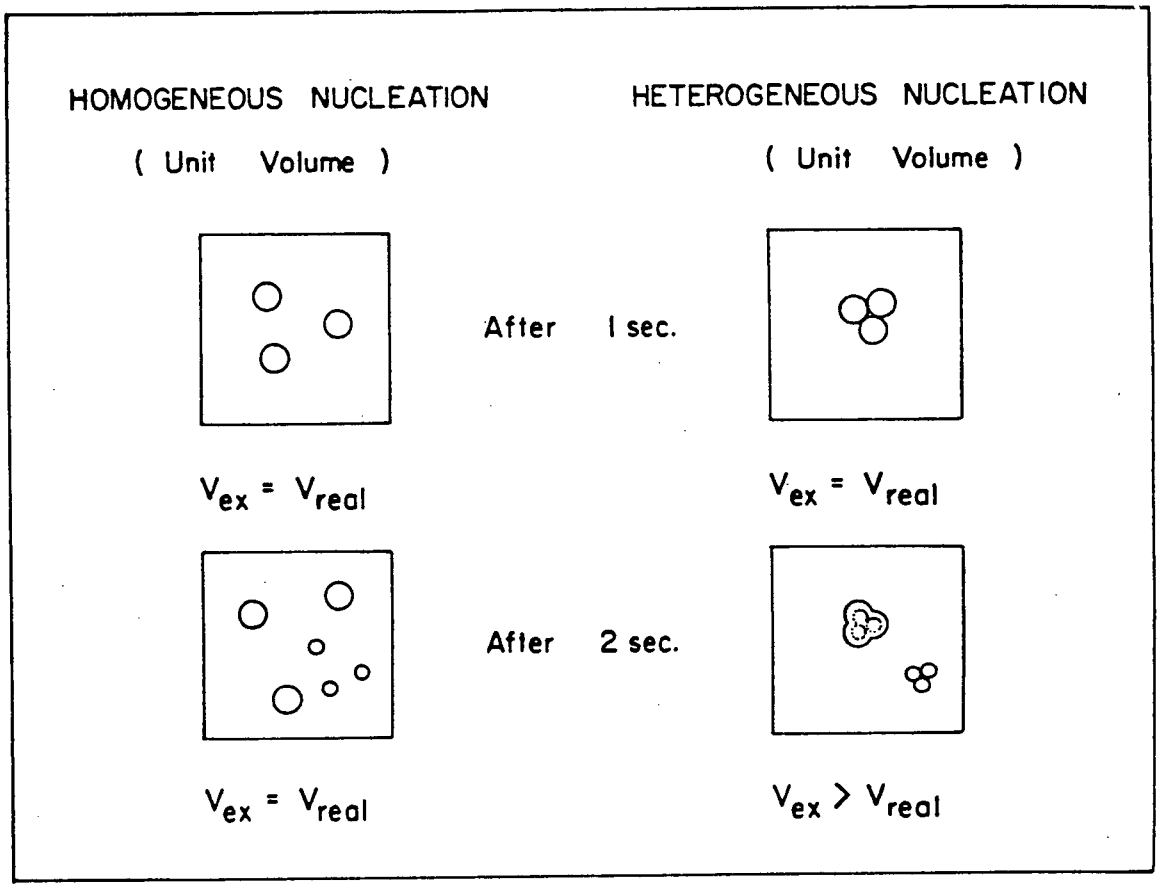

Fig. 3.22 Schematic representation of homogeneous and heterogeneous reaction kinetics.

As can be seen, the rate of the inhomogeneous reaction will be slower than that of a homogeneous reaction due to greater impingement in the inhomogeneous reaction.

The time dependent variation of 'I' for an isothermal reaction would be expected to have the form shown in Fig. 3.23. Because extensive impingement would not take place at the earlier stages of the transformation, the rates of the homogeneous and the heterogeneous reactions should not be very different. Similarly towards the completion of the reaction where the reaction rates would be very slow and where there would not be much volume untransformed for nucleation and/or growth to take place in. The difference between the rates of homogeneous and heterogeneous reactions would diminish.

Both homogeneous and inhomogeneous reaction kinetics were determined using isothermal kinetic data generated with the salt pot. The experimentally determined nucleation and growth rates were used in the Johnson and Mehl equation (Equation 2.4), with n = 4, to determine the progress of the homogeneous reaction. (As assumed by J.M when deriving their rate equation.) The Avrami equation (Equation 2.5), in terms of the empirical constants 'n' and 'b' was used to follow the kinetics of the inhomogeneous (i.e. real) reaction.

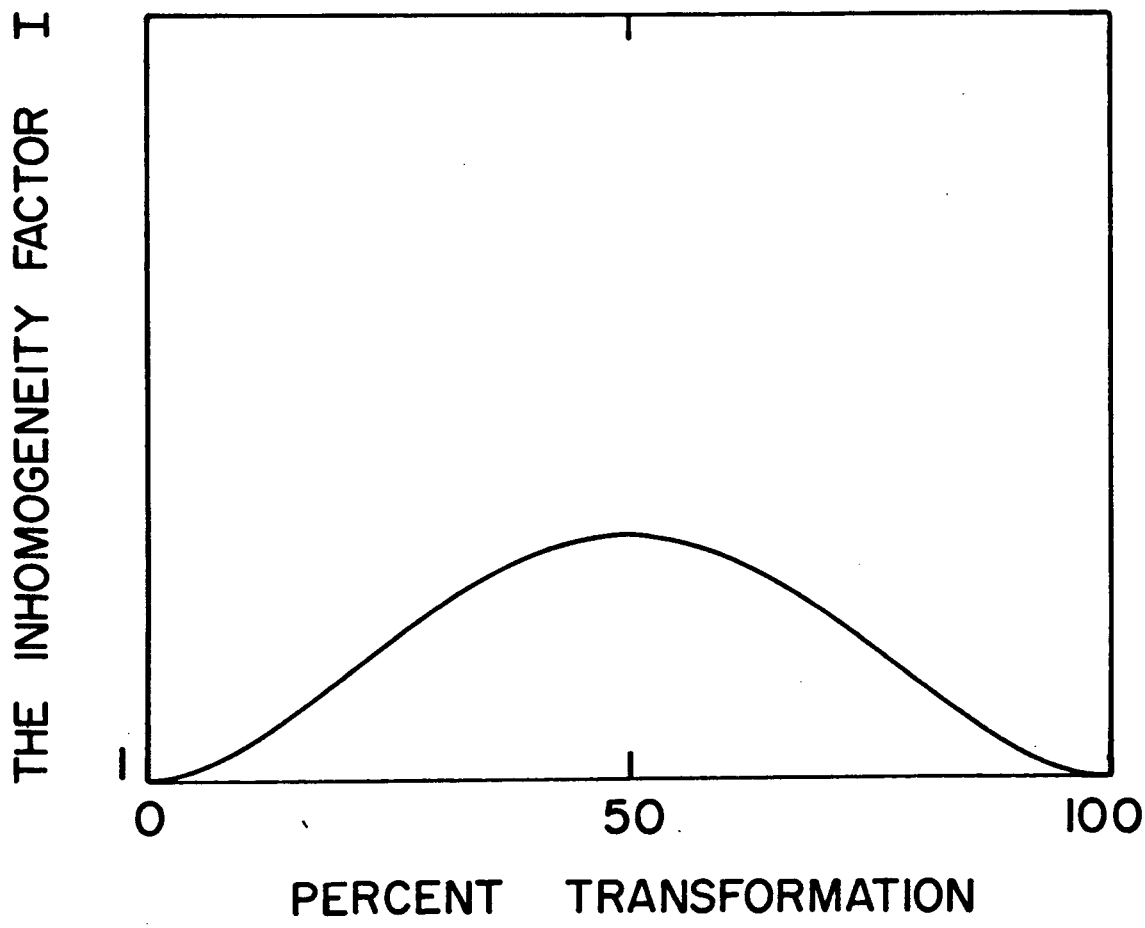

Fig. 3.23 Predicted variation of the "Inhomogeneity Factor", I, with percent transformed of pearlite.

The effect of grain size on the "inhomogeneity factor" at different isothermal reaction temperatures can be seen in Fig. 3.24. The observed departures from the predicted behaviour could be due to two possible considerations;

1. The nucleation effect: For the total range of grain sizes the possibility of a larger number of nodules located at high energy sites such as multi-grain intersections increases due to the greater availability of these sites in the fine grained material. This in turn increases the overall number of nodules that exhibit approximately spherical growth (as explained earlier in relation to Fig. 3.20).
2. The impingement effect: Due to the relative proximity of nucleation sites in small grained specimens, the pearlite nodules will start impinging more rapidly than in large grained samples where nucleation sites are far apart. Greater impingement of the pearlite nodules will give rise to relatively larger deviations from spherical growth.

These two competing effects may be used to explain some of the abnormal behaviour seen on Fig. 3.24. In the 640°C graph (Fig. 3.24 a), the largest grain size samples are seen to deviate significantly from the expected behaviour. This could be explained by the nucleation effect

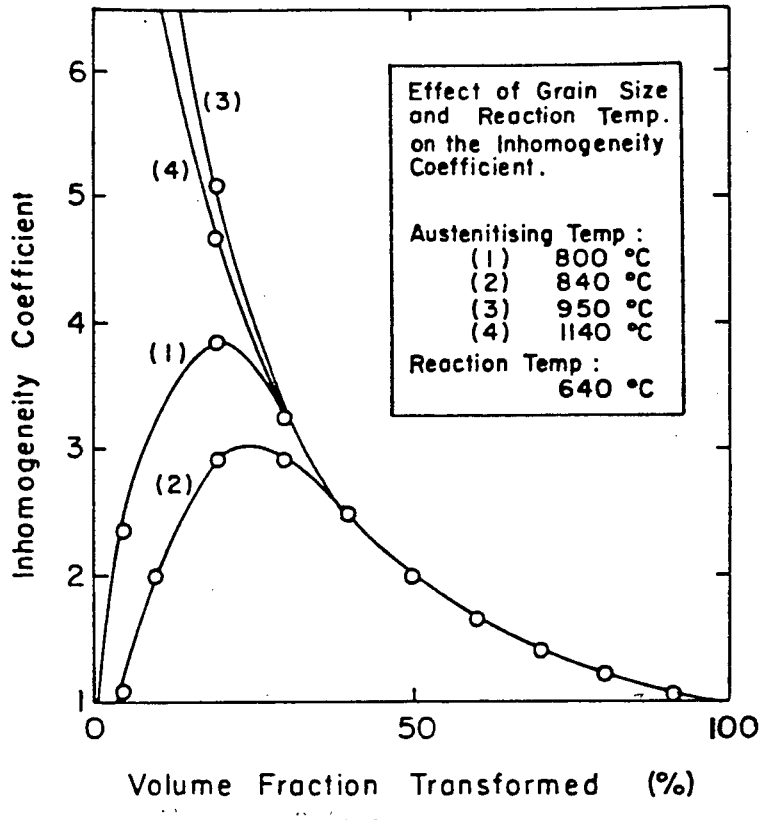

Fig. 3.24a Experimental variation of 'I', for the isothermal reaction temperature of 640°C.

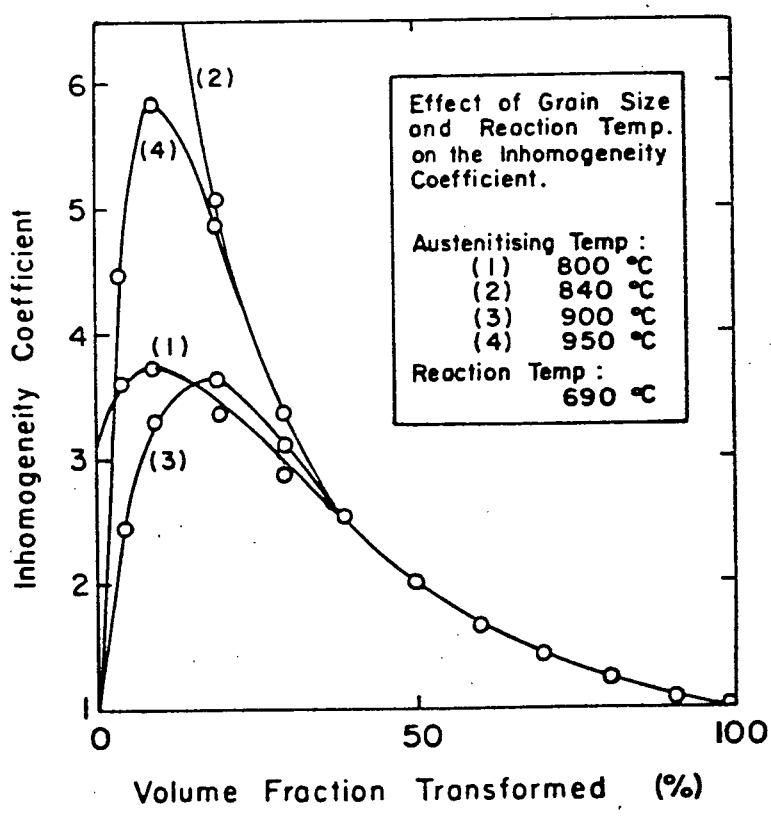

Fig. 3.24b Experimental variation of 'I', for the isothermal reaction temperature of 690°C.

which would give rise to non-spherical growth that would increase the inhomogeneity factor.

The contribution to the total volume transformed of nodules nucleating in the first 20% of the reaction was calculated by using the equation: (For the derivation of this equation see Appendix 1.)

$$\frac{V_{o/20}}{V_{90}} = \frac{t_{90}^4 - (t_{90} - t_{20})^4}{t_{90}^4} \qquad \ldots 3.12$$

where

$V_{o/20}$ = Volume transformed by nodules nucleating in the first 20% at 90% transformation.

V_{90} = Total volume transformed at 90% transformation.

By using the time to 90% transformation for, V_{90}, a calculation was carried out to determine the contribution to the total volume of nodules nucleating in the first 20% of the isothermal pearlite transformation (i.e. t_{20} = time to 20% transformation). The results of this calculation can be seen on Table 3.14. for the range of grain sizes and isothermal reaction temperatures investigated.

TABLE 3.14 The Influence of Grain Size and Isothermal Reaction Temperature on Volume Contributions.

Contribution to the Total Volume Transformed, by Nodules which Nucleated in the First 20% of the Transformation, at 90% Total Volume Transformed (%)	Austenitising Temperature (°C)	Reaction Temperature (°C)
85	950	690
93	840	690
94	800	690
88	900	690
97	1100	640
96	950	640
82	840	640
86	800	640

In all instances the nodules nucleating in the first 20% of the reaction contribute to at least 80% of the total volume transformed at 90% transformation. The results clearly support the description of the experimental behaviour as "effective site saturation". This means that, the temperature dependent growth process dominates the transformation event.

This observation can be coupled with an important thermodynamic consideration of the transformation process. Due to the greater volume of the pearlite phase a positive pressure would develop in the structure with increasing percent transformation. Le Chatelier's principle states that the system should move to minimize this effect, i.e. to reduce the amount transformed in areas adjacent to the growing nodules. In this case, the increased pressure should reduce the transformation temperature, thereby stabilizing the austenite to lower temperatures. The result would be to reduce the effectiveness of nucleation sites adjacent to existing nodules. Therefore this condition would also encourage "effective site saturation".

An "effective-site saturation" criterion can be formulated to test its validity for other grades of steel. By using 85% for the contribution to total volume at 90%

transformation, of nodules nucleating in the first 20% of the transformation in equation 3.12 the following relationship can be obtained (Appendix A2):

$$t_{20} \geq 0.38\ t_{90} \qquad \ldots 3.13$$

where

t_{20} : time to 20% transformation

t_{90} : time to 90% transformation

This "effective site saturation" criterion has been tested for all experimental results of this study (Table 3.15) and for isothermal kinetic data reported in the literature for different grades of steel (Table 3.16). The results show that for the total range of grain sizes, isothermal reaction temperatures and steel compositions investigated, the "effective site saturation" criterion is a sufficient condition for the applicability of the additivity principle.

TABLE 3.15 The "Effective Site Saturation" Criterion, $\frac{t_{20}}{t_{90}} \geq 0.38$, Values Calculated for Experimental Results Determined for the 1080 Steel Used in this Study.

Reaction Temperature °C	Grain Size A.S.T.M.	t_{20}	t_{90}	$\frac{t_{20}}{t_{90}}$	Source
640	9.1	3.22	8.38	0.38	1080 Steel
640	7.8	3.08	8.93	0.34	
640	7.3	6.8	12.7	0.53	
640	3	31.76	55.14	0.58	
690	9.1	51.1	101.4	0.51	
690	7.8	119.0	243.0	0.49	
690	7.4	918	2275	0.40	
690	7.3	847	2301	0.37	

TABLE 3.16 Calculated values of $\frac{t_{20}}{t_{90}} \geq 0.38$, the "Effective Site Saturation: Criterion, for Isothermal Reactions Reported in Literature.

Reaction Temperature °C	Grain Size A.S.T.M.	t_{20}	t_{90}	$\frac{t_{20}}{t_{90}}$	Source
500	5½	4.2	5.5	0.76	0.78%C plain carbon steel[37]
540	5½	4.8	6.5	0.74	
600	5½	6.4	10	0.64	
630	5½	8	20	0.40	
650	4½	23	42	0.54	0.80%C plain carbon steel[37]
660	4½	70	92	0.76	
690	4½	700	1100	0.63	
662	5	4.7	6.5	0.72	1.10%C steel[37]
691	5	80	200	0.40	0.57%C steel[37]
689	1	35	46	0.75	0.93%C steel[37]
715	-	95	200	0.48	SKD-6 steel[38]
670	-	340	830	0.41	
615	5-7	3.25	5.4	0.62	0.82%C plain carbon steel[72]
630	5-7	5.6	9.8	0.57	
660	5-7	32.4	72	0.45	
670	5-7	58	163	0.36	

Chapter 4

4.1 SUMMARY

The following conclusions summarize the results, discussion and interpretation of experiments performed to examine the kinetics of nucleation and growth of pearlite in eutectoid plain-carbon steels; a wide range of austenite grain sizes and transformation temperatures were included in this study:

1. The Avrami equation (Equation 2.5), as modified by Tamura et al,[39,40] to include a grain size parameter, can be used to characterize the pearlite transformation

$$X = 1 - \exp(-b \frac{t^n}{d^m}) \qquad \text{...Equation 2.8}$$

2. The measured magnitude of the grain size exponent 'm' in Equation 2.8, indicates that edge nucleation of pearlite should dominate. Metallographic observations confirm that the predominant pearlite nucleation site is austenite grain corners and/or grain edges; it is difficult to separate these two nucleation sites by metallographic observation.

3. The austenite grain growth kinetics of this 1080 steel can be characterized by using the relationship developed by Alberry et al.,[49] to predict microstructure in the HAZ of weldments: (Equation 2.16). This expresses the final grain size in terms of the peak temperature and holding time at peak temperature.

$$D^{3.57} - D_o^{3.57} = 2.98 \times 10^{12} \exp\left(\frac{-460{,}000 \mp 1000}{RT}\right) t \quad \text{...Equation 2.15}$$

4. The existing criteria that define the conditions under which the additivity principle is applicable, an isokinetic temperature range, as defined by Avrami[19] and saturation of available nucleation sites of pearlite, as outlined by Cahn,[20,35,61] were shown to be insufficient in explaining the austenite-to-pearlite transformation.

5. An alternative, sufficient condition for the applicability of the additivity principle to predict continuous cooling data from isothermal transformation data has been proposed. This condition was termed "effective site saturation" to express the essentially growth dominated nature of the pearlite reaction and the relative insignificance of the pearlite nucleation

event after the early stages of the transformation. Calculations based on the measured pearlite nucleation and growth rates have shown that the relative contribution of pearlite nodules nucleating in the first 20% of the transformation to the total volume transformed at the end of the transformation is very high; at least 80% of the total volume transformed.

6. The "effective site saturation" criterion (Equation 3.13) has been shown to be a sufficient condition for permitting the use of the additivity principle, for a range of grain sizes, isothermal transformation temperatures and steel grades. It can be summarized as follows:

$$t_{20} > 0.38\ t_{90} \qquad \text{...Equation 3.13}$$

4.2 RECOMMENDATIONS FOR FUTURE WORK

1. Although salt pots have been used as the most suitable equipment for the accurate determination of nucleation and growth kinetics due to the large number of specimens involved, they have been shown to provide a very limited cooling rate. The very slow cooling rates (in the order of 25-30 °C/s), obtained on transferring a specimen from one salt

pot to another salt pot makes isothermal tests near the nose of the TTT curve impossible; the transformation initiates during cooling to the isothermal temperature. Therefore, for the satisfactory correlation of nucleation and growth kinetics with isothermal kinetic data near and below the TTT nose and a complete fundamental understanding of the whole range of transformation, an experimental technique which can achieve significantly higher cooling rates is a necessity. If disc-shaped flat specimens could be heated rapidly by using electrical resistance heating, two-directional water spraying or water jets could achieve faster cooling rates.

2. The upper and lower limits to the applicability of the additivity principle could be better defined by studying the nucleation and growth kinetics of pearlite in very small grained specimens (A.S.T.M. 12), and in very large grained specimens (A.S.T.M. 1).

3. A more extensive metallographic study of the effect of flat and curved grain boundaries and the effect of nucleation at multi-grain intersections, grain edges and grain surfaces on the growth morphology of the pearlite nodules could better clarify the phenomena of departure from spherical growth of pearlite nodules.

BIBLIOGRAPHY

1. English Translation (1583) of "The Anonymous Booklet, Von Stahel and Eysen" (Nuremberg 1532) History of Metallography. C. S. Smith.

2. Tylecote, R.F. "A History of Metallurgy" Published by the Metals Society, 1976, London.

3. Davenport, E.S., Bain, E.C. "Transformation of Austenite at Sub-critical Temperatures". Trans. AIME. 90, 117 (1930).

4. Carpenter, H.C.H., Robertson, J.M. "The Austenite-Pearlite Inversion". J.I.S.I. No. 11, p.345, (1931).

5. Mehl, R.F., Hagel, W.C. "The Austenite-Pearlite Reaction". Progress in Metal Physics, 6, pp.74-134, (1942).

6. Davenport, E.S. "Isothermal Transformation in Steels". Trans. A.S.M., Vol. 27, p.837, (1939).

7. Bain, E.C. "Factors Affecting the Inherent Hardenability of Steel". Trans. A.S.S.T., Vol. 20, p.385, (1932).

8. Reed-Hill, R.E. Physical Metallurgy Principles, p.702, D. Van Nostrand, N.Y., 1973.

9. Grange, R.A., Kiefer, J.M. "Transformation of Austenite on Continuous Cooling and its Relation to Transformation at Constant Temperature". Trans. A.S.M. 29, p.85, (1941).

10. Samuels, L. E. 'Optical Microscopy of Carbon Steels' Metals Park, Ohio, A.S.M., 1980.

11. Scheil, E. "Initiation time of the Austenite Transformation". Archiv. Eisenhüttenwesen, 8, pp.565-567, (1935).

12. Steinberg, S. "Relationship between Rate of Cooling, Rate of Transformation, Undercooling of Austenite, and Critical Rate of Quenching". Metallurgy, 13(1), pp. 7-12, (1938).

13. Hollomon, J. H., Jaffe, L.D. "Anisothermal Decomposition of Austenite". Trans. A.I.M.M.E. 167, 419, (1946).

14. Krainer, H. "The Conditions for Thorough Hardening of Steel". Archiv. Eisenhüttenwesen 9, pp. 619-622, (1936).

15. Lange, H. "Austenite Decomposition in Plane Carbon Steel". Mitt. K.W.I. Eisenforschung 22, pp.229-240, (1940).

16. Lange, H., Hansel, H. "The Course of Austenite Transformation in the Undercooled State, according to Investigations on Pure Plain Carbon Steels". Mitt. K.W.I. Eisenforschung 19, pp. 199-208, (1937).

17. Manning, G.K., Lorig, C.H. "The Relationship between Transformation at constant Temperature and Transformation During Cooling. Trans. A.I.M.M.E. 167.

18. Avrami, M. "Kinetics of Phase Change". J. Chem. Phy. 7, pp. 1103-1112, (1939); 8, pp.212-224, (1940); 9, pp.177-184, (1941).

19. Johnson, W.A., Mehl, R.F. "Reaction Kinetics in Processes of Nucleation and Growth". Trans. A.I.M.M.E. 135, pp.416-442, (1939).

20. Cahn, J.W. - "The Kinetics of Grain-Boundary Nucleated Reactions" Acta Met. 4, Sept. (1956), p.449.

21. Umenoto, M., Komatsubara, N., Tamura, I. "Prediction of Hardenability Effects from Isothermal Transformation Kinetics". J. Heat Treating, Vol. 1, No. 3, pp.57-64, (1980).

22. Dorn, J.E., De Garmo, E.D., Flanigan, A.E. "Nucleation and Growth Rates in Pearlite". Trans. A.S.M. Dec. pp.1022-1036, (1941).

23. Agarwal, P.K., Brimacombe, J.K. "Mathematical Model of Heat Flow and Austenite-Pearlite Transformation in Eutectoid Carbon Steel Rods for Wire". Met. Trans. B, Vol. 12B, pp.121-133, (1981).

24. Krauss, G. "Principles of Heat Treatment of Steel". Metals Park, Ohio, A.S.M. 1980 .

25. Bain, E.C. "On the Rates of Reactions in Solid Steel". Trans. A.I.M.E. Vol. 100, pp.13-46, (1932).

26. Bain, E.C. "Factors Affecting Hardenability of Steel". Trans. A.S.S.T., Vol. 20, pp.385-428, (1932).

27. Vilella, J.R., Bain, E.C. "Revealing the Austenite Grain Size of Steel". Metal Progress, Vol. 30, No. 3, pp.39-45, (1936).

28. Bain, E.C. "Austenitic Grain Size, Estimation and Significance". Steel, May, Vol. 98, p.66, (1936).

29. Bain, E.C. "Grain Size and Hardenability in Steels to be Heat Treated". Steel, Vol. 100, p.33, (1938).

30. Mehl, R.F. "Physics of Hardenability". Hardenability of Alloy Steels, Published by A.S.M., p.1, 1938.

31. Mehl, R.F. "The Structure and Rate of Formation of Pearlite". Trans. A.S.M., pp. 813-862, Dec. (1941).

32. Christian, J.W. "The Theory of Transformations in Metals and Alloys". Pergamon Press, p.21, (1965).

33. Rothenau, G.W., Boas, G. "Electron Optical Observations of Transformations in Eutectoid Steel". Acta Met. 2, 875, (1954).

34. Clemm, P.J., Fisher, J.C. "The Influence of Grain Boundaries on the Nucleation of Secondary Phases". Acta Met. 3, 70, (1955).

35. Cahn, J.W. "On the Kinetics of the Pearlite Reaction". Trans. A.I.M.E. 209, 140, (1957).

36. Lyman, T., Troiano, A.R. "Isothermal Transformation of Austenite in 1 percent Carbon, High Chromium Steels" Trans. A.I.M.E. 162, 196, (1945).

37. Hull, F.C., Colton, R.A., Mehl, R.F. "Rate of Nucleation and Rate of Growth of Pearlite". Trans. A.I.M.M.E., 150, pp.185-207, (1942).

38. Umemoto, M., Horiuchi, K., Tamura, I. "Transformation Kinetics of Bainite During Isothermal Cooling and Continuous Cooling". Trans. I.S.I.J., Vol. 22, pp. 854-861, (1982).

39. Umemoto, M., Nishioka, N., Tamura, I. "Prediction of Hardenability from Isothermal Transformation Diagrams". J. Heat Treating, Vol. 2, No. 2, pp.130-138, (1981).

40. Umemoto, M. Tamura, I. "Continuous Cooling Transformation Kinetics of Steels". Trans. I.S.I.J., Vol. 21, pp.383-392, (1981).

41. Carpenter, H.C.H., Elam, L.F. "Crystal Growth and Recrystallization in Metals". J. Inst. Met. 24, 83, (1920).

42. Sutoki, T. Scientific Report, Tohoku University 17, 857, (1928).

43. Harker, D., Parker, E.A. Trans. A.M.S. 34, 156, (1945).

44. Burke, J.E., Turnbull, D. "Recrystallization and Grain Growth". Progress in Metal Physics, Vol. 3, pp.220-292.

45. Nielsen, J.P. "Recrystallization, Grain Growth and Texture". A.S.M. Seminar Series, pp.141-164, A.S.M. Metals Park, Ohio.

46. Feltham, P., Copley, P.S. "Grain Growth in alpha-brasses". Acta Met. 6, 539, (1958).

47. Hannerz, N.E., de Kazinczy, R. "Kinetics of Austenite Grain Growth in Steel". J.I.S.I. 208, pp.475-481, (1970).

48. Hu, H., Roth, B.B. "On the Time Exponent of Isothermal Growth". Met. Trans. 1, pp.3181-3184, (1970).

49. Alberry, P.J., Chew, B., Jones, W.K.C. "Prior Austenite Grain Growth in HAZ of a 0.5 Cr-Mo-V Steel. Metals Technology, June, pp.317-325, (1977).

50. Ikawa, H., Oshige, H., Noi, S., Date, H., Uchikawa, K. "Relation Between Welding Conditions and Grain Size in Weld HAZ". Trans. Japan Welding Soc. Vol. 9, No. 1, pp.47-51, (1978).

51. "Grain Size Determination" - Metallography, Structures and Phase Diagrams - A.S.M. Metals Handbook Vol. 8, 8th Edition Metals Park, Ohio.

52. Roberts, G.A. Ph.D. Thesis submitted by G.A. Roberts Carnegie Institute of Technology. Pittsburgh, Pennsylvania. May 1942.

53. Bastien, P., Maynier, Ph. Dollet, J. "Prediction of Microstructure via Empirical Formulae Based on CCT Diagrams". Hardenability Concepts with Applications to Steel. Ed. D.V. Doane and J.S. Kirkaldy. Publication of A.I.M.E., 1978.

54. Arnold, G., McWilliam, R. "The Thermal Transformations of Carbon Steel". J.I.S.I. No. 2, p.27, (1905).

55. Benedics, C. "The Nature of Troostite". J.I.S.I. No. 2, p.352, (1905).

56. Hull, F.C., Mehl, R.F. "The Structure of Pearlite". Trans. A.S.M. pp.381-474, June (1942).

57. Modin, S. Jernkontorets Ann., 142, 37 (1958).

58. HIllert, M. "The Formation of Pearlite". Decomposition of Austenite by Diffusional Processes, Ed. V.F. Zackay and H.I. Aaronson. A.I.M.M.E. Publications, 1962.

59. Mirkin, I. L., Blanter, M.E. Metallurg Vo.. 11, No. 12, p.43, (1936).

60. Scheil, E., Lange-Weise, A. "Statistische Ge fügeuntersuchungern", Vol. 2, p.93, (1937-1938).

61. Cahn, J.W., Hagel, W.C. "Theory of the Pearlite Reaction". Decomposition of Austenite by Diffusional Processes. Ed. V.F. Zackay and H.I. Aaronson A.I.M.E. Publ. 1962.

62. Brown, D., Ridley, N. "Rates of Nucleation and Growth and Interlamellar Spacing of Pearlite in a Low-alloy Eutectoid Steel". J.I.S.I. 204, pp.811-816, (1966).

63. Brown, D., Ridley, N. "Kinetics of the Pearlite Reaction in High-Purity Nickel Eutectoid Steels". J.I.S.I. 207, pp.1232-1240, (1969).

64. Darken, L.S., Fisher, R.M. "Some Observations on the Growth of Pearlite". Decomposition of Austenite by Diffusional Processes. Ed. V.F. Zackay and H.I. Aaronson A.I.M.E. Publ. (1962).

65. Parcel, R.W., Mehl, R.F. "Effect of Molybdenum and of Nickel on the Rate of Nucleation and the Rate of Growth of Pearlite". Journal of Metals, pp.771-780, July 1952.

66. Cahn, J.W. "Transformation Kinetics During Continuous Cooling". Vol. 4, p.572, November 1956.

67. Modin, H., Modin, S. "Metallurgical Microscopy" John-Wiley and Sons, N.Y., pp.159-161, 1973.

68. Scheil, E. Zeitschrift fur Metallkunde, 37, 123, (1946).

69. Brandt, W.H. "Solution of the Diffusion Equation Applicable to the Edgewise Growth of Pearlite" J. Appl. Phy. 16, 139, (1945).

70. Zener, C. "Kinetics of the Deocomposition of Austenite". Trans. A.I.M.E. 167, 550, (1946).

71. Hillert, M. Jernkontorets Ann. 141, 757 (1957).

72. Jayaraman, R. "Mathematical Modelling of Transformations in Steels". M.A.Sc. Thesis. The University of British Columbia, 1983.

73. Hawbolt, E.B., et al., "The Characterization of Transformation Kinetics of Carbon Steels under Industrial Process Conditions" Progress Reports 2-4 to prepared for the A.I.S.I. 1980-1983.

74. Aaronson, H.I. "Pro-Eutectoil Ferrite and Cementite Reactions" Decomposition of Austenite by Diffusional Processes. Ed. V.F. Zackay, H.I. Aaronson, Publ. A.I.M.E. 1962.

75. Sorby, H.C., J.I.S.I., No. 1, 1886, p.140.

76. Hawbolt, E.B., Chau, B., Brimacombe, J.K. "Kinetics of Austenite-Pearlite Transformation in Eutectoid Carbon Steel", Accepted for publication in Met. Trans. 1983.

Appendix 1

VOLUME CONTRIBUTIONS

APPENDIX 1

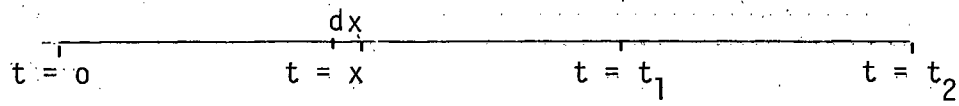

Number of nuclei nucleating during a time dx = N dx

where 'N' is the volumetric nucleation rate.

The extended volume of growth of these nuclei at time $t = t_2$ is:

$$\sigma . N dx . G^3(t_2-x)^3$$

where

σ = shape factor

$= \frac{4}{3}$ for spherical growth.

G = growth rate (mm/s)

Therefore the extended volume (V_{ex}) of growth of nuclei nucleating between $t = o$ and $t = t_1$ at time $t = t_2$ is:

$$V_{ex}^{t_2}{}_{o/t_1} = \int_o^{t_1} \sigma . G^3(t_2-x)^3 N dx$$

$$= \frac{\sigma N G^3}{4} [t_2^4 - (t_2-t_1)^4] \qquad \ldots A1.1$$

The total extended volume (i.e. from t = o to t = t_2), is:

$$V_{ex}^{t_2} = \frac{NG^3 t_2^4}{4} \qquad \ldots A1.2$$

∴ The fractional volume contributed by the nuclei, nucleating between t = o and t = t_1, to the total transformed volume at t = t_2 is:

$$\frac{V_{ex_{o/t_1}}^{t_2}}{V_{ex}^{t_2}} = \frac{t_2 - (t_2 - t_1)^4}{t_2^4} \qquad \ldots A1.3$$

(Ref 72)

N.B.

It must be noted that $V_{ex_{o/t_1}}^{t_2}$ is not the extended volume transformed at $t=t_1$, rather it is the extended volume at t = t_2 of pearlite nodules nucleating between t = 0 and t = 1 and growing up to t = t_2. Thus

$\frac{V_{ex_{o/t_1}}^{t_2}}{V_{ex}^{t_2}}$ is considered to be equivalent to $\frac{V_{true(t_1)}^{t_2}}{V_{true}^{t_2}}$,

since both extended volumes are corrected to true volume at t_2.

Appendix 2

THE EFFECTIVE SITE SATURATION CRITERION

APPENDIX 2

$$\frac{V_{ex_{o/t_1}}^{t_2}}{V_{ex}^{t_2}} = \frac{t_2^4 - (t_2-t_1)^4}{t_2^4} \qquad \ldots A2.1$$

when

$$t_1 = t_{20}$$

$$t_2 = t_{90}$$

and

$$\frac{V_{ex_{o/t_1}}^{t_2}}{V_{ex}^{t_2}} = 0.85$$

The "effective site saturation" criterion is:

$$\frac{t_{90}^4 - (t_{90}-t_{20})^4}{t_{90}^4} \geq 0.85 \qquad \ldots A2.2$$

Therefore

$$t_{20} \geq 0.38\ t_{90} \qquad \ldots A2.3$$